

AD\_\_\_\_\_

AWARD NUMBER: DAMD17-02-C-0073

TITLE: Overuse Injury Assessment Model

PRINCIPAL INVESTIGATOR: James H. Stuhmiller, Ph.D.  
Bryant L. Sih, Ph.D.  
Weixin Shen, Ph.D.  
Kofi Amankwah, Ph.D.  
Charles Negus, Ph.D.

CONTRACTING ORGANIZATION: Titan Corporation  
San Diego, California 92121-1002

REPORT DATE: March 2006

TYPE OF REPORT: Annual

PREPARED FOR: U.S. Army Medical Research and Materiel Command  
Fort Detrick, Maryland 21702-5012

DISTRIBUTION STATEMENT: Approved for Public Release;  
Distribution Unlimited

The views, opinions and/or findings contained in this report are those of the author(s) and should not be construed as an official Department of the Army position, policy or decision unless so designated by other documentation.

<b>REPORT DOCUMENTATION PAGE</b>				<i>Form Approved</i> <b>OMB No. 0704-0188</b>	
Public reporting burden for this collection of information is estimated to average 1 hour per response, including the time for reviewing instructions, searching existing data sources, gathering and maintaining the data needed, and completing and reviewing this collection of information. Send comments regarding this burden estimate or any other aspect of this collection of information, including suggestions for reducing this burden to Department of Defense, Washington Headquarters Services, Directorate for Information Operations and Reports (0704-0188), 1215 Jefferson Davis Highway, Suite 1204, Arlington, VA 22202-4302. Respondents should be aware that notwithstanding any other provision of law, no person shall be subject to any penalty for failing to comply with a collection of information if it does not display a currently valid OMB control number. <b>PLEASE DO NOT RETURN YOUR FORM TO THE ABOVE ADDRESS.</b>					
<b>1. REPORT DATE (DD-MM-YYYY)</b> 01-03-2006		<b>2. REPORT TYPE</b> Annual		<b>3. DATES COVERED (From - To)</b> 22 Feb 2005 – 21 Feb 2006	
<b>4. TITLE AND SUBTITLE</b>  Overuse Injury Assessment Model				<b>5a. CONTRACT NUMBER</b> DAMD17-02-C-0073	
				<b>5b. GRANT NUMBER</b>	
				<b>5c. PROGRAM ELEMENT NUMBER</b>	
<b>6. AUTHOR(S)</b> James H. Stuhmiller, Ph.D.; Bryant L. Sih, Ph.D.; Weixin Shen, Ph.D.; Kofi Amankwah, Ph.D.; and Charles Negus, Ph.D.  E-Mail: <a href="mailto:James.Stuhmiller@L-3com.com">James.Stuhmiller@L-3com.com</a>				<b>5d. PROJECT NUMBER</b>	
				<b>5e. TASK NUMBER</b>	
				<b>5f. WORK UNIT NUMBER</b>	
<b>7. PERFORMING ORGANIZATION NAME(S) AND ADDRESS(ES)</b>  Titan Corporation San Diego, California 92121-1002				<b>8. PERFORMING ORGANIZATION REPORT NUMBER</b>	
<b>9. SPONSORING / MONITORING AGENCY NAME(S) AND ADDRESS(ES)</b> U.S. Army Medical Research and Materiel Command Fort Detrick, Maryland 21702-5012				<b>10. SPONSOR/MONITOR'S ACRONYM(S)</b>	
				<b>11. SPONSOR/MONITOR'S REPORT NUMBER(S)</b>	
<b>12. DISTRIBUTION / AVAILABILITY STATEMENT</b> Approved for Public Release; Distribution Unlimited					
<b>13. SUPPLEMENTARY NOTES</b>					
<b>14. ABSTRACT</b>  This report covers progress made in the development of a model to predict both injury and performance during basic training. Previously, we developed preliminary performance enhancement and metabolic demand models to complement stress fracture models developed earlier. In this report, we describe our work in the further development of the performance model, with a focus on run performance. We also introduce a statistical prediction method to compare our model accuracy with, and describe the development of preliminary overuse and acute injury models. We further refine the software conceptual design and describe the implementation of a simplified version of the software. Additional datasets were also acquired and organized, which were used for model development and validation.					
<b>15. SUBJECT TERMS</b> stress fracture, basic training, bone, gait, performance, metabolic cost					
<b>16. SECURITY CLASSIFICATION OF:</b>			<b>17. LIMITATION OF ABSTRACT</b>  UU	<b>18. NUMBER OF PAGES</b>  115	<b>19a. NAME OF RESPONSIBLE PERSON</b> USAMRMC
<b>a. REPORT</b> U	<b>b. ABSTRACT</b> U	<b>c. THIS PAGE</b> U			<b>19b. TELEPHONE NUMBER (include area code)</b>



**communications**

**Applied Technologies**

---

# **Overuse Injury Assessment Model, Part I: Training, Overuse Injury, and Performance Modeling**

**Part I of Annual Report:** J3181-06-296  
under Contract No. DAMD17-02-C-0073

Prepared by:

Bryant L. Sih, Ph.D.  
Weixin Shen, Ph.D.

**L-3 Communications/Jaycor**  
3394 Carmel Mountain Road  
San Diego, California 92121-1002

**Prepared for:**

Commander  
**U.S. Army Medical Research and Materiel Command**  
504 Scott Street  
Fort Detrick, Maryland 21702-5012

# Summary

This document describes the work performed on the development of the Training, Overuse Injury, and Performance (TOP) Model. The primary objective is to develop a software product that incorporates training regimen plans in the prediction of training performance and injury outcomes.

Currently, there is a need for guidance on minimizing injuries and maximizing performance during basic combat training. Most research has involved field studies where a significant number of subjects (hundreds to thousands) are monitored and a statistical procedure such as factor analysis is performed to determine relevant measures for injury and performance. Unfortunately, the results are only applicable to similar populations and training regimens, offering no guidance or predictability for different scenarios. To demonstrate the inability of a statistical approach to accurately predict training outcomes, a Test Index Cluster (TIC) analysis was performed on several training datasets and the decline in accuracy noted.

For the preliminary version of the TOP Model, a run performance and a lower-body acute/mishap injury algorithm was implemented. The performance model is based on a review of the literature and takes into account training regimen in predicting performance, as measured by the running portion of the military Physical Fitness Test. We find that the performance model has the same level of accuracy as a statistically-based analysis when the model uses parameter values consistent with those found in the literature. However, unlike a statistical analysis, the model is able to maintain the accuracy across different regimens. Despite previous literature suggesting otherwise, we were unable to find any significant factors that correlated with lower-body acute injury suggesting this type of injury is primarily random in the dataset analyzed. Thus, a probability-based model was employed.

To demonstrate usability, a conceptual TOP Model design is included in this document. Features include the ability to import and modify subject and regimen data, specify analyses to run, and produce relevant reports using a user friendly interface. In addition, a preliminary Web-based version of the software has been written with the ability to import data and access the run performance and lower-body acute/mishap injury models.

There are several limitations that will need to be addressed in the future. First, the existing performance and acute/mishap injury models will need to be refined and validated against additional datasets. Second, an overuse injury and stress fracture model needs to be developed. And third, the TOP Model software program will need to be updated and documentation written based on user feedback.

In summary, the TOP Model incorporates performance and injury models based on research found in the literature to predict training outcomes. We demonstrate the main advantage of the software, which is its ability to account for different training situations. Additional models and refinements are planned as future work in this area.

# Contents

	<u>Page</u>
<b>1. INTRODUCTION .....</b>	<b>1</b>
1.1 OBJECTIVE .....	1
<b>2. TEST INDEX CLUSTER ANALYSIS .....</b>	<b>3</b>
2.1 METHOD .....	3
2.2 STATISTICAL ANALYSIS OF EXISTING PERFORMANCE DATA .....	4
2.2.1 TIC Predictive Capability Validation .....	4
2.2.2 Common Variables Identified by TIC Analysis of Different Datasets .....	5
2.3 DISCUSSION .....	6
<b>3. MODEL DEVELOPMENT.....</b>	<b>8</b>
3.1 RUN PERFORMANCE PREDICTION MODEL.....	8
3.1.1 Literature Review.....	8
3.1.2 Methods.....	12
3.1.3 Results .....	18
3.1.4 Discussion.....	19
3.2 ACUTE/MISHAP INJURY PREDICTION MODEL .....	20
3.2.1 Literature Review.....	20
3.2.2 Methods.....	20
3.2.3 Results .....	21
3.2.4 Discussion.....	22
<b>4. SOFTWARE APPLICATION DEVELOPMENT .....</b>	<b>23</b>
4.1 SOFTWARE CONCEPTUAL DESIGN IMAGES .....	24
4.2 PRELIMINARY SOFTWARE SCREENSHOTS.....	32
<b>5. KEY ACCOMPLISHMENTS.....</b>	<b>36</b>
<b>6. REPORTABLE OUTCOMES .....</b>	<b>37</b>
<b>7. CONCLUSIONS.....</b>	<b>38</b>
<b>8. LITERATURE.....</b>	<b>39</b>
<b>APPENDIX A. AVAILABLE DATASETS.....</b>	<b>42</b>

# Illustrations

	<u>Page</u>
<b>1. Simple 2-component systems model of training and performance. ....</b>	<b>9</b>
<b>2. Experimental results for 2 subjects, EWB (left) and RHM (right). ....</b>	<b>10</b>
<b>3. A summary diagram of the run performance algorithm. ....</b>	<b>17</b>
<b>4. TOP Model flow diagram.....</b>	<b>23</b>

# Tables

	<u>Page</u>
1. Test Index Cluster (TIC) analysis results for male and female recruits undergoing basic combat training at Ft. Jackson with “Standardized” Training. ....	3
2. Validation of TIC accuracy.....	5
3. Independent TIC analysis results for five different sets of recruits. ....	6
4. Performance model literature review summary.....	8
5. Summary of model constants and statistics for least-squares regression of criterion performance on predicted performance. ....	10
6. Indicators of goodness-of-fit of performance for various systems models of training effects. ....	12
7. Estimates of $k_1$ from running studies found in the literature.....	16
8. A comparison of the accuracy of a Test Index Cluster (TIC) analysis to that of the run performance model for male recruits undergoing basic combat training at various Army training sites. ....	18
9. A comparison of the accuracy of a Test Index Cluster (TIC) analysis to that of the run performance model for female recruits undergoing basic combat training at various Army training sites. ....	19
10. Variables used in a t-test to compare those that sustained an acute injury to those that did not. ....	21
11. Summary of the datasets available for model development.....	42

# 1. Introduction

The purpose of basic combat training (BCT) is to prepare recruits for the rigors of military life, including acquiring a high fitness level. However, recruits may be injured or fail to reach the desired fitness level (as measured by performance tests such as the military Physical Fitness Test or PFT). Thus, there is a need for guidance on minimizing injuries and maximizing performance during BCT.

Most work has involved field studies where a significant number of subjects (hundreds to thousands) are monitored and a statistical procedure such as factor analysis is performed to determine relevant measures for injury and performance. For example, Allison et al. (2005) analyzed the data from a Ft. Jackson BCT study and identified the key predictors to the negative outcomes of BCT (injury, APFT test failure, and attrition) using a Test Index Cluster (TIC) approach. While the predictors vary for different groups and variables, the results clearly show that gender and initial fitness as measured by initial APFT scores are strongly correlated to the negative outcomes of the training.

These types of analyses are hindered by the inability to identify the relative importance of individual training activities, the difficulty in combining data from different sources, and the limited amount of available data. Most importantly, the results are only applicable to the similar populations and training regimens, offering no guidance or predictability for different scenarios.

What is needed is prediction tool that can account for different populations and training regimens, packaged in a software program that can be easily accessed. Thus, the primary objective is to deliver a product to the military community, including USARIEM, CHHPM, base commanders and fitness advisors, which incorporates training plans into the prediction scheme and improves prediction in differing regimens.

## 1.1 Objective

This document describes the work performed in the following areas:

1. Reviewed the TIC approach, quantifying accuracy and demonstrating limitations of this method.
2. Developed a performance model that takes into account training regimen in predicting performance, as measured by the running portion of the PFT.
3. Developed an acute injury model that take into account training regimen in predicting mishap-type (sprains, blisters, etc.) injuries.
4. Produced an initial application software that, by integrating results obtained by Allison et al. (2005) and related research efforts with regimen-based performance



and injury models, provides a tool where users can easily predict the negative outcomes of BCT for different regimens.

5. Identified the gaps in current model output and recommend future research efforts.

## 2. Test Index Cluster Analysis

As mentioned in the Introduction, previous work often utilizes a statistical approach to determine risk factors for various outcomes of interest. In this section, the Test Index Cluster (TIC) Analysis method is described and its accuracy demonstrated as it relates to BCT performance measures. We show how this method, while accurate for similar training regimens and populations, is not able to accurately predict outcomes for new training protocols or varying groups of people. Other statistically-based methods will have similar limitations.

### 2.1 Method

The purpose of the TIC analysis is to identify relevant predictor variables and the most appropriate cutoff values with which to classify individuals into “high” and “low” risk groups. The procedure is as follows:

- Unpaired t-test to eliminate irrelevant variables
- Receiver-Operator Curve Analysis (ROC) to optimize variable cutoff values
- Logistic Regression to identify statistically significant variables
- Test Index Cluster Analysis to quantify the accuracy of identified variables in the prediction

Additional information on TIC analysis can be found in Allison et al. (2005) or statistical text books.

The dataset used to develop the TIC analysis by Allison et al. (2005) was from a group of recruits undergoing BCT at Fort Jackson circa 2003 using the Army “Standardized” Physical Training Regimen (See the Appendix: Dataset F). Variables included basic anthropometry (age, height, weight, race, and gender), initial PFT test results, educational level, and military service time. From this group of recruits, the variables forming the TIC were determined.

To investigate the limitations of TIC accuracy, the TIC results were applied to three additional datasets: Army BCT at Ft. Jackson with “Traditional” Physical Training, Army BCT at multiple training sites using “Traditional” Physical Training, and Marine Corps BCT at MCRD-San Diego. Additional details on these datasets can be found in the appendix, where they are labeled Datasets F, G, and E.

A separate, independent TIC analysis was also performed on each of these datasets to determine if there are any common variables that identify high risk individuals regardless of training regimen.

## 2.2 Statistical Analysis of Existing Performance Data

### 2.2.1 TIC Predictive Capability Validation

In Allison et al. (2005), the TIC analysis classified individuals as likely or not likely to pass the final PFT (combined run, push-ups, and sit-ups score). Male and female recruits were analyzed separately. The data indicated that 11.8% of male recruits and 18.4% of female recruits did not pass the final PFT.

The results of the TIC analysis are shown in Table 1. In summary, items identified for males include initial push-ups and sit-ups, while females are best predicted for passing the final PFT using initial sit-ups, runtime, and age. In both groups, the TIC analysis is not sensitive ( $< 0.15$ ) but has high specificity ( $> 0.95$ ). More importantly, positive post-test probability was substantially greater for both genders when classified as high risk by the TIC analysis (58.4% and 83.7% of males and females, respectively, of the high risk group did not pass the final PFT).

Table 1. Test Index Cluster (TIC) analysis results for male and female recruits undergoing basic combat training at Ft. Jackson with “Standardized” Training.

Male	Final PFT	
	Fail	Pass
Any 2 or more	7	5
One or less	47	399

Female	Final PFT	
	Fail	Pass
All 3 items	5	1
Two or less	51	254

**For males, two items were identified:  $< 13$  initial push-ups and  $< 21$  initial sit-ups. A recruit with these two items had a significantly greater chance of failing the final PFT (Sensitivity = 0.13; Specificity = 0.99; Positive pretest probability = 11.8%; Positive post-test probability = 58.4%; Negative post-test probability = 10.5%). For females, three items were identified:  $< 10$  initial sit-ups, unable to run a mile in less than 10.71 min, and being less than 20.5 years in age. A recruit with these three times had a significantly greater chance of failing the final PFT (Sensitivity = 0.09; Specificity = 1.00; Positive pretest probability = 18.4%; Positive post-test probability = 83.7%; Negative post-test probability = 17.1%).**

Applying the same TIC variables to the additional datasets resulted in a reduction in accuracy (Table 2). In general, the TIC was most accurate when applied to other Ft. Jackson-based recruits and least accurate when applied to the Marine Corps training, which has the most different training regimen.

Table 2. Validation of TIC accuracy.

Prevalence		Positive Test Probability
TIC Basis		
Army BCT at Ft. Jackson with Standardized Training		
Male	12%	58%
Female	18%	84%
TIC Prediction		
Army BCT at Ft. Jackson with Traditional Training ( <b>F</b> )		
Male	13%	50%
Female	21%	25%
Army BCT at various training centers with Traditional Training ( <b>G</b> )		
Male	16%	32%
Female	21%	Unable to calc.
Marine Corp BCT at MCRD-SD ( <b>E</b> )		
Male	12%	Unable to calc.

**Positive Test Probability is the percent of those in the “high risk” group that failed the final PFT. The Army BCT at Ft. Jackson with Standardized Training was the basis used to identify relevant variables. However, when these variables were used to predict the probability of failing the final PFT in other datasets (different training regimens and training centers), accuracy was substantially reduced. In some cases, the TIC analysis was unable to identify any recruits of high risk (noted with “unable to calculate”). Additional details about the datasets can be found in the appendix (bold letters indicate dataset).**

### 2.2.2 Common Variables Identified by TIC Analysis of Different Datasets

Each of the five datasets used in the validation analysis above (Table 3) was analyzed with a similar set of measures to determine if any variables were common to all datasets. Not all datasets contained education level or military service time so these were not included in the TIC analysis. In addition, several modifications were necessary for the MCRD-SD dataset. Pull-ups and crunches were substituted for push-ups and sit-ups, respectively, as the Marine Corps PFT test is slightly different than the Army counterpart. Also, the original final PFT failure rate was only 0.3% (2 out of 572), making a TIC analysis impossible. To account for this, the failing score was artificially raised until the failure rate matched the Army dataset (11.8%).

The results of applying a separate TIC analysis to each dataset can be found in Table 3. There is a substantial increase in the positive post-test probability for all datasets. The analysis consistently finds initial sit-ups and crunches as a predictor, suggesting that core strength is an important predictor physical fitness ability as it relates to the PFT.

Table 3. Independent TIC analysis results for five different sets of recruits.

<b>Prevalence</b>		<b>Positive Test Probability</b>
<b>Army BCT at Ft. Jackson with Traditional Training (F)</b>		
Male	13%	60%
	TIC identified:	Initial sit-ups < 22
Female	18%	58%
	TIC identified:	Initial sit-ups < 22
<b>Army BCT at various training centers with Traditional Training (G)</b>		
Male	16%	50%
	TIC identified:	Initial sit-ups < 12
Female	21%	53%
	TIC identified:	Initial sit-ups < 13
<b>Marine Corp BCT at MCRD-SD (E)</b>		
Male	12%	60%
	TIC identified:	Initial pull-ups < 2 Initial crunches < 34 Initial runtime > 12.01 min for 1.5 miles Height > 71.5 inches

**The common variable identified is sit-ups/crunches, suggesting that core strength is important for passing the final PFT. Additional details on these datasets can be found in the appendix. Additional details about the datasets can be found in the appendix (bold letters indicate dataset).**

## 2.3 Discussion

The purpose of the TIC analysis is to classify individuals into two different groups, whose likelihood of a desired outcome is different (high or low risk). In the preceding analysis, failing the final PFT was used but injury likelihood would also be an appropriate outcome to predict using TIC.

There are several advantages and disadvantages to using the TIC approach. A feature is that it is an established, objective approach, commonly used in the evaluation of medical diagnostic tests. In addition, because it is statistically-based, this method can quantify the accuracy of the prediction easily. The major short coming of the TIC (or any other statistical approach) is that the prediction is not applicable to new situations, such as different training regimens, as was demonstrated above.

For BCT, where there are different training regimens at different physical locations, a model-based approach has the potential to be more robust, as it is based on the physical and biological mechanisms of performance and injury. A more robust method would be of value to the military in optimizing training and maximizing recruit potential.

### 3. Model Development

Having established that a statistically-based method such as TIC is not robust because it does not account for training differences such as regimen, we develop more appropriate models that can account for these differences. The initial effort was spent on developing a predictive model for run performance. In addition, an acute/mishap model was also developed. This section describes the work done on both of these models.

#### 3.1 Run Performance Prediction Model

Run performance was chosen as the initial performance exercise to predict because of the large body of gait research found in the literature. The purpose of this section is to describe model development and validate the model by comparing its accuracy to the TIC method.

##### 3.1.1 Literature Review

A performance model literature review was performed (Table 4). Additional literature was found on other performance models but was not chosen for the model work described in this document and is, thus, excluded in the literature review for brevity.

Table 4. Performance model literature review summary.

Source	Data Summary
(Morton et al. 1990)	“Banister” model. Uses exponential decay fitness and fatigue components with reasonable results.
(Busso 2003)	Banister model with a time varying fatigue component to account for increased fatigue from multiple training sessions. Appears more realistic than previous versions.

**R. H. Morton, J. R. Fitz-Clarke, and E. W. Banister. Modeling human performance in running. J.Appl.Physiol. 69 (3):1171-7, 1990.**

In this model, referred to as the “Banister Model,” training is quantified using duration and heart rate and includes a weighting factor to emphasize high intensity training. The model has two components: fitness and fatigue. Both are exponential decay type equations that increase or reduce the ability to perform at a given time based on the current training dosage. See Figure 1.

In this model, training is quantified by a pseudointegral (training impulse based on minutes of exercise) where heart rate is normalized.

$$w(t) = D \left( \frac{HR_{ex} - HR_{rest}}{HR_{max} - HR_{rest}} \right) Y \quad (3.1)$$

where  $D$  is the duration of exercise,  $HR_{ex}$  is the average hear rate during exercise,  $HR_{rest}$  is the resting heart rate, and  $HR_{max}$  is the maximal HR. The weighting factor  $Y$  is to emphasize high intensity training and is defined as

$$Y = e^{bx} \quad (3.2)$$

where  $x$  equals the heart rate ratio term of Eq. (3.1) and  $b$  is a coefficient that depends on gender (1.92 for men and 1.67 for women).

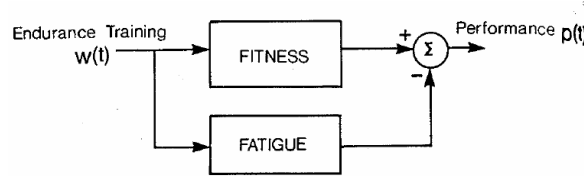


**Figure 1. Simple 2-component systems model of training and performance.**

**Diagram shows how training input sows  $w(t)$  affects both fitness and fatigue. The summer (S) combines these responses, fitness positively and fatigue negatively, into a single performance output  $p(t)$ .**

In the simplified model of Figure 1, two factors, fitness  $g(t)$  and fatigue  $h(t)$ , are recurrently affected each time training  $w(t)$  is undertaken, so that

$$g(t) = g(t-i)e^{-i/\tau_1} + w(t) \quad (3.3)$$

and

$$h(t) = h(t-i)e^{-i/\tau_2} + w(t) \quad (3.4)$$

where  $g(t)$  and  $h(t)$  are arbitrary fitness and fatigue response levels, respectively, at the end of day  $t$ ,  $i$  is the intervening period between the current days' training and that previously undertaken, and  $\tau_1$  and  $\tau_2$  are decay time constants of these respective effects.

Model performance at time  $t$ ,  $p(t)$ , is given by the simple linear difference

$$p(t) = k_1g(t) - k_2h(t) \quad (3.5)$$

where  $k_1$  and  $k_2$  are positive dimensionless weighting factors for fitness and fatigue, respectively.

In this study, the model had good predictive power for two subjects tested for maximal performance. The dosage was variable, not block and the training lasted 28 days. This was followed by a 50 day cessation of training (other than the performance tests). The model parameters were derived using a least-squares regression and were able to predict performance reasonably well ( $r^2 = 0.71$ ,  $p = 0.001$  and  $r^2 = 0.96$ ,  $p = 0.0001$  for the two subjects). Application of the model with the derived parameters to new subjects was not done. See Table 5 and Figure 2.



Table 5. Summary of model constants and statistics for least-squares regression of criterion performance on predicted performance.

Subject	$\tau_1$	$\tau_2$	$k_1$	$k_2$	$r^2$	$F$ Statistic	df	$P$	SE
<i>EWB</i>	50	11	1	1.8	0.71	59	4,21	$\leq 0.001$	$\pm 13$
<i>RHM</i>	40	11	1	2.0	0.96	252	4,18	$\leq 0.0001$	$\pm 7$

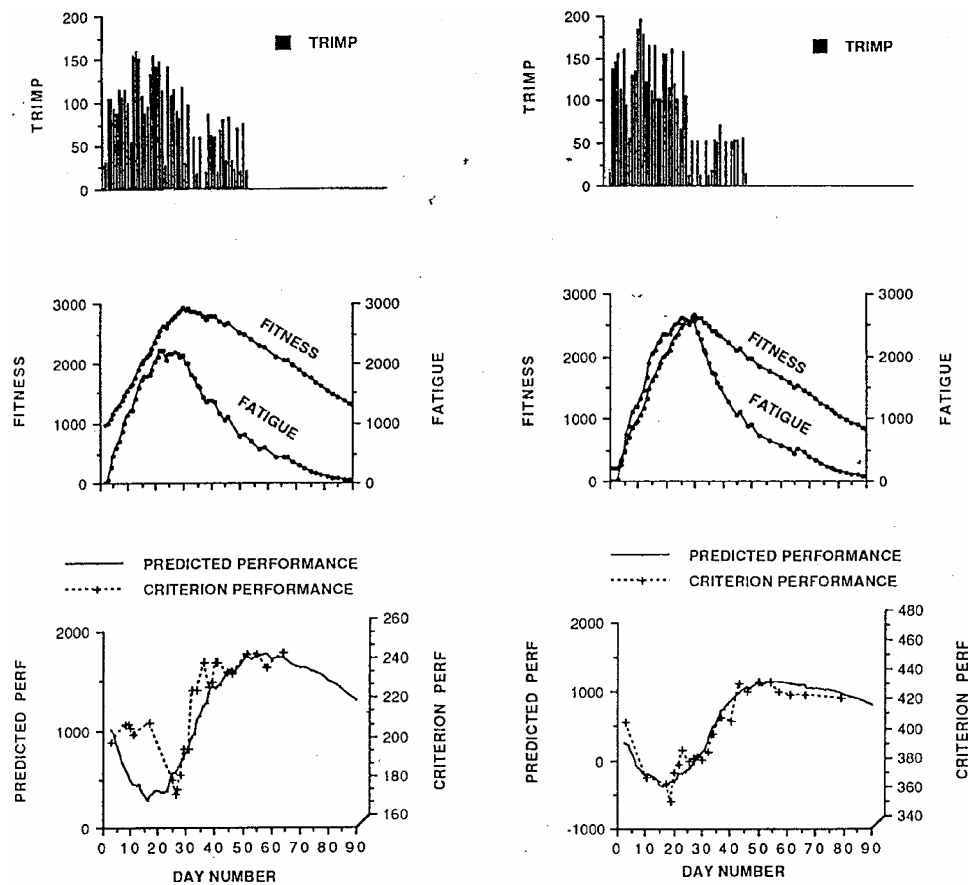


**Figure 2. Experimental results for 2 subjects, *EWB* (left) and *RHM* (right).**

**Top:** distribution of daily training impulse throughout training (28 days) and tapering phases of experiment. **Middle:** fitness and fatigue curves calculated from training impulse. These represent fitness and fatigue appropriate to a least-squares iterative matching of predicted to actual performance for each subject. **Bottom:** best matching of predicted and criterion performance scores from modeling process (solid and dashed lines, respectively). A good degree of fit may be observed.

**T. Busso. Variable dose-response relationship between exercise training and performance. Med.Sci.Sports Exerc. 35 (7):1188-1195, 2003.**

This article proposes a modification to the Banister model and tests it (and three previous variations) to a cycling ergometer training regiment. The model generally used in the literature was initially proposed by Banister et al.<sup>1</sup> This model is defined by a transfer function composed of two first-order filters characterized by the two gain terms  $k_1$  and  $k_2$ , and the two time constants  $\tau_1$  and  $\tau_2$  (Model 2-Comp). To test the statistical significance of the second component, the two-component model was compared with a systems model comprising only one first-order filter (Model 1-Comp) with an impulse response  $k_1 e^{-t/\tau_1}$ . Another third-order model (Model 3-Comp), proposed by Calvert et al.<sup>2</sup>, has two negative components and one positive component to single out the fatigue effect on the time course of training adaptation. The impulse response of this systems model is  $k_1(e^{-t/\tau_1} - e^{-t/\tau_1'}) - k_2 e^{-t/\tau_2}$ . For each model, the performance  $p(t)$  is obtained by the convolution product of the training doses  $w(t)$  with the impulse response added to basic level of performance noted  $p^*$ .  $W(t)$  is considered to be a discrete function, i.e., a series of impulse each day,  $w^i$  on day  $i$ . The convolution product becomes a summation in which model performance  $\hat{p}^n$  on day  $n$  is estimated by mathematical recursion from the series of  $w^i$ .  $\hat{p}^n$  is thus estimated for models used in this study as follows:

$$\text{Model 1-Comp: } \hat{p}^n = p^* + k_1 \sum_{i=1}^{n-1} w^i e^{-(n-i)/\tau_1} \quad (3.6)$$

$$\text{Model 2-Comp: } \hat{p}^n = p^* + k_1 \sum_{i=1}^{n-1} w^i e^{-(n-i)/\tau_1} - k_2 \sum_{i=1}^{n-1} w^i e^{-(n-i)/\tau_2} \quad (3.7)$$

$$\text{Model 3-Comp: } \hat{p}^n = p^* + k_1 \sum_{i=1}^{n-1} w^i \left[ e^{-(n-i)/\tau_1} - e^{-(n-i)/\tau_1'} \right] - k_2 \sum_{i=1}^{n-1} w^i e^{-(n-i)/\tau_2} \quad (3.8)$$

The model proposed in this study assumes that the gain term for the negative component is a state variable varying over time in accordance with system input. Performance output for the model proposed in this study is computed as follows:

$$\hat{p}^n = p^* + k_1 \sum_{i=1}^{n-1} w^i e^{-(n-i)/\tau_1} - \sum_{i=1}^{n-1} k_2^i w^i e^{-(n-i)/\tau_2} \quad (3.9)$$

in which, the value of  $k_2$  at day  $i$  is estimated by mathematical recursion using a first-order filter with a gain term  $k_3$  and a time constant  $\tau_3$

<sup>1</sup> BANISTER, E. W., T. W. CALVERT, M. V. SAVAGE, and T. BACH. A systems model of training for athletic performance. *Aust. J. Sports Med.* 7:57–61, 1975.

<sup>2</sup> CALVERT, T. W., E. W. BANISTER, M. V. SAVAGE, and T. BACH. A systems model of the effects of training on physical performance. *IEEE Trans. Syst. Man. Cybern.* 6:94–102, 1976.

$$k_2^i = \sum_{j=1}^i w^j e^{-(i-j)/t_3} \quad (3.10)$$

The daily training quantity was computed in arbitrary units from work done during training sessions and trials. The work done during warm-up and recovery was not considered in the computation. The tests to measure  $P_{lim5'}$  (average power during a 5 minute all-out cycling ergometer exercise) and  $\dot{V}O_{2max}$  were both arbitrarily ascribed to 100 training units (t.u.). Each 5-min bout of exercise for training sessions was weighted by intensity referred to  $P_{lim5'}$  (i.e., mean power output/ $P_{lim5'} \times 100$ ). A training session composed of four bouts of exercise at 85% of  $P_{lim5'}$  would be thus ascribed to  $4 \times 85 = 340$  t.u. The regiment for this experiment consisted of 2 weeks of performance measures only (no training) 8 weeks of 3 sessions/week of training, a week of performance testing only, followed by 4 weeks of 5 sessions/week and another two weeks of performance testing only.

The results show that the most accurate version contains a fatigue component varying in time to account for increases in the fatigue effect from repeated training sessions (Proposed Model, Table 6). However, the accuracy of this model under different training regiments is unknown.

Table 6. Indicators of goodness-of-fit of performance for various systems models of training effects.

Subject No.	N	Model-1Comp df = 2		Model-2Comp df = 4		Model-3Comp df = 5		Proposed Model df = 5	
		Adj.R <sup>2</sup>	SE	Adj.R <sup>2</sup>	SE	Adj.R <sup>2</sup>	SE	Adj.R <sup>2</sup>	SE
1	45	0.920	7.91	0.933*	7.26	0.933	7.26	0.958†,‡	5.73
2	45	0.883	10.97	0.896	10.37	0.897	10.25	0.954†,‡	6.86
3	40	0.807	12.35	0.817	11.98	0.816	12.04	0.947†,‡	6.43
4	45	0.815	10.51	0.850*	9.42	0.850*	9.43	0.931†,‡	6.39
5	46	0.860	9.13	0.943†	5.84	0.943†	5.83	0.944†	5.79
6	45	0.858	10.98	0.871	10.46	0.873	10.40	0.931†,‡	7.63
Mean ± SD		0.857 ± 0.042	10.31 ± 1.56	0.885 ± 0.048	9.22 ± 2.27	0.885 ± 0.049	9.20 ± 2.27	0.944 ± 0.011	6.47 ± 0.71

Model-1Comp, model using one first-order component; Model-2Comp, model using two first-order components; Model-3Comp, model using one first-order component and one second-order component; proposed model, model proposed in this study with two components where the gain term for negative component varies by using one further first-order filter; N, number of measurements of performance; Adj.R<sup>2</sup>, adjusted coefficient of determination; SE, standard error. Statistical difference from Model-1Comp: \*  $P < 0.05$ ; †  $P < 0.001$  and from Model-2Comp: ‡  $P < 0.001$ .

### 3.1.2 Methods

#### Model

There are several characteristics of a performance model that must be incorporated in order for it to be functional under a wide range of conditions. The model output must be bounded with a limit on the maximum and minimum values so that impossibly fast or slow (e.g., negative velocity) situations are not predicted. In addition, the output should be asymptotic, approaching high fitness slowly since it is well established that smaller performance gains are made as fitness improves. Finally, the model needs to be simple

since there are a limited number of measurements made (PFT runtimes) during a training regimen from which the model may be fit and parameters estimated.

The literature review above suggests that a “Banister-type” two-component model (performance enhancement and fatigue) would be ideal. However, since this would require four parameter estimates and fatigue is a short-term effect which is of limited interest, a single-component model without fatigue was developed. The performance model chosen is:

$$P = P_0 + (P_{\max} - P) g_1 \otimes W \quad (3.11)$$

where  $P$  is normalized performance,  $P_0$  is initial or pre-training performance,  $P_{\max}$  is an individual's maximum  $P$ ,  $g_1$  is the performance enhancement component,  $W$  are daily training dosages, and  $\otimes$  is the convolution function. Additional details on each of the model variables are discussed below.

### **Performance, $P$ , Definition**

There are several requirements that dictate the form of performance  $P$ , the model prediction or output. Primarily,  $P$  must be based on a measurable event. This is to allow a numeric calculation and prediction value. In addition, it is well established that specific exercises influence performance differently depending on the event (e.g., swimming will not appreciably increase run performance) and a model based on an exact event can account for the effect of different exercises in the final performance prediction. In the model presented, the event is the final PFT run.  $P$  also needs to be bounded to prevent prediction of impossible performances. This is accomplished by defining  $P$  as normalized run velocity:

$$P = V_{\text{event}} / V_{\max} \quad (3.12)$$

where  $V_{\text{event}}$  is the final PFT run velocity and  $V_{\max}$  is the estimated World Record velocity for the final PFT run distance using the “Purdy Points System” (Gardner and Purdy 1970; Purdy 1974a; Purdy 1974b; Purdy 1975; Purdy 1977). Thus, if  $P$  is predicted from Eq.. (3.11) and  $V_{\max}$  is known, it is possible to predict  $V_{\text{event}}$ . Knowing the velocity and distance of the event, it is trivial to determine runtime, the usual measure of PFT run performance. Note that, by definition,  $P = 1$ , only for the World Record holder.

### **Initial Performance, $P_0$**

$P_0$  (Eq.. (3.11)) is the initial performance level of the recruit and is defined as:

$$P_0 = V_{\text{IST}} / V_{\max} \quad (3.13)$$

where  $V_{\text{IST}}$  is the initial PFT run velocity, which is calculated from runtime and distance. Since the initial PFT run is often a shorter distance than the final PFT, the following is

used to estimate the initial run time  $t_2$ , if the recruit had run at the longer final PFT distance for the initial PFT:

$$t_2 = t_1 \left( \frac{d_2}{d_1} \right)^{1.06} \quad (3.14)$$

where  $d_1$  and  $t_1$  are the measured initial distance and time, respectively, and  $d_2$  is the final PFT distance (Riegel 1981).

### **Maximum Performance Potential**

Like  $P_0$ ,  $P_{\max}$  is a normalized run velocity:

$$P_{\max} = \text{indiv } V_{\max} / V_{\max} \quad (3.15)$$

where  $\text{indiv } V_{\max}$  is an individual's maximum possible performance level achievable (i.e., not everyone has the capacity to train up to a performance level of 1) and is assumed to be an inherent, constant value attainable only with perfect training. To estimate  $\text{indiv } V_{\max}$ , the following assumptions are made. First, since runtimes for the 1.5-3 mile range of the PFT are greater than 6 minutes, this run is primarily a test of aerobic capacity. Second,  $\text{VO}_{2\max}$  (the maximum rate of oxygen consumption) is the gold-standard measure for aerobic capacity and is primarily dependent on hereditary factors (80-93% according to McArdle et al. 1991). To estimate  $\text{VO}_{2\max}$ , a nonexercise estimate was used for both male and females (George et al. 1997):

$$\text{Male: } \text{VO}_{2\max} = 67.350 + 1.921(\text{PA-R}) - 0.381(\text{age}) - 0.754(\text{BMI}) \quad (3.16)$$

$$\text{Female: } \text{VO}_{2\max} = 56.363 + 1.921(\text{PA-R}) - 0.381(\text{age}) - 0.754(\text{BMI}) \quad (3.17)$$

where PA-R is the NASA/Johnson Space Center Physical Activity Rating [0-7], age is in years, and BMI is body mass index. Since Eq.. (3.15) is based on a recruit's maximum theoretical velocity, PA-R was assumed to be 7. In addition,  $\text{VO}_{2\max}$  was increased by 15% for training effects (McArdle et al. 1991).  $\text{indiv } V_{\max}$  can then be estimated by determining the final PFT velocity that would give an individual's  $\text{VO}_{2\max}$  (Daniels 1979). Using this formulation,  $P_{\max}$  is estimated to be 0.6-0.8 for most subjects.

### **Training Dosage, W, Definition**

To formulate an algorithm estimating the effects of training, the following assumptions were made. First, the training dosage,  $W$  (Eq.. (3.11)), is exercise dependent and that different exercises affect performance differently. Second, the dosage rate is nonlinear and limited, to reflect the inability to sustain high power anaerobic/sprint exercises. Note that this does not limit the overall amount of  $W$  since dose rate is multiplied by time to give dose.

As reviewed earlier, previous models found in the literature use work on a cycle ergometer (Busso 2003) or normalized heart rate (Morton et al. 1990) as a quantifiable dosage measure. Morton et al. (1990) also accounted for anaerobic effects with a lactate threshold factor (Eqs. (3.1)-(3.2)). Not having access to either work or heart rate, rate of oxygen consumption or  $\text{VO}_2$  was chosen instead since it is well established that heart rate and  $\text{VO}_2$  are linearly related (e.g., McArdle et al. 1991).

$W$  was based on the work of Morton et al. (1990), replacing heart rate with oxygen consumptions measures in Eqs. (3.1)-(3.2):

$$W = W_{\text{rate}} \times \text{duration} \times e^{bW_{\text{rate}}} \quad (3.18)$$

where  $W_{\text{rate}}$  is bound by normalizing  $\text{VO}_2$  using  $\text{VO}_{2\text{max}}$  and resting metabolic rate ( $RMR$ ),

$$W_{\text{rate}} = \frac{(\text{VO}_2 - RMR)}{(\text{VO}_{2\text{max}} - RMR)} \quad (3.19)$$

duration is time in minutes, and  $b$  is the lactate threshold factor used by Morton et al. (1990), 1.92 and 1.67 for men and women, respectively. Since  $\text{VO}_2$  is dependent on the exercise and intensity, it was assumed that only walking/marching and running had a significant training affect on final runtime performance.  $\text{VO}_2$  estimates for walking and running were calculated from the regressions developed by Epstein et al. (1987) and Pandolf et al. (1977), which estimates  $\text{VO}_2$  for walking and running under different velocities, terrain, grade, and load carriage conditions.  $RMR$  was estimated using the popular Harris-benedict equations (Harris and Benedict 1919).

To calculate dosage,  $W$ , for a given subject on a given day, a subject's  $W_{\text{rate}}$  and duration was calculated for each exercise (walking or running). All  $W$  for a given day was summed for a recruit's final daily total.

### Model Parameters for $g_1$

The final model parameters needed to compute  $P$  (Eq. (3.11)) are the coefficients in the performance enhancement component,  $g_1$ , which is defined in a similar manner to Eq. (3.3) of Morton et al. (1990):

$$g_1 = k_1 e^{-t/\tau_1} \quad (3.20)$$

where  $t$  is time (days),  $k_1$  is a linear coefficient (unitless) and  $\tau_1$  is a time constant (days).

Under ideal conditions, military datasets containing training regimens and initial and final PFT runtimes could be used to determine  $k_1$  and  $\tau_1$ . However, since recruits are not required to run maximally, but only to pass the maximum allotted runtime, the final PFT run does not appear to represent an objective measure of training enhancement. Therefore, a literature review was conducted and  $k_1$  was estimated using running studies where the

training protocol and changes in performance were measured (Table 7).  $\tau_1$  was assumed to be 40 days, a value estimated by Busso (2003) using a similar model. From the literature review, the average  $\pm$ s.d. value for  $k_1$  was found to be  $(1.84 \pm 1.86) \times 10^{-4}$ . A value of  $2.0 \times 10^{-4}$  was found to predict the final PFT run failure rate similar to the observed failure rate for both Army and Marine Corps datasets, which is within the range of values seen in the literature.

Table 7. Estimates of  $k_1$  from running studies found in the literature.

<b>Source</b>	<b><math>k_1</math></b>
(Flynn et al. 1998)	$1.1314 \times 10^{-4}$
(Smith et al. 1999)	$4.5431 \times 10^{-4}$
(Loy et al. 1993)	No ht, wt given
(Mutton et al. 1993)	$1.5991 \times 10^{-4}$
(Foster et al. 1995)-Run	$7.0655 \times 10^{-5}$
(Foster et al. 1995)-Control	$8.4935 \times 10^{-6}$
(Burtcher et al. 1996)	Only 12 days
(Smith et al. 2003)-T70	$4.065 \times 10^{-5}$
(Smith et al. 2003)-T60	$2.4045 \times 10^{-4}$
(Houmard et al. 1994)	Only 7 days
<b>Mean</b>	<b><math>1.84 \times 10^{-4}</math></b>
<b>SD</b>	<b><math>1.86 \times 10^{-4}</math></b>

For the Eq. (3.20),  $k_1$  was assumed to be  $2.0 \times 10^{-4}$  based on this review.

### Analysis Procedure

Having described the algorithm used to estimate run performance (see Figure 3), we can now proceed with predicting final PFT runtimes and whether a recruit's performance is adequate to pass. Of interest is not only the model's ability to predict a runtime, but the accuracy of the prediction compared to other methods. Thus, the model is compared to the Test Index Cluster (TIC) method described previously.

The datasets chosen are the male and female recruits that underwent Army BCT at various training centers. Unfortunately, details of the Non-Standardized BCT regimen are unknown at this time. However, the Standardized BCT regimen produced similar training effects (Knapik et al. 2004) and, thus, was assumed to be equivalent for the purposes of calculating training dose. Additional details on the datasets can be found in the appendix (Dataset G).

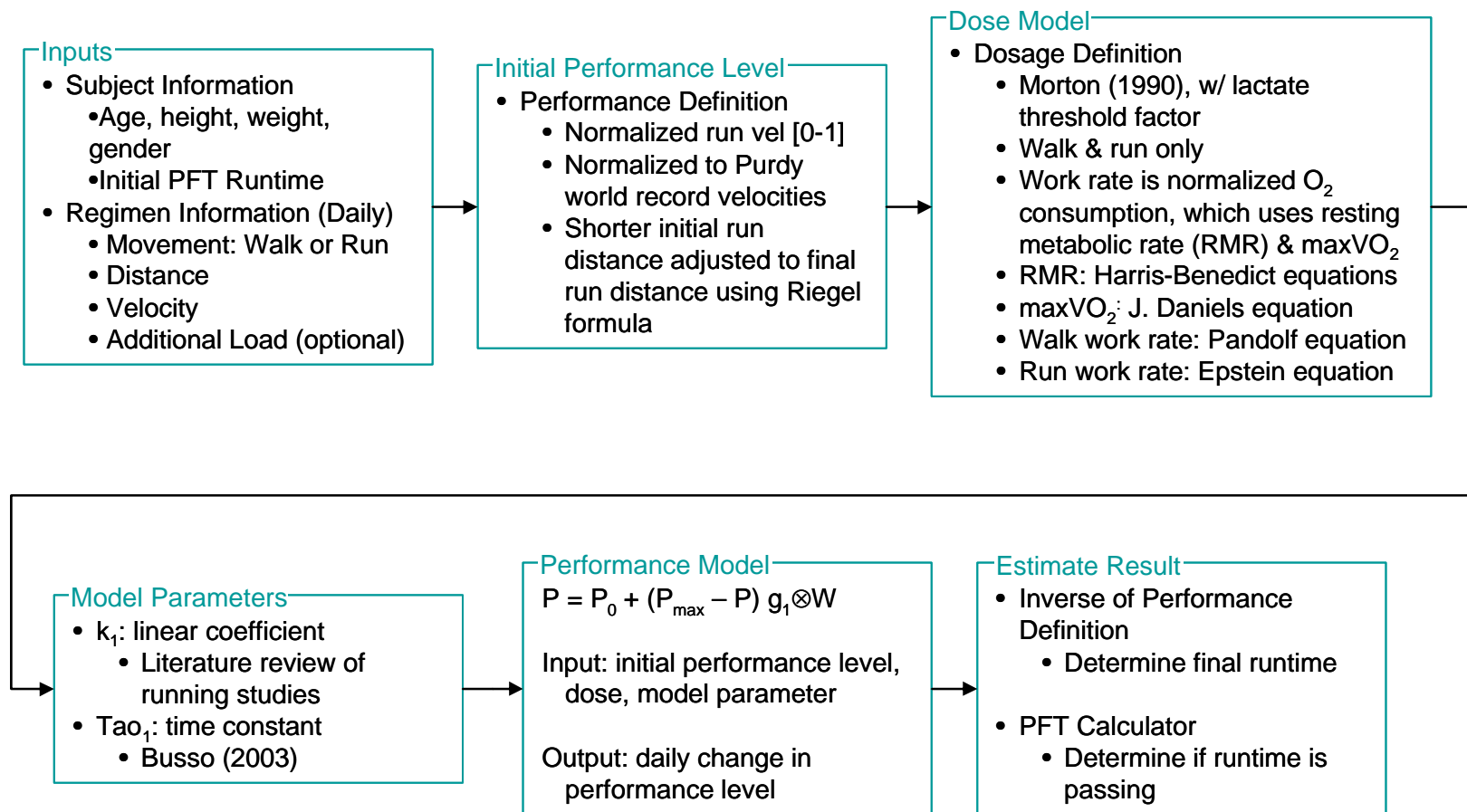


**Figure 3. A summary diagram of the run performance algorithm.**



For both the model and the TIC comparison, subject height, weight, and gender as well as initial PFT push-ups, sit-ups, and runtimes were used. A separate TIC analysis was performed for each gender whereas the model used different algorithms to account for gender. Both the TIC and model predicted final PFT run pass or fail, which could be compared to each recruit's actual performance to determine accuracy.

### 3.1.3 Results

#### Male Recruits

The initial prevalence (overall failure rate) was 4% for the males on the final PFT run. The TIC analysis identified only initial PFT runtime as a significant predictor, with a time of 20:17 or slower. Both the TIC and model predictions are comparable, with similar diagnostic accuracy (88% for TIC and 84% for the model) and positive post-test probabilities (Table 8).

Table 8. A comparison of the accuracy of a Test Index Cluster (TIC) analysis to that of the run performance model for male recruits undergoing basic combat training at various Army training sites.

TIC	Final PFT Run	
	Fail	Pass
IST Run > 20:17	9	47
IST Run < 20:17	11	428

Model	Final PFT Run	
	Fail	Pass
Predict Fail	10	67
Predict Pass	10	409

**For the TIC, one item was identified: a runtime > 20:17 on the initial PFT run. A recruit with this item had a significantly greater chance of failing the final PFT (Sensitivity = 0.45; Specificity = 0.90; Positive pretest probability = 4%; Positive post-test probability = 16%; Negative post-test probability = 3%). For the performance model, accuracy was similar (Sensitivity = 0.50; Specificity = 0.86; Positive pretest probability = 4%; Positive post-test probability = 13%; Negative post-test probability = 2%).**

#### Female Recruits

The initial prevalence (overall failure rate) was 8% for the females on the final PFT run. The TIC analysis identified only initial PFT runtime as a significant predictor, with a

time of 22:55 or slower. Both the TIC and model predictions are comparable, with similar diagnostic accuracy (80% for TIC and 87% for the model) and positive post-test probabilities (Table 9).

Table 9. A comparison of the accuracy of a Test Index Cluster (TIC) analysis to that of the run performance model for female recruits undergoing basic combat training at various Army training sites.

TIC	Final PFT Run	
	Fail	Pass
IST Run > 22:55	7	39
IST Run < 22:55	14	202

Model	Final PFT Run	
	Fail	Pass
Predict Fail	4	18
Predict Pass	17	237

**For the TIC, one item was identified: a runtime > 22:55 on the initial PFT run. A recruit with this item had a significantly greater chance of failing the final PFT (Sensitivity = 0.33; Specificity = 0.84; Positive pretest probability = 8%; Positive post-test probability = 15%; Negative post-test probability = 6%). For the performance model, accuracy was similar (Sensitivity = 0.19; Specificity = 0.93; Positive pretest probability = 8%; Positive post-test probability = 18%; Negative post-test probability = 7%).**

### 3.1.4 Discussion

For both the male and female datasets, the run performance model prediction accuracy was comparable to a TIC analysis when subject height, weight, and gender as well as initial PFT push-ups, sit-ups, and runtimes were used. Thus, the model gives reasonable results using parameters and values found in the literature and suggests that the model has the potential to predict PFT runtimes accurately. Unlike a TIC analysis, however, the model does not require a separate independent analysis for each different condition. This robustness is demonstrated by using the same model for both male and female recruits and still having reasonable results compared to two independent TIC analyses.

In the previous TIC analyses (Table 1 and Table 2), accuracy was substantially better. This was due to the addition of several more variables in the analysis such as age and the prediction of not just runtime but total final PFT failure. We anticipate that additional measures such as pre-fitness and smoking history questionnaire data as well as health risk

behavior and psychological information will improve both the TIC and model accuracy for final PFT runtime prediction. A major benefit of the model is that it has been designed to be able to account for regimen differences. Unfortunately, the incomplete training regimen information used in the current model limits the accuracy to the same level as a TIC analysis.

### **3.2 Acute/Mishap Injury Prediction Model**

Acute or mishap injuries are a specific set of injuries common to large training regimen protocols such as a military's BCT program. This type of injury was chosen because the random nature of the injury suggests a simple statistical model may be developed easily. The purpose of this section is to describe the initial model development.

#### **3.2.1 Literature Review**

While most literature focuses on overuse injury, there is some support that there are multiple factors contributing to the likelihood of sustaining an acute injury during military life. These include the amount of physical training such as vigorous activity (Almeida et al. 1999) and running distance (Jones et al. 1994; Jones and Knapik 1999), as well as recreational sports (Lauder et al. 2000). In addition, military occupational specialty was also found to be a factor, with more physically active occupations having a higher risk (Foulkes 1995). Nonactivity related factors include being previously injured (Evans et al. 2005) and psychological factors (Gregg et al. 2002).

#### **3.2.2 Methods**

##### **Preliminary Analysis**

The initial dataset chosen to explore the nature of this injury was the dataset where recruits undergoing Army BCT at various training centers were monitored and the week of injury occurrence noted. An acute injury was limited to the lower body (pelvis, leg, or foot) and defined as a strain/sprain, sudden fracture, dislocation, tear, contusion, or laceration. Out of 1,019 recruits, 213 injuries were reported (prevalence of 21%) (See Appendix A, Dataset G).

As noted previously, a t-test is the first step of a TIC analysis and this was used to compare injured to noninjured for a wide variety of measures (Table 10). Unlike the studies reported in the literature, no significant differences were found for these measures suggesting that an acute/mishap injury is predominantly random in this group. Thus, neither a TIC analysis nor a physiologically-based injury model will be able to predict this type of injury from this dataset and a statistical approach was used.

Table 10. Variables used in a t-test to compare those that sustained an acute injury to those that did not.

<b>Subject Characteristics</b>	
	Gender, Height, Weight, Body Mass Index, Race, Smoking History
<b>Fitness</b>	
	Pre-fitness Level, Initial PFT Runtime, Push-ups, Sit-ups & Score
<b>Previous Injury</b>	
	Previous Civilian Injury, Previous BCT Injury
<b>Training Regimen</b>	
	Weekly Training Dose (see pg. 15)

**No significant differences were found for a dataset containing recruits undergoing Army BCT at a variety of training centers (See Appendix: Dataset G).**

### Model

Having established that acute injuries are random for the dataset chosen, we assumed that the chance of injury each day is independent of other days and that injury follows a binomial distribution (either injured or not). Using the above dataset (213 injuries from 1019 recruits during 61 days of Army BCT), there is a 20.9% chance of injury per recruit or a  $p$  of 0.34%, the chance of injury per recruit per day). Since the probability of a recruit sustaining at least one injury during BCT is the complement of the probability of the recruit getting no injuries during BCT:

$$P_{\text{BCT}} = 1 - (1 - p)^n \quad (3.21)$$

where  $n$  is the number of days in BCT.

Binomial distribution properties allow the calculation of both the mean number of injuries expected:

$$N_{\text{BCT}} = n_{\text{subj}} \times P_{\text{BCT}} \quad (3.22)$$

and the standard deviation:

$$SD_{\text{BCT}} = \sqrt{n_{\text{subj}} \times P_{\text{BCT}} \times (1 - P_{\text{BCT}})} \quad (3.23)$$

where  $n_{\text{BCT}}$  is the number of recruits.  $P_{\text{BCT}}$  and  $SD_{\text{BCT}}$  can then be expressed as a percent of the population by dividing by the number of recruits.

### 3.2.3 Results

Due to time constraints, this model was not validated against additional datasets. Thus, future tasks include validating and refining the model against additional datasets and training regimens such as those described in the appendix.

### **3.2.4 Discussion**

Despite not validating the model, it is clear that there are several limitations to the statistical approach described primarily because none of the risk factors identified in the literature were found to be statistically significant for this dataset. Most notably, the calculated training dosage was not significantly higher on high injury days, which means that the current training regimen measure is not capturing the causes of acute injury. We hypothesize that the types of acute injuries are wide ranging (sprain, contusions, etc.) and will need to be treated separately before the risk factors found in the literature are revealed.

## 4. Software Application Development

The preliminary run performance and acute/mishap injury algorithms described previously were used as the basis for a web-based software to predict performance and injury. The initial version of the Training, Overuse Injury, and Performance (TOP) Model was implemented to demonstrate the feasibility of an “all-in-one” prediction tool to help in the design of training regimens and to identify individuals who may be at risk for injury or low performance because of the regimen. A flow diagram was designed prior to software development to insure that the TOP Model was modular, allowing updates to be easily incorporated. In addition, a key design element is that the large volume of data (training regimen and subject information) requires precise control over the flow of data (Figure 4).

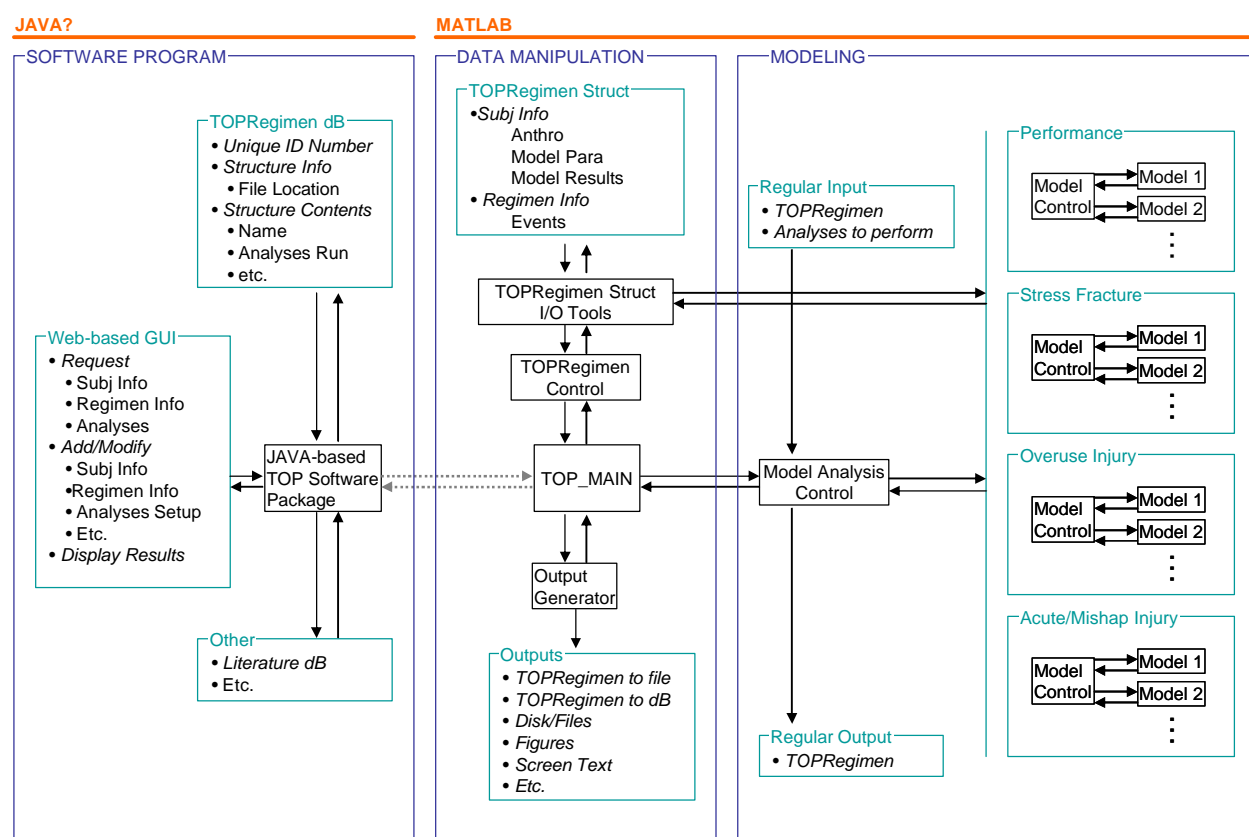



**Figure 4. TOP Model flow diagram.**

There are several design requirements for the TOP Model software. Because a key advantage of a model-based approach compared to a statistical analysis is the ability to account for different training regimens, an efficient graphical user interface (GUI) is needed to allow users to modify regimen definitions as they see fit. Also, model outputs should be easy to interpret, with an error range to allow user's to quickly ascertain model predictions. And finally, the software should be easy to use, with a simple step-by-step procedure to allow novice users to produce results quickly.

#### **4.1 Software Conceptual Design Images**

The following pages are conceptual design of the TOP Model software. Key features are highlighted with yellow callouts. Being unable to create a software program of this complexity in the time allotted, a simplified version was implemented. Screenshots of the functional preliminary software are shown on pages 34 through 37.



# TOP

## Training, Overuse Injury, and Performance Modeling

[Home](#) | [Account](#) | [TOP 0.1](#) | [Tools](#) | [Data](#) | [Document](#) | [Logout](#) | [Help](#)

TOP Assessment

Define New or Edit Subjects

Define New or Edit Regimens

Model Information

Welcome

The Training, Overuse Injury, and Performance Model (TOP) is a software framework for assessing the effects of training on performance and injury. This software will:

- Identify those who are at "high risk" of injury for a given training regimen
- Compare training regimens for differences in both performance and injury potential
- Recommend training regimens for those who at "medium risk" of injury to reduce their risk

It applies state-of-the-art biomechanical, computational, and statistical models to predict performance improvements and the likelihood of injury.

This site hosts the TOP web application software where users can define or select subject population parameters, define or select training regimens, and perform a prediction analysis.

TOP is developed and maintained under the sponsorship of USARIEM.

**How to use TOP 0.1**

To define subject characteristics, click [here](#) or on the "Define Subjects" on the left navigation bar and follow the instructions in the main work area.


To define a training regimen, click [here](#) or on the "Define Regimens" on the left navigation bar and follow the instructions in the main work area.

To start an TOP assessment project, click [here](#) or on the "TOP Assessment" on the left navigation bar and follow the instructions in the main work area.

Click [here](#) or on the "Document" on the top title bar to find related literature.

[Next](#)

All data, documentation and models accessible from a centralized location



# TOP

## Training, Overuse Injury, and Performance Modeling

[Home](#) | [Account](#) | [TOP 0.1](#) | [Tools](#) | [Data](#) | [Document](#) | [Logout](#) | [Help](#)

TOP Assessment

1. Select/Define TOP Project

2. Select Subjects

3. Select Regimen

4. Run TOP Analysis

5. Report

Define New or Edit Subjects

Define New or Edit Regimens

Model Information

Start a TOP Project

TOP Assessment interfaces will guide the user through the steps necessary to run a TOP prediction analysis and generate a report.

The following are needed before running a TOP Assessment:

- A TOP Project, which specifies the measures to be predicted.
- A population of subjects with defined or measured characteristics such as height, weight, and initial fitness. Characteristics depend on the Project specifications.
- A training regimen, which specifies the exercises done and intensity level of the exercises


**Tips**

- Step 1 (Select/Define TOP Project) has to be completed first
- Use the "Next" button or the links to complete the necessary steps
- Checkmarks (✓) indicated completed steps
- Click on "Report" to view previously archived TOP Assessment results

[Next](#)

Multiple methods to perform analysis allow users of differing familiarity to analyze the data





# TOP

## Training, Overuse Injury, and Performance Modeling

[Home](#) | [Account](#) | [TOP 0.1](#) | [Tools](#) | [Data](#) | [Document](#) | [Logout](#) | [Help](#)

TOP Assessment

1. Select/Define TOP Project
2. Select Subjects
3. Select Regimen
4. Setup Analysis Report
5. Run TOP Analysis
6. Report

Define New or Edit Subjects

Define New or Edit Regimens

Model Information

Instruction

Select an existing or create a new TOP Project. Selected projects can also be modified or deleted.

TPI Projects

New

New/Modify

Delete

Project Name	Description	Performance	Overuse Inj	Acute Inj
<input checked="" type="radio"/> MCRD-SD 2005 Analysis 1	BCT: MCRD-SD 2005	✓		
<input type="radio"/> Army-Ft Jackson 2003 Analysis 3	BCT: Ft Jackson 2003	✓	✓	✓
<input type="radio"/> MCRD-PI 1995 Analysis 1	BCT: MCRD-PI 1995		✓	✓

New

New/Modify

Delete


Print

Next >

Assessment settings saved in Projects for future retrieval, review, and modification

All steps involved in assessment clearly shown

Specify assessments to be done



# TOP

## Training, Overuse Injury, and Performance Modeling

[Home](#) | [Account](#) | [TOP 0.1](#) | [Tools](#) | [Data](#) | [Document](#) | [Logout](#) | [Help](#)

TOP Assessment

1. Select/Define TOP Project
2. Select Subjects
3. Select Regimen
4. Run TOP Analysis
5. Report

Define New or Edit Subjects

Define New or Edit Regimens

Model Information

Instruction

Select the analyses to perform.

TOP Project Setup

Cancel

Save

Project Name:

Project Description:

Analysis Categories

Performance

Overuse Injury

Mishap/Acute Injury

☒ FPFT
☒ Run
☐ Upper Body Strength
☐ Core Strength

☒ Stress Fracture
☒ Lower Body
☐ Upper Body


☒ Lower Body
☐ Upper Body

Analysis Options

☒ Individual subject potential (red/yellow/green)
☐ Compare training regimens
☐ Evaluate pre-training exercises on subject potential (red/yellow/green)

Cancel

Save



## TOP

### Training, Overuse Injury, and Performance Modeling

Home | Account | TOP 0.1 | Tools | Data | Document | Logout | Help

**TOP Assessment**

1. Select/Define TOP Project ✓
2. **Select Subjects**
3. Select Regimen
4. Setup Analysis Report
5. Run TPI Analysis
6. Report

Define New or Edit Subjects

Define New or Edit Regimens

Model Information

**Instruction**

Select an existing or create a new set of subjects. Selected populations can also be modified or deleted.

---

**Subjects**


[New](#) [New/Modify](#) [Delete](#)

	Subject Populations	N	Gender	Description
<input checked="" type="radio"/>	MCRD-SD 2005	572	M	MCRD-SD males from 2005, performance measures only
<input type="radio"/>	Army-Ft Jackson 2003	934	M,F	Ft Jackson males and females from 2003
<input type="radio"/>	MCRD-PI 1995			
<input type="radio"/>	High BMI Females	1000	F	Virtual subjects with BMI > 30

[New](#) [New/Modify](#) [Delete](#)

"Regimens" web page would be similar to Subjects page

Subject and Regimen data can be imported from Excel spreadsheets



## TOP

### Training, Overuse Injury, and Performance Modeling

Home | Account | TOP 0.1 | Tools | Data | Document | Logout | Help

**TOP Assessment**

1. Select/Define TPI Project ✓
2. Select Subjects ✓
3. Select Regimen ✓
4. Setup Analysis Report ✓
5. Run TOP Analysis ✓
6. **Report**

Report Archive

Define New or Edit Subjects

Define New or Edit Regimens

Model Information

**About the TOP Assessment Report**

The following is the assessment predictions for the MCRD-SD 2005 project.

---

**Report Summary**

• Date of analysis: Tue Nov 15 18:28:24 PST 2005

• Project name: MCRD-SD 2005

Performance Improvement	37%
Overuse Injury Rate	10.7%
Mishap/Acute Injury Rate	24%
March Distance: Total	47 miles
Run Distance: Total	23 miles

• Click [here](#) for Performance Result details

• Click [here](#) for Overuse Injury Result details

• Click [here](#) for Acute Injury Result details

• Click [here](#) for Performance vs. Injury Cross-Analyses

Not shown: Customize report output

Not shown: Summary page contains links to more details for advance users

Not shown: Links to simple high/moderate/low output formats





# TOP

## Training, Overuse Injury, and Performance Modeling

- Home
- Account
- TOP 0.1
- Tools
- Data
- Document
- Logout
- Help

- TOP Assessment
- Define New or Edit Subjects
  - Subject List
  - Edit Individual Data**
- Define New or Edit Regimens
- Model Information

Instruction

Add or edit various subject data using the tabs and fields. For missing data, leave fields blank.

MCRD-SD 2005 Subject 001

**Import individual subject information**

Import Cancel Save

Anthropometry Bone Information Fitness & Performance Health & Lifestyle

Height (m)

Weight (kg)

Age (yrs)

Sex


Leg Length

Shoe Size

Edit additional subject information via tabs, e.g., Fitness, Behavioral, and Injury Questionnaire responses

TOTAL NUMBER OF SUBJECTS: 572

Import Cancel Save



# TOP

## Training, Overuse Injury, and Performance Modeling

- Home
- Account
- TOP 0.1
- Tools
- Data
- Document
- Logout
- Help

- TOP Assessment
- Define New or Edit Subjects
  - Subject List
  - Edit Statistical Distributions**
- Define New or Edit Regimens
- Model Information

Instruction

Create a new set of subjects or edit an existing set. Selected populations can also be modified or deleted. For a single individual's analyses, specify a population of one.

MCRD-SD 2005 Subject Statistical Distribution

Import Cancel Save

Anthropometry Bone Information Fitness & Performance Health & Lifestyle

	Mean	SD
Height (m)	<input type="text"/>	<input type="text"/>
Weight (kg)	<input type="text"/>	<input type="text"/>
Age (yrs)	<input type="text"/>	<input type="text"/>
Sex	<input type="text"/>	<input type="text"/>
Leg Length	<input type="text"/>	<input type="text"/>
Shoe Size	<input type="text"/>	<input type="text"/>

Enter desired mean, standard deviation and number of subjects for program to automatically generate a virtual population.

TOTAL NUMBER OF SUBJECTS:

Import Cancel Save



# TOP

## Training, Overuse Injury, and Performance Modeling

Home | Account | TOP 0.1 | Tools | Data | Document | Logout | Help

- TOP Assessment
- Define New or Edit Subjects
- Define New or Edit Regimens
- Model Information

Instruction

Create a new regimen or edit an existing one. Selected regimens can also be deleted.

Regimens


Report New New Study Delete

Name	Days	Branch	Description
<input checked="" type="radio"/> BCT: MCRD-SD 2005	84	MC	Daily running mileage for MCRD-SD
<input type="radio"/> BCT: Ft Jackson 2003	63	Army	Daily Exercises for Ft Jackson
<input type="radio"/> BCT: MCRD-PI 1995			

Report New New Study Delete

Report as hourly, daily or weekly schedules

Quickly import regimen data in Excel or other formats.



# TOP

## Training, Overuse Injury, and Performance Modeling

Home | Account | TOP 0.1 | Tools | Data | Document | Logout | Help

- TOP Assessment
- Define New or Edit Subjects
- Define New or Edit Regimens
- Model Information

Instruction

Create a new regimen or edit an existing one. Selected regimens can also be deleted.

BCT: MCRD-SD 2005

Report Cancel Save

Week 2: Live Fire Week

Select specific exercise...

	M	T	W	Th	F	S	Su
8:00							
10:00	Run				Run		
12:00							
14:00			PFT Test				
16:00						March	
18:00							

Run Distance  Duration   
Pace  Effort   
Footwear


Stretches Drills PFT's

Run March Wt Lifting

Run Sprint Ability Run Cross-Country

Parameters depend on exercise selected

...and drag to appropriate time



- TOP Assessment
- Define New or Edit Subjects
- Define New or Edit Regimens
- Model Information
  - Overview
  - Performance
  - Overuse Injury
  - Mishap/Acute Injury

**TOP**  
**Training, Overuse Injury, and Performance Modeling**

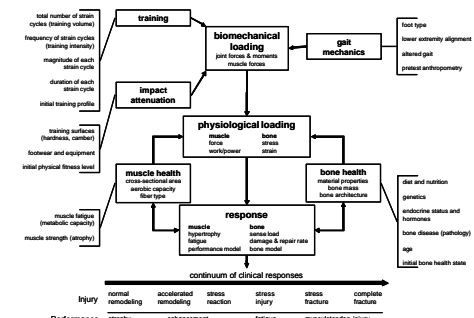
[Home](#) | [Account](#) | [TOP0.11](#) | [Tools](#) | [Data](#) | [Document](#) | [Logout](#) | [Help](#)

Introduction

The following models were used to for the TOP assessment.


Overview

The Training, Overuse Injury, and Performance Model (TOP) uses a mechanistic approach where external factors such as training regimen as well as internal variables such as fitness level are presumed to affect both performance and injury in a specific manner.



Performance Model

The performance component of the TOP model is based on the dose-response model described in Busso (2003). For the TOP model, dose is defined as the distance run or marched and the response is an increase in performance level.



Browse Database:

☐ All Literature

☐ Internal documents

☐ Journal papers

Search Database:

☐ Keyword

☐ Title


☐ Author

☐ Report number

**TOP**  
**Training, Overuse Injury, and Performance Modeling**

[Home](#) | [Account](#) | [TOP 0.1](#) | [Tools](#) | [Data](#) | [Document](#) | [Logout](#) | [Help](#)

Literature



Searchable database of all relevant documents

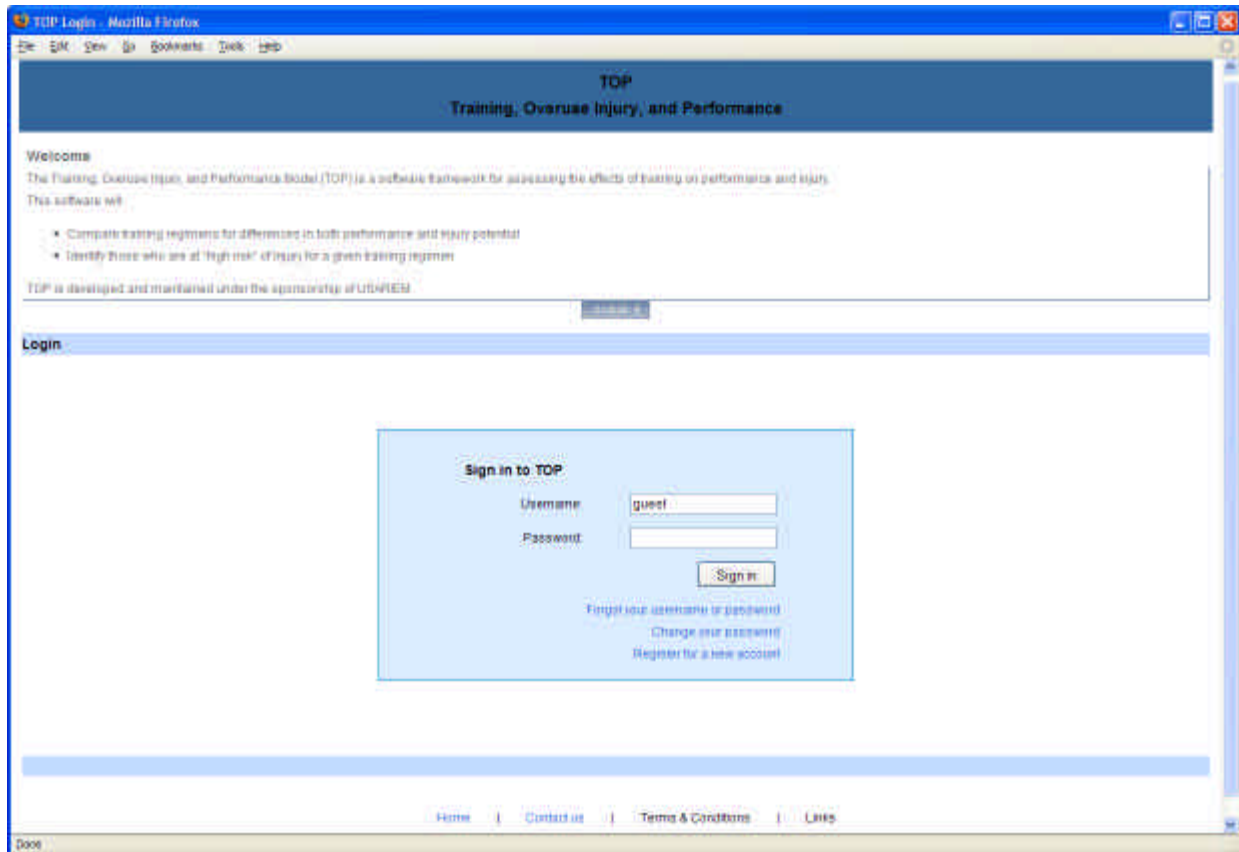
Instructions

The literature database allows the user to browse through the collection of documents or to search for a specific document.

- **Browsing**
  - To browse the entire collection of documents.
  - 1) Click the [All literature](#) box on the left side menu under the title Browse.
  - 2) Click the 'Start Browsing' button to retrieve list of documents for browsing.
- To browse a predefined subset of the entire document collection.
  - 1) Click the box next to the desired subset of documents (e.g., Technical reports).
  - 2) Click the 'Start Browsing' button to retrieve the subset of documents for browsing.
- **Searching**
  - To search for a specific document.
  - 1) Enter the search terms into the search box on the left side menu under the title Search.
  - 2) Select whether the search terms are related to the title, author, report number, or key words of the document.
  - 3) Click the 'Start Searching' button to retrieve the list of search results.
- **Literature Results**
  - Once the list of documents is retrieved, it is displayed as a list of references with hyperlinks to the abstract and full document. The results can be sorted according to author name, year, type of document, or report number. To sort the documents, choose the desired sorting method from the pull down menu on the right side of the page.


## 4.2 Preliminary Software Screenshots

The following are screenshots from the preliminary TOP Model software version. Note that not all functions have been built-in at this time but the run performance and acute/mishap models described earlier have been incorporated.



Training, Overuse Injury, and Performance - Mozilla Firefox

File Edit View Go Bookmarks Tools Help



Introduction  
Select Training Regimen  
Select Subject Population  
Select & Run Analysis  
Results

**TOP**  
**Training, Overuse Injury, and Performance**

Home | Document Logout Help

**Instruction**

The Training, Overuse Injury, and Performance Model (TOP) is a software framework for assessing the effects of training on performance and injury risk.

- Compare training regimens for differences in both performance and injury potential
- Identify those who are at "high risk" of injury for a given training regimen

**Start a TOP Simulation**

The TOP software interface will guide the user step-by-step to setup and run a training simulation. The following are needed before running a TOP simulation:

- Predefined training regimen(s) in Excel format. Existing regimens available for analysis are cataloged by the software. Additional regimens can be imported as well.
- Predefined subject information in Excel format. Existing subjects available for analysis are cataloged by the software. Additional files can be imported as well.

**Tips**

Simply click on "Next" after completing each step to ensure all steps are completed.  
Click on the links to the left at anytime to access the different steps.  
Click on the "Expand" tab for additional information about each step.

The TOP algorithm takes into account both training regimen and subject characteristics. Regimens are characterized by the amount of daily marching and running. Subject measures such as height, weight, and fitness ability are also accounted for.


The performance model(s) are based on algorithms shown to predict changes in performance with exercise, which have been published in the literature. Similarly, the overuse injury and stress fracture algorithms are based on known biological mechanisms leading to tissue damage, as published in the literature. The metaprocessor requires one assumed to primarily be random events and injury rates are based on statistical methods.

Additional details can be found in the "Expand" tabs throughout this program and in the Literature Database.

Next >

Training, Overuse Injury, and Performance - Mozilla Firefox

File Edit View Go Bookmarks Tools Help



Introduction  
Select Training Regimen  
Select Subject Population  
Select & Run Analysis  
Results

**TOP**  
**Training, Overuse Injury, and Performance**

Home | Document Logout Help

**Instruction**

Select existing regimen(s) or import additional ones to be analyzed. Select regimen(s) by marking the check box.

See RegimenExample.xls for an Excel file properly formatted for a training regimen.

Each training is reported by exercise, with different exercises requiring different measures (number of repetitions, speed, distance, etc.). In addition, specific days are specified where initial performance measures are measured and final measures are predicted, such as the initial PFT and CPFT, respectively.

Regimens

Excel Import < Previous Next >


	Name >	Days >	Branch >	Description >
<input type="checkbox"/>	Amy Standardized BCT	61	US Army-BCT	Standardized Training (CHPPM No. 12-HF-67728-04)
<input checked="" type="checkbox"/>	Marine BCT	85	US Army-BCT	2003 Training Regimen Estimate

Excel Import < Previous Next >



Training, Overuse Injury, and Performance - Mozilla Firefox

File Edit View Go Bookmarks Tools Help



Introduction  
Select Training Regimen  
Select Subject Population  
Select & Run Analysis  
Results

TOP  
Training, Overuse Injury, and Performance

Home | Document Logout Help

Instruction

Select an existing population or import a new set of subjects. Only one population may be analyzed at a time.  
The population dataset consists of individuals with known measures such as height, weight, and initial fitness level. These are used in conjunction with the training regimen to predict performance and injury potential on an individual basis.

Subject


Exit Report Previous Next

Subject Population	N	Description
<input type="radio"/> HCMO-All	1018	Henderson Combat Medic Data 97 - All Subjects
<input type="radio"/> HCMO-F	336	Henderson Combat Medic Data 97 - Females Only
<input checked="" type="radio"/> HCMO-M	681	Henderson Combat Medic Data 97 - Males Only
<input type="radio"/> max	85	
<input type="radio"/> MCRD-SD	571	MCRD-SD 2005 Recruits

Exit Report Previous Next

Training, Overuse Injury, and Performance - Mozilla Firefox

File Edit View Go Bookmarks Tools Help



Introduction  
Select Training Regimen  
Select Subject Population  
Select & Run Analysis  
Results

TOP  
Training, Overuse Injury, and Performance

Home | Document Logout Help

Instruction

Select one or more different analysis categories and analysis options. Selected categories have not yet been implemented. Click them to begin simulation.

Confirm and Run Analysis

Please wait: 20 % completed

Analysis Categories

Performance Overuse injury MenapAcute injury

☐ FPFT-Score ☐ Lower Body ☒ Lower Body

☒ FPFT-Run ☐ Upper Body ☐ Upper Body

☐ Upper Body Strength ☐ Stress Fracture

☐ Core Strength

Analysis Options


☒ Population Results

☐ Identify high risk individuals

Run Stop

Training, Overuse Injury, and Performance - Mozilla Firefox

File Edit View Go Bookmarks Tools Help



Introduction  
Select Training Regimen  
Select Subject Population  
Select & Run Analysis  
Results

**TOP**  
Training, Overuse Injury, and Performance

Home | Document Logout Help

About the TOP Assessment Report  
The following is the assessment predictions for the specified population and regimen.

**Summary** [Previous](#)

Regimen Information

- name: Marine BCT
- description: 2003 Training Regimen Estimate

Subject Information

- Population Name: HCMO-M
- Description: Henderson Combat Medic Data 97 - Males Only

Analysis Categories

- Lower Body
- FPFT-Run

Analysis Options

- Identify high risk individuals
- Population Results

Population Results

	Marine BCT
FPFT Run-Overall Fail, Pred Rate	15.0 %
Lowbody Acute inj-Overall Inj, Pred Rate	25.2±1.5 %
FPFT Run-Pct at High Risk (fail odds: >10%)	99.6 %
FPFT Run-Pct at Low Risk (fail odds: <5%)	0.4 %

Done

## 5. Key Accomplishments

We have:

- Developed a run performance model based on concepts reported in the literature
- Developed a probability-based lower-body acute/mishap injury model
- Created a conceptual design of the Training, Overuse Injury, and Performance (TOP) Model and implemented a simplified version
- Acquired and organized multiple datasets which are used for model development and validation

## 6. Reportable Outcomes

We have shown:

- Run performance changes due to military training can be modeled effectively using algorithms and parameters based on those found in the literature.
- A run performance model has the potential to predict outcomes for different training situations while being more robust since it can maintain the same level of accuracy as a statistically-based approach.
- If acute/mishap injuries are random, they can be modeled using a probability-based approach.
- It is feasible to create a user friendly software program to run different performance and injury models, allowing users to quickly modify training protocols and determine the effect.

## 7. Conclusions

This document describes the work in developing a prediction software package (TOP Model) that can account for different populations and training regimens, which may be of use to the military community, where maximizing performance while minimizing injury for a large population is important. In the initial version of the software, run performance and acute/mishap injuries were modeled. Unlike most statistically-based algorithms, the models included a training “dosage” to account for different regimens. The preliminary results suggest that this approach is as accurate as a statistical method but with the added advantage of being more robust. The TOP Model has the ability to make accurate predictions under a wider range of training situations.

Despite these initial achievements, there are several limitations to the software that will need to be addressed in the future. The current version of the TOP Model software lacks some key features including the ability to easily modify subject and regimen parameters. As the software becomes more evolved into a final product, a user’s manual and demonstration datasets will also be needed. Current limitations to the regimen-based algorithms include the lack of validation against additional datasets due to low quality regimen data and the incorporation of only a few known risk factors. Overuse injury and stress fracture algorithms have not yet been developed as well. The following future tasks should address some of these limitations:

- Validate run performance model with additional datasets
- Validate acute/mishap injury model with additional datasets
- Develop an overuse injury model
- Acquire additional datasets for further model development and validation
- Update TOP Model software and documentation based on user feedback.

## 8. Literature

- Allison, S. C., Knapik, J. J., Creedon Jr., J. F., and Sharp, M. A. (2005). "Development Of Test Item Clusters For Predicting Negative Outcomes In Basic Combat Training." U.S. Army Research Institute of Environmental Medicine, Natick, MA. Personal communication.
- Almeida, S. A., Williams, K. M., Shaffer, R. A., & Brodine, S. K. (1999). "Epidemiological patterns of musculoskeletal injuries and physical training." Med Sci Sports Exerc **31**(8): 1176-82.
- Burtscher, M., Nachbauer, W., Baumgartl, P., & Philadelphia, M. (1996). "Benefits of training at moderate altitude versus sea level training in amateur runners." Eur J Appl Physiol Occup Physiol **74**(6): 558-563.
- Busso, T. (2003). "Variable dose-response relationship between exercise training and performance." Med Sci Sports Exerc **35**(7): 1188-1195.
- Daniels, J. (1979). Oxygen power: Performance tables for distance runners Unknown binding, J. Daniels and J. Gilbert.
- Epstein, Y., Stroschein, L. A., & Pandolf, K. B. (1987). "Predicting metabolic cost of running with and without backpack loads." Eur J Appl Physiol **56**(5): 495-500.
- Evans, R., Reynolds, K., Creedon, J., & Murphy, M. (2005). "Incidence of acute injury related to fitness testing of U.S. Army personnel." Mil Med **170**(12): 1005-1011.
- Flynn, M. G., Carroll, K. K., Hall, H. L., Bushman, B. A., Brolinson, P. G., & Weideman, C. A. (1998). "Cross training: indices of training stress and performance." Med Sci Sports Exerc **30**(2): 294-300.
- Foster, C., Hector, L. L., Welsh, R., Schrager, M., Green, M. A., & Snyder, A. C. (1995). "Effects of specific versus cross-training on running performance." Eur J Appl Physiol Occup Physiol **70**(4): 367-372.
- Foulkes, G. D. (1995). "Orthopedic casualties in an activated National Guard Mechanized Infantry Brigade during Operation Desert Shield." Mil Med **160**(3): 128-31.
- Gardner, J. B. & Purdy, J. G. (1970). "Computer generated track scoring tables." Med Sci Sports **2**(3): 152-161.
- George, J. D., Stone, W. J., & Burkett, L. N. (1997). "Non-exercise VO<sub>2</sub>max estimation for physically active college students." Med Sci Sports Exerc **29**(3): 415-423.
- Gregg, R. L., Banderet, L. E., Reynolds, K. L., Creedon, J. F., & Rice, V. J. (2002). "Psychological factors that influence traumatic injury occurrence and physical performance." Work **18**(2): 133-139.

- Harris, J. & Benedict, F. (1919). A biometric study of basal metabolism in man Washington D.C., Carnegie Institute of Washington.
- Houmard, J. A., Scott, B. K., Justice, C. L., & Chenier, T. C. (1994). "The effects of taper on performance in distance runners." Med Sci Sports Exerc **26**(5): 624-631.
- Jones, B. H., Cowan, D. N., & Knapik, J. J. (1994). "Exercise, training and injuries." Sports Med **18**(3): 202-14.
- Jones, B. H. & Knapik, J. J. (1999). "Physical training and exercise-related injuries. Surveillance, research and injury prevention in military populations." Sports Med **27**(2): 111-25.
- Knapik, J. J., Darakjy, S., Scott, S., Hauret, K., Canada, S., Marin, R., Palkoska, F., VanCamp, S., Piskator, E., Rieger, W., & Jones, B. H. (2004). "Evaluation of Two Army Fitness Programs: The TRADOC Standardized Physical Training Program for Basic Combat Training and the Fitness Assessment Program." U.S. Army Center for Health Promotion and Preventative Medicine, Aberdeen Proving Ground, MD. USACHPPM Project No. 12-HF-5772B-04.
- Lauder, T. D., Baker, S. P., Smith, G. S., & Lincoln, A. E. (2000). "Sports and physical training injury hospitalizations in the army." Am J Prev Med **18**(3 Suppl): 118-128.
- Loy, S. F., Holland, G. J., Mutton, D. L., Snow, J., Vincent, W. J., Hoffmann, J. J., & Shaw, S. (1993). "Effects of stair-climbing vs run training on treadmill and track running performance." Med Sci Sports Exerc **25**(11): 1275-1278.
- McArdle, W. D., Katch, F. I., & Katch, V. L. (1991). Exercise Physiology: Energy, Nutrition, and Human Performance Malvern, PA, Lea & Febiger.
- Morton, R. H., Fitz-Clarke, J. R., & Banister, E. W. (1990). "Modeling human performance in running." J Appl Physiol **69**(3): 1171-7.
- Mutton, D. L., Loy, S. F., Rogers, D. M., Holland, G. J., Vincent, W. J., & Heng, M. (1993). "Effect of run vs combined cycle/run training on VO<sub>2</sub>max and running performance." Med Sci Sports Exerc **25**(12): 1393-1397.
- Pandolf, K. B., Givoni, B., & Goldman, R. F. (1977). "Predicting energy expenditure with loads while standing or walking very slowly." J Appl Physiol **43**(4): 577-581.
- Purdy, J. G. (1974a). "Computer generated track and field scoring tables: I. Historical development." Med Sci Sports **6**(4): 287-294.
- Purdy, J. G. (1974b). "Least squares model for the running curve." Res Q **45**(3): 224-238.
- Purdy, J. G. (1975). "Computer generated track and field scoring tables: II. Theoretical foundation and development of a model." Med Sci Sports **7**(2): 111-115.

- Purdy, J. G. (1977). "Computer generated track and field scoring tables: III. Model evaluation and analysis." Med Sci Sports **9**(4): 212-218.
- Riegel, P. S. (1981). "Athletic records and human endurance." Am Sci **69**(3): 285-290.
- Smith, T. P., Coombes, J. S., & Geraghty, D. P. (2003). "Optimising high-intensity treadmill training using the running speed at maximal  $\dot{V}O_2$  uptake and the time for which this can be maintained." Eur J Appl Physiol **89**(3-4): 337-343.
- Smith, T. P., McNaughton, L. R., & Marshall, K. J. (1999). "Effects of 4-wk training using  $\dot{V}_{max}/T_{max}$  on  $\dot{V}O_{2max}$  and performance in athletes." Med Sci Sports Exerc **31**(6): 892-896.



## Appendix A. Available Datasets

The project currently has seven different datasets containing subject information ranging from fitness test scores to injury and anthropometry measures. Some datasets also contain questionnaire responses on initial fitness level, hormone regulation and previous injuries. Unfortunately, limited information on the training regimen these recruits participated in is known. Table 11 summarizes the information contained in each dataset.

Table 11. Summary table of the datasets available for model development.

	<b>A</b>	<b>B</b>	<b>C</b>	<b>D</b>	<b>E</b>	<b>F</b>	<b>G</b>
Location	MCRD-PI 1995	MCRD-PI 1999	MCRD-SD 1993	MCRD-SD 2003	MCRD-SD 2005	Ft Jackson 1998	Various Army Cntrs
Source	NHRC	NHRC	NHRC	MCRD-SD	MCRD-SD	ARIEM	BAMC
N <sub>subjects</sub>	2963	821	1286	3782	572	350	1019
<b>Fitness Testing</b>							
IST Data		✓		✓	✓	✓	✓
Mid-PFT Data							
Other Fitness Tests						✓	
FPFT Data				✓	✓	✓	✓
<b>Injury Status</b>							
Stress Fracture	✓	✓	✓				✓
Overuse Injury	✓	✓	✓				✓
Mishap/Acute Injury	✓	✓	✓				✓
<b>Questionnaire</b>							
Initial Fitness Level	✓	✓	✓				✓
Hormone Regulation	✓	✓	✓				✓
Previous Injuries	✓	✓	✓				✓
<b>Anthropometry</b>							
Gender	F	F	M	M	M	M	M, F
Ht, Wt, Age	✓	✓	✓		✓	✓	✓
Detailed Anthro	✓		✓			✓	
<b>Training Regimen</b>							
N <sub>days</sub>	83	83	82	85	85	63	63/70
Regimen	BCT	BCT	BCT	BCT	BCT	BCT	BCT/AIT
Regimen Details	Good	---	OK	Low	---	---	---



**communications**

**Applied Technologies**

---

# **Overuse Injury Assessment Model, Part II: NMS-biodynamics—A Biomechanical Modeling Toolbox**

**Part II of Annual Report: J3181-06-297**

Prepared by:

Kofi Amankwah, Ph.D.

Weixin Shen, Ph.D.

**L-3 Communications/Jaycor**

San Diego, California 92121-1002

**Prepared for:**

Commander

**U.S. Army Medical Research and Materiel Command**

504 Scott Street

Fort Detrick, Maryland 21702-5012

# **Abstract**

The human body is a complex, highly nonlinear system. Biomechanical modeling has become an important tool in understanding the neuromuscular and skeletal components of this system. The object of this work has been to develop a flexible suite of modeling components that can be assembled rapidly to address a majority of biomechanical questions. Currently, the NMS-biodynamics application has the basic components needed to build biomechanical models. Models can be built to solve kinematic, inverse dynamic, and static forward dynamic problems. Future efforts will incorporate optimization algorithms for muscle force sharing problems and methods for implementing various neuromuscular control systems. This report will outline the topics relevant to biomechanical modeling and illustrate the power and flexibility of the NMS-biodynamics application.

# Contents

	<u>Page</u>
<b>1. INTRODUCTION .....</b>	<b>1</b>
1.1 MODELING THE HUMAN NEUROMUSCULAR SYSTEM.....	1
1.2 OBJECTIVE .....	2
1.3 FEATURES .....	2
<b>2. BIOMECHANICAL MODELING ENGINE .....</b>	<b>3</b>
<b>3. BIOMECHANICAL ANALYSIS .....</b>	<b>4</b>
3.1 KINEMATICS .....	4
3.2 INVERSE DYNAMICS .....	5
3.2.1 <i>Muscle Force Sharing</i> .....	5
3.3 FORWARD DYNAMICS .....	6
3.3.1 <i>System Control</i> .....	7
3.4 ENERGETICS .....	7
<b>4. MODEL COMPONENTS.....</b>	<b>9</b>
4.1 MECHANICAL.....	9
4.2 ACTUATOR.....	9
4.3 CONTROL.....	10
<b>5. EXAMPLE APPLICATIONS.....</b>	<b>12</b>
5.1 HEAD NECK MODEL: INVERSE PROBLEM.....	12
5.1.1 <i>Building Model</i> .....	12
5.1.2 <i>Simulation Results</i> .....	13
5.2 HEAD NECK MODEL: FORWARD PROBLEM.....	14
5.2.1 <i>Building Model</i> .....	15
5.2.2 <i>Simulation Results</i> .....	16
<b>6. SUMMARY .....</b>	<b>18</b>
<b>7. REFERENCES.....</b>	<b>19</b>
<b>APPENDIX A. BIOMECHANICAL MODELING ELEMENTS.....</b>	<b>21</b>
A.1 SEGMENTS.....	21
A.2 JOINTS .....	22
A.3 PASSIVE ELEMENTS .....	22
A.3.1 <i>Spring and Damper Parallel (1 DOF)</i> .....	22
A.3.2 <i>Spring and Damper Parallel (3 DOF)</i> .....	22
A.3.3 <i>Spring and Damper Series (1 DOF)</i> .....	22
A.4 ACTIVE ELEMENTS .....	23

# Illustrations

	<u>Page</u>
<b>5-1. FOUR SEGMENT MODEL FOR THE INVERSE DYNAMICS PROBLEM.....</b>	<b>13</b>
<b>5-2. CALCULATED JOINT FORCES AND MOMENTS REQUIRED TO MAINTAIN THE STATIC POSTURE OF THE MODEL. ....</b>	<b>14</b>
<b>5-3. FOUR SEGMENT MODEL FOR THE FORWARD DYNAMICS PROBLEM.....</b>	<b>15</b>
<b>5-4. CALCULATED JOINT TRAJECTORIES.....</b>	<b>16</b>
<b>A-1. RIGID BODY.....</b>	<b>21</b>
<b>A-2. PLANAR JOINT. ....</b>	<b>21</b>
<b>A-3. PARALLEL SPRING AND DAMPER (1 DOF).....</b>	<b>22</b>
<b>A-4. PARALLEL SPRING AND DAMPER (3 DOF).....</b>	<b>22</b>
<b>A-5. SERIES SPRING AND DAMPER (1 DOF).....</b>	<b>22</b>
<b>A-6. MUSCLE. ....</b>	<b>23</b>

# 1. Introduction

## 1.1 Modeling the Human Neuromuscular System

The modeling, simulation, and analysis of the human neuromuscular system has become an increasingly important area of research. This has been driven by two factors: the basic desire to understand the fundamental mechanisms of the neuromuscular system, and by the increasing desire to improve health and reduce injuries to humans by optimizing products and physical training used by them. For the military, the desire to improve health and reduce injuries is a continual challenge. The military researchers face challenges to develop better equipment to enhance soldiers' performance, improve training regiments to increase soldiers' strength and reduce injury, and design better methods to assess the medical status of soldiers during training and combat.

To address these types of challenges, one approach is to perform only experiments or field observations and then analyze the measurements as the primary research result. This experimental approach, however, suffers several limitations. The human body is a complex, highly nonlinear system; therefore significant variations in the measurements of one subject and between subjects can be expected. Consequently large numbers of subject are required to obtain statistically significant results. Even with statistically significant results, the underlying mechanisms remain unknown due to the empirical nature of statistics. Consequently, the results can only answer the question posed by the experiment. Human experimental work requires large amounts of resources. It is difficult to control large numbers of subjects over long periods of time, and lastly it is ethically impossible to perform certain experiments on human subjects.

More recently, biomechanical modeling has become an important part of understanding the human neuromuscular and skeletal systems. With modeling, the human body is represented with sets of mathematical relationships and related parameters. Through computer simulations the model can be put through various scenarios to examine the effects on the health and performance of the body. In addition, by varying the model parameters during a simulation a better understanding can be gained of the underlying mechanisms of the neuromuscular system and the influence of those mechanisms on the health and performance of the body. Accordingly, the advantages of modeling are that many more tests can be performed rapidly, with fewer resources, and with no need for concerns about subject safety. Biomechanical models however, must be developed and validated with experimental data to ensure their results are credible.

The construction of an accurate model begins with experimentation, but through development and utilization of the model further lines of research are discovered. Modeling

helps the researcher understand which mechanisms are most influential. Therefore, a combination of experimentation, analysis, modeling and simulation are needed to confront the complexity of the neuromuscular and skeletal systems of the human body.

## **1.2 Objective**

Once a biomechanical model is developed it can be a very powerful tool for analysis. However developing a model can be time consuming process due to the validation process. Consequently, various modeling applications have been developed to ease model development. These modeling applications however are targeted at a specific type of biomechanical problem, do not allow for rapid development, or do not allow for easy integration with other analysis software. Therefore our objective is to develop a neuromuscular and skeletal modeling application that provides a flexible suite of modeling tools that can be assembled rapidly to address a majority of biomechanical questions.

## **1.3 Features**

The product will be designed and implemented to ease the development and analysis of biomechanical problems. The key features of the product include:

1. **Powerful:** The software engine will be the Simulink and SimMechanics platform by Mathworks.
2. **Reliable:** The components and algorithms will be rigorously developed and tested.
3. **Efficient:** Models will be assembled from standardized components through a graphical interface. Therefore, users are spared from basic programming and can concentrate on the advanced aspects of the model. In addition, components describing subsystems specific to certain biomechanical problems will also be provided.
4. **Consistent:** Developing models in a systematic way will make the comparison of results easier. Benchmark data and problems will also be included to aid calibration of model results.
5. **Flexible:** Users will be provided with the components and algorithms to solve a majority of biomechanical problems. The components will be modular so that model assembly and component improvements are easily accomplished.
6. **Open:** The toolbox will allow for the addition of new algorithms and components. The open structure ensures that the toolbox will remain relevant as this research area matures.
7. **Manageable:** Simulation results will be stored in a systematic and easily retrievable way.

## 2. Biomechanical Modeling Engine

Matlab and the Simulink platform (MathWorks, [www.mathworks.com](http://www.mathworks.com)) form the basis of the mathematical engine underlying the neuromuscular and skeletal modeling application. Matlab is a high level language that provides users with a robust set of functions and algorithms to perform computationally intensive calculations. Simulink is a platform developed by MathWorks for model-based design. It consists of a graphical interface where models are built by connecting blocks representing mathematical operations, signal processing functions, and control system components. With this platform, models can be developed rapidly and solved with the algorithms included in the platform. SimMechanics is a toolbox for Simulink that contains specific blocks such as masses, springs, dampers, and joints (constrained motions) for solving rigid body dynamics problems.

The advantages of using Matlab are the power of its included functions and algorithms, and that the high level language allows for easy programming. The graphical interface of Simulink provides a rapid means for building models without typing code, and SimMechanics provides the functions necessary to solve static and dynamic rigid body problems. Also, the basic rigid body, force and joint components of SimMechanics allow for custom blocks representing biomechanical components such as bones, muscles, and ligaments to be built.



### **3. Biomechanical Analysis**

Biomechanical problems are diverse in nature. For example, one might want to understand the trajectory of the ankle, knee, and hip angles during walking or optimize muscle activation during a movement to minimize fatigue. These diverse problems however can be segregated into four types: kinematic, inverse dynamic, forward dynamic, and energetic. The following sections will describe each type of problem and the ability of the software to address each one.

#### **3.1 Kinematics**

For a forward kinematic problem, the goal is to determine the endpoint position and velocity of the system given the positions and velocities of each joint, and the dimensions of the rigid bodies. The inverse kinematic problem determines the joint positions and velocities given the endpoint position and velocity of the system. For a forward kinematic problem, there is a single answer. However for the inverse problem there can be multiple answers depending on the complexity of the system. Consequently, additional constraints must be included to obtain a unique solution. Examples of constraints include limits on the range of motion (ROM) of the joints or minimizing the total moment of the configuration.

If the endpoint of the system is not grounded then the system is an open chain. The degrees of freedom of the open chain equal the number of joints in the system. However if the endpoint is grounded then all of the joints are not independent. The angle at one joint will affect one or more of the other joints. The advantage of this constraint is it can make the inverse answer unique with no additional constraints. The disadvantage however is the mathematical model of the system is stiff. Therefore numerical simulations must take very small steps or numerical drift will cause the solution to be incorrect.

For biomechanical analysis, often the goal is to examine the trajectories of the joint angles during a specific task. Accelerometers attached to the body or optical tracking systems or both are employed to accomplish this goal. By placing accelerometers on different segments, the movement of the segments relative to each other can be examined. For optical tracking systems, passive or active markers are placed on the segments of the subject. Cameras from the tracking system then record the position of the markers with respect to time.

NMS-biodynamics can solve either type of kinematic problem. Knowing the joint positions and velocities, and the rigid body dimensions, the toolbox can configure the model appropriately and return the endpoint characteristics of the system. For inverse problems, NMS-biodynamics will use optimization techniques to determine the joint positions and velocities for a given endpoint condition.

## 3.2 Inverse Dynamics

For an inverse dynamics problem, the goal is to calculate the joint forces and moments needed for a specific system configuration. To solve this problem, the necessary data are the kinematics of the system and the external forces applied to the system. With the data and the equations of motion of the system, a solution can then be calculated.

The necessary kinematic data can be measured from accelerometers mounted on body segments or from a motion capture system. With accelerometers, the acceleration data is integrated to get the required velocities and displacements. With a motion capture system, the displacement data are differentiated to obtain velocities and accelerations.

The externally applied forces in a biomechanical analysis of human systems are usually ground reaction forces. Force plates can measure these reaction forces. For other applied forces such as the impact during a vehicle crash, a human surrogate with force transducers is initially used to measure the applied force.

For the equations of motion of the system the inertial properties of the body segments must be known. These properties can be obtained through direct measurement on the subject. There are also regression equations to calculate these values based on a number of anthropometric measurements such as body weight, stature and specific geometric dimensions of individual segments.

To solve an inverse dynamics problem with NMS-biodynamics the user first builds their block model specifying the inertial properties of the body segments and how the segments are connected. Then the user specifies the joint kinematics at every degree of freedom as a function of time and any externally applied forces as functions of time. When the system is fully described, NMS-biodynamics can begin the simulation. The user does not need to develop the equations of motion and constraint equations, because NMS-biodynamics does it for them. The simulation output is the forces and moments at each of the joints as a function of time.

### 3.2.1 *Muscle Force Sharing*

For a biomechanical analysis, the next step after solving the inverse problem is to determine the muscle forces necessary to generate those joint forces and moments, and joint reaction forces from passive structures (e.g. ligaments and tendons). However, since each joint in the human body is spanned by a number of muscles, the estimation of muscle forces is an indeterminate problem (Collins, 1995). Techniques to solve this force sharing problem are based on either grouping muscles with similar function thus eliminating redundancy or applying optimization criteria to solve the muscle force distribution (Crowninshield, 1978; Hardt, 1978; Patriarco et al., 1981; Vaughan et al., 1982; Cholewicki and McGill, 1994). The first approach leads to oversimplification and unsatisfactory results.

The second approach is usually called inverse optimization or static optimization. Inverse optimization is numerically efficient and has been successfully applied, but it also suffers from certain drawbacks. No consensus on the optimization cost function has been reached. Secondly, the inverse optimization cannot guarantee the continuity of the solution. Muscle dynamics are not reflected in the inverse optimization procedure, although some recent work (Happee, 1994; Happee and van der Helm, 1995) has been done to include muscle dynamics as constraints in the optimization. Finally the lack of reliable validation procedures also limits the application of inverse optimization. Currently, electromyogram (EMG) signals, which describe the input into the muscular system, are usually recorded to see if they match with the muscle force pattern calculated from the optimization.

With the joint forces and moments known, NMS-biodynamics will allow the user to select a muscle force sharing criteria. The software will then calculate the forces needed in each muscle to generate the appropriate joint force and moment.

### **3.3 Forward Dynamics**

A forward dynamics problem is the opposite of the inverse problem. For this problem, the goal is to determine the motion of the system as a function of time. To calculate the solution, the necessary data are the joint forces and moments at each degree of freedom, and all externally applied forces.

The joint forces and moments are generated by the actuators that cross that joint. For biomechanical analysis, muscles, tendons, and ligaments are the actuators of the system. Tendons and ligaments are passive elements that produce force based on their length or velocity. Muscle is an active element. The neuronal input to muscle determines its level of activation and therefore the force generated by the muscle.

To solve a forward dynamics problem with NMS-biodynamics, the user first builds their block model specifying the inertial properties of the body segments and how the segments are connected. If muscles are included, the user then specifies the activation levels of each muscle as functions of time. If no muscles are included, the joint torques as functions of time are specified. Any externally applied forces as functions of time are also specified. When the system is fully described, NMS-biodynamics can begin the simulation. The user does not need to develop the equations of motion and constraint equations, because NMS-biodynamics does it for them. The simulation output is the motion of each joint as a function of time.

### **3.3.1 System Control**

Solving the forward dynamic problem provides the motion of the system for given forces and moments. To control the movement however, without predefining it requires a control system. The two types of control systems are open loop and closed loop.

The easiest type of control system is an open loop system. With open loop control, a desired motion is obtained by setting the activation levels to predefined levels to generate the necessary muscle forces and consequently the necessary joint forces and moments. The disadvantage of open loop control is that if the motion is not as expected there is no means for the control system to know. Consequently, the system may have a very different motion and may become unstable.

A variation of open loop control is feedforward control. With this type of control, the potential disturbances to the system are well known. A sensor measures the disturbances as they appear and the control system adjusts the input appropriately to obtain the desired output. However the output is not measured so the control system still has no means to determine if the actual output is equal to the desired output.

With closed loop control, the input signal is not just a function of time but also a function of one or more output variables. For example, the muscle activation would be a function of time and a function of the joint positions and velocities. In practice this means that some of the outputs are fed back to adjust the input appropriately to ensure the desired motion is obtain. Consequently if the system is disturbed the actual output will be different for the desired output so the input will be changed to correct for this mismatch. This ability to correct for disturbances to the system is the advantage of closed loop control.

The Simulink engine of NMS-biodynamics was designed for solving control system theory problems. Therefore NMS-biodynamics has the ability to simulate conventional open loop and closed loop systems. Additionally, more advanced control systems including feed-forward and neural networks can be developed within NMS-biodynamics.

## **3.4 Energetics**

The energetic aspect of human biomechanical systems deals with the mechanical power as well as the metabolic cost associated with human movements. The metabolic cost can be separated into different terms according to their sources. The activation heat accounts for the energy used to activate muscles. The maintenance heat is used to maintain the muscle forces. The shorting heat is related to the extra heat produced as a consequence of the shortening of muscle. The mechanical work is the product of muscle force doing work. And the dissipation of energy in passive structures also contributes to the total metabolic costs. Although research work has led to some empirical relations, the actual metabolic cost

is usually determined from the measured oxygen consumption, which is related to the metabolic cost.

Different methods are available to estimate the mechanical power during human movement. Some methods calculate the power based on external work necessary to move the center of mass of a human body. However, the actual dynamics of each segment is lost in these methods. Some other methods provide the mechanical power due to the movement of each segment. These models cannot account for the synergy of muscles over a single joint. Although it is recognized that the actual mechanical work and thus the metabolic cost has to come from the muscles, currently researchers have not been very successful in calculating muscle power due to the difficulties in determining muscle forces.

NMS-biodynamics has the ability to calculate the mechanical energy used by a biomechanical system. Using empirical equations from the literature (Bhargava et al., 2004; Umberger et al., 2001) muscle energy can also be calculated. However a method to easily calculate the total metabolic energy is not currently available.

## 4. Model Components

Humans as a living biomechanical system are a complex neural-muscular-skeletal system combining motion generation components, adaptive control, reflexes, self-analysis and learning (Barnes, Oggero et al. 1997). All human movements are complex motions characterized by the coordination of neural control, muscle activation, and skeletal motion generation. The central neural system sets the goal to be achieved. The neuromuscular system correspondingly controls the pattern of the muscle activation. The muscle forces drive the skeletal system to generate or adjust the motion. In modeling, the different components of the human biomechanical system are represented by different mathematical systems.

### 4.1 Mechanical

The mechanical components of a human biomechanical system are the segments or rigid bodies that represent the skeletal system, and the joints that connect those bodies. The governing equation of motions can be obtained from the Newton-Euler formulations, Lagrange formulations, or Kane's method. The resulting sets of equations include kinematic data (velocities and accelerations), kinetic data (forces and moments) and inertial properties of body segments (mass and moment of inertia).

Deformable bodies have also been used in some models. For example, long bones can be represented as deformable beams. Finite element models and other models based on continuum mechanics are also used to model the mechanical subsystem. Simulation of specific structures, such as the foot, benefits from the use of deformable body representation. However due to the modeling complexity of continuum mechanics, rigid body formulations are mostly used in biomechanical analysis.

NMS-biodynamics is a rigid body toolbox for biomechanical analysis. It includes rigid bodies that can be customized by changing the inertia matrix and mass of the body. The toolbox also has the ability to connect the bodies with many types of joints including: revolute, transverse, and universal.

### 4.2 Actuator

The human biomechanical system has two types of actuators. Ligaments are passive tissues that constrain the movements of body segments. Muscles are active tissues that generate the forces needed to move body segments.

As mechanical elements, ligaments store and dissipate energy. Therefore they are modeled as combinations of springs and dampers. Simple models use linear equations for

these elements, but cubic or exponential functions can also be implemented (Amankwah et al., 2004; Gottlieb and Agarwal, 1978; Yoon and Mansour, 1982).

Muscles generate active force through the contraction of muscle fibers and passive force through the stretching of tendon. Simple musculotendon models involve only the active elements and no passive elements. More complex models involve both the passive and the active elements. To determine the muscle force and joint torque generated, it is also necessary to include the muscle origin and insertion points to determine the line of action of the muscle. Thus muscle force calculations become highly integrated with the geometry of the physical system. Additional challenges to musculotendon force calculations include muscles that span more than one joint and redundancies presented by multiple muscles spanning a joint.

The NMS-biodynamics toolbox includes elements to model the passive and active characteristics of ligaments and muscles. The toolbox includes springs and dampers that can model linear and nonlinear systems. For muscles, musculotendon models have been developed to include passive properties and the active properties of force-length and force-velocity. The flexibility of the toolbox allows for many different musculotendon models to be developed and utilized.

### **4.3 Control**

Control of the human body is conducted through the central nervous system (CNS), which is comprised of the brain and the spinal column. The CNS provides signals via the peripheral nervous system to muscles to actuate them in coordinated manners to produce desired functions. Exactly how the CNS determines those signals, and how the CNS optimizes for overdetermined situations is still an area of research. As mentioned above, some accepted methods for solving the muscle force sharing problem include minimizing the sum of the squared muscle stresses (Crowninshield and Brand, 1981) and minimizing the sum of the squared muscle forces (Collins and De Luca, 1993).

For biomechanical modeling, the simplest strategy is to have no control system; therefore the control system is open loop. Consequently the muscle forces need to be precalculated for the desired movement and any substantial disturbance to the system will cause an error in the output. With a closed loop control system, the model receives feedback from its output, and therefore is more able to respond to disturbances and adapt to changing conditions. Biomechanical research has implemented closed loop control systems through traditional approaches such as PID (proportional, integral, derivative) control and through new approaches such as adaptive control and neural networks (Ferrante et al., 2004; Ferrarin et al., 2001; Winter et al., 1998; Soetanto et al., 2001).

NMS-biodynamics toolbox was built in the Matlab Simulink environment. This is a significant advantage for implementing control systems, because Simulink was designed for developing control system models. Therefore complex control systems can easily be built and integrated with biomechanical models created with the toolbox.



## 5. Example Applications

### 5.1 Head Neck Model: Inverse Problem

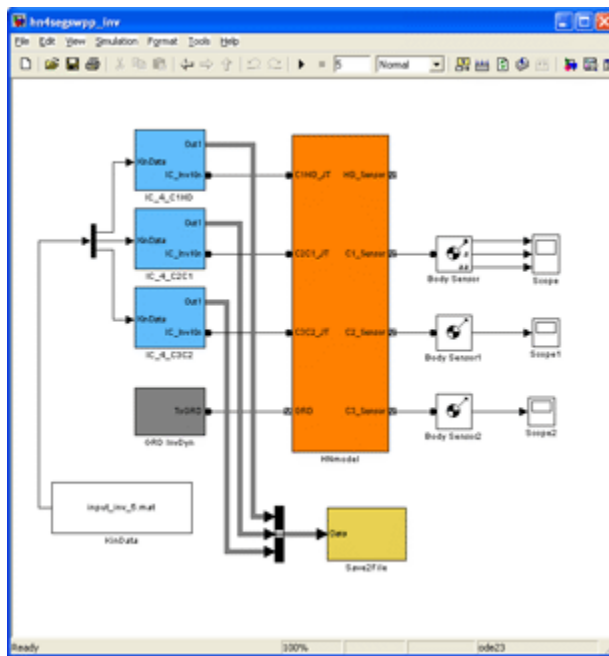
This section provides an example of developing and simulating a model with the NMS-biodynamics toolbox. The next subsections will discuss assembling the model, setting its parameters, and running an inverse simulation to determine the joint forces and moments needed to maintain a given posture. Then the simulated results will be presented and discussed. The goal of this example is to illustrate the power of this software and the speed with which a biomechanical model can be developed.

#### 5.1.1 Building Model

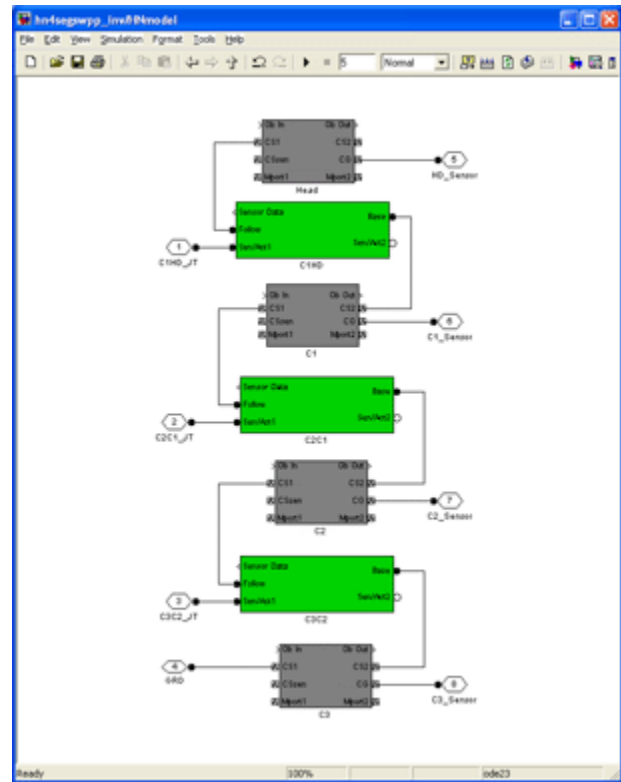
The head neck model (Figure 5-1) contains rigid bodies representing the head, and the spinal vertebrae of C1, C2, and C3. The joints between each of these segments are planar joints, which allow translation along the X and Y axis, and rotation about the Z axis. Passive elements at each of the joints provide joint elasticity and viscosity. No muscles are included in this example model, and gravity acts in the  $-Y$  direction.

Other elements needed for a complete model include a ground block, blocks to prescribe the motion of each degree of freedom, and a block to save the output data. The model via the C3 segment is connected to the ground block with an in-plane joint, which allows translation along the X and Y axes. For each joint, a motion block (e.g. IC\_4\_C1HD) prescribes the kinematics for each degree of freedom of the joint. During the simulation, the kinematic data is loaded from a file. The data from the simulation is saved to a file with the aid of the Save2File block. Additionally, sensor blocks are attached to the head neck model to view the results during the simulation.

The model parameters are defined in the passdata.dat and segdata.dat files. The segdata.dat defines the mass, moment of inertia, and the location and rotation of the body relative to the proximally connected body. The passdata.dat defines the equation relating the elastic and viscous properties to the position and velocity for each degree of freedom. The equation can be linear or nonlinear. To initialize the model parameters and prepare the model for simulation, the last step is to execute a function which loads the parameter values from the .dat files and applies them to the model.



(a) Head Neck model overview



(b) Exploded view of HN Model  
(orange area of Fig. 5-1a)

**Figure 5-1. Four segment model for the inverse dynamics problem.**

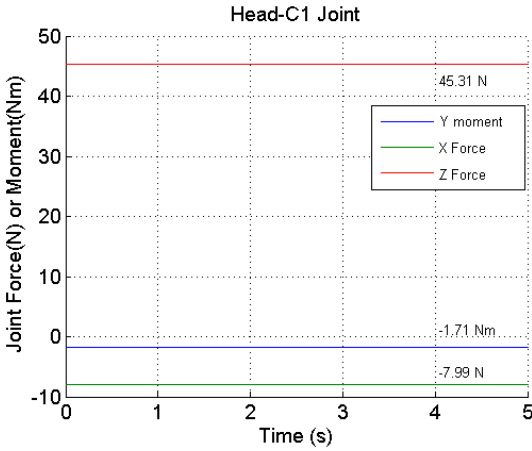
### 5.1.2 Simulation Results

For this inverse dynamics example, the model was simulated while positioned in a static posture. During the simulation, the forces and torques needed at each degree of freedom were calculated so that the model maintained its posture (Table 5-1). The calculated results (Figure 5-2) were then saved to an output file.

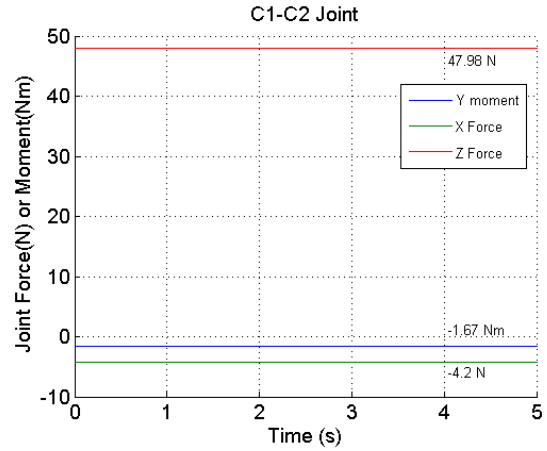
Table 5-1. Kinematic input to model

Joint	Rotation about Y-axis Angle (°)	X Position (m)	Z Position (m)
C1 – HD	5	0	0
C2 – C1	5	0	0
C3 – C2	5	0	0

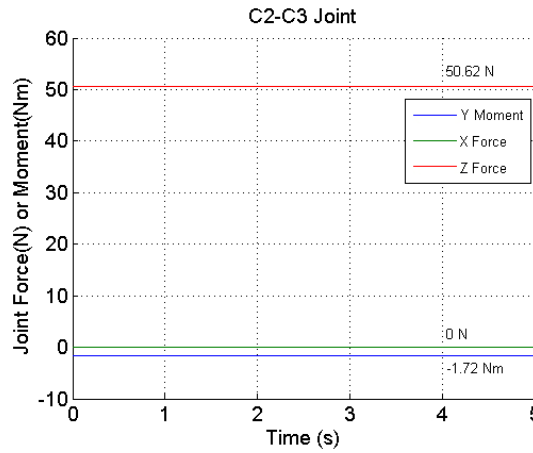
The velocities and accelerations were all set to zero.



(a) C1-Head joint



(b) C2-C1 joint



(c) C3-C2 joint

**Figure 5-2. Calculated joint forces and moments required to maintain the static posture of the model.**

Using NMS-biodynamics, a user is able to rapidly build and simulate models without the need to derive the equations of motion. Through this inverse simulation example, a four segment model was built and simulated. The simulation was able to calculate the necessary forces and moments for the model to hold a static posture.

## 5.2 Head Neck Model: Forward Problem

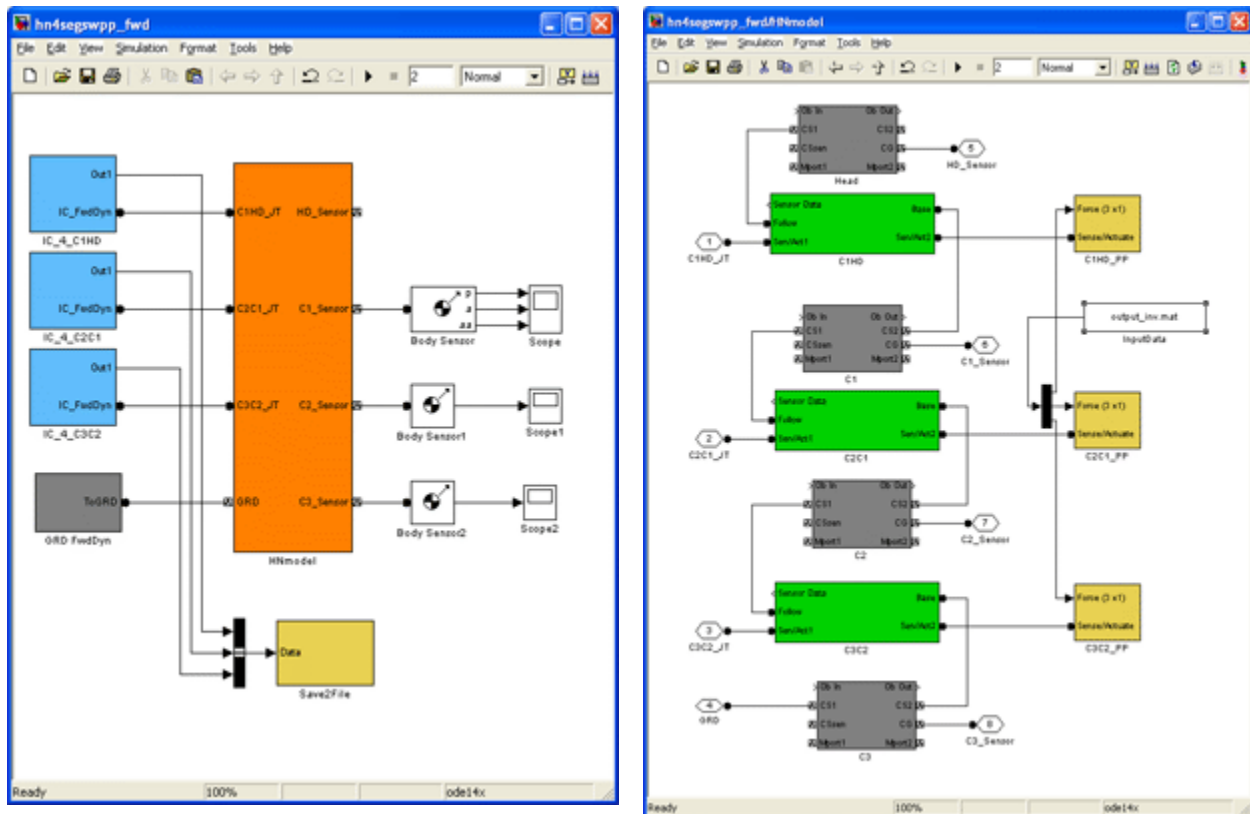
This section provides an example of simulating a head neck model to solve a forward dynamics problem. In this example, the joint forces and moments are known and the trajectories of the joint angles and positions are calculated. Because the method of building the model is very similar to the method used in the inverse problem example, the subsection about building the model will be brief. The simulated results will then be presented and

discussed. The goal of this example is to illustrate the power of the NMS-biodynamics toolbox and the speed with which a solution to forward dynamics problems can be achieved.

### 5.2.1 Building Model

As with the model described for the inverse problem, the head neck model (Figure 5-3) contains rigid bodies representing the head, and the spinal vertebrae of C1, C2, and C3. The joints between each of these segments are planar joints. Passive elements at each of the joints provide joint elasticity and viscosity and no muscles are included.

Similar to the inverse problem model a ground block and a block to save the output data is included. The difference with this model is that the blocks which prescribe the joint motions are removed. Those blocks are replaced with blocks (e.g. IC\_4\_C1HD) which prescribe the joint forces and moments.



(a) Head Neck Model overview

(b) Exploded view of HN Model  
(orange area of Fig. 5-3a)

**Figure 5-3. Four segment model for the forward dynamics problem.**

To initialize the model parameters and prepare the model for simulation, a function is executed to load the parameter values from the appropriate .dat files and apply them to the model. The applied joint forces and moments data are used by the simulation at each time step to determine the joint angle and position trajectories.

### 5.2.2 Simulation Results

For the forward dynamics example, the model was simulated with constant joint forces and moments (Table 5-2). During the simulation, the resulting joint trajectories were calculated (Figure 5-4) are then saved to an output file.

Table 5-2. Force and moment inputs to the model

Joint	Y Moment (Nm)	X Force (N)	Z Force (N)
C1 – HD	-1.71	-7.99	45.31
C2 – C1	-1.67	-4.20	47.98
C3 – C2	-1.72	0.00	50.62

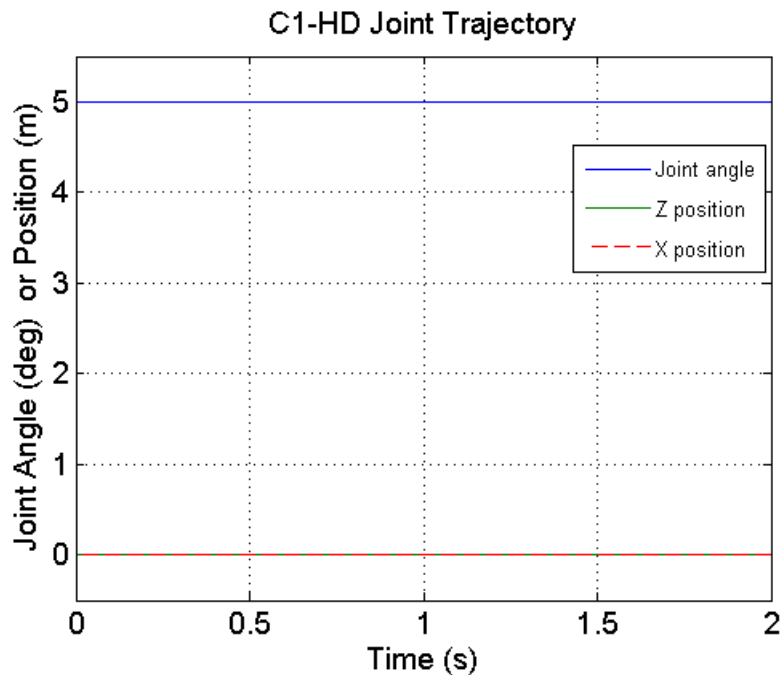


**Figure 5-4. Calculated joint trajectories.**

*The joint positions and angles at the C1-Head, C2-C1, and C3-C2 joints remained constant over time. For brevity, only the results for the C1-Head joint are shown.*

The initial position of the model was the same as the inverse problem example. Therefore if the same forces and moments calculated for the inverse problem were applied in the forward problem the model should remain stationary. The results illustrate the model did not move. Consequently, using the NMS-biodynamics toolbox a user can solve a forward dynamics problem to determine the trajectory of a model with time.

## 6. Summary

The objective of this current version of the NMS-biodynamics toolbox was to develop a set of basic tools that would allow one to rapidly build biomechanical models. To do this we have developed a basic set of elements to accomplish this task. The elements include a rigid body, a planar joint, viscoelastic joint properties, and a muscle model (Appendix A). Through the examples it was shown that the toolbox can solve static inverse and forward dynamics problems. The current toolbox can also solve dynamic inverse problems. Future tasks will include incorporating algorithms to solve the muscle force sharing problem and methods for solving quasi static forward dynamics problems.

## 7. References

- Amankwah, K., Triolo, R. J., Kirsch, R., (2004). Effects of spinal cord injury on lower-limb passive joint moments revealed through a nonlinear viscoelastic model. *J. Rehabil. Res. Dev.* 41, 15-32.
- Bhargava, L. J., Pandy, M. G., Anderson, F. C., (2004). A phenomenological model for estimating metabolic energy consumption in muscle contraction, *J. Biomech.* 37, 81-88.
- Cholewicki, J., McGill, S. M., (1994). EMG assisted optimization: a hybrid approach for estimating muscle forces in an indeterminate biomechanical model. *J. Biomech.* 27, 1287-9.
- Collins, J. J., (1995). The redundant nature of locomotor optimization laws, *J. Biomech.* 28, 251-267.
- Collins, J. J., De Luca, C. J., (1993). Open-loop and closed-loop control of posture: a random-walk analysis of center-of-pressure trajectories. *Exp. Brain Res.* 95, 308-318.
- Crowninshield, R. D., (1978). Use of optimization techniques to predict muscle forces. *J. Biomech. Eng.* 100, 88-92.
- Crowninshield, R. D., Brand, R. A., (1981). A physiologically based criterion of muscle force prediction in locomotion. *J. Biomech.* 14, 793-801.
- Ferrante, S., Pedrocchi, A., Ianno, M., De, M. E., Ferrarin, M., Ferrigno, G., (2004). Functional electrical stimulation controlled by artificial neural networks: pilot experiments with simple movements are promising for rehabilitation applications. *Funct. Neurol.* 19, 243-252.
- Ferrarin, M., Palazzo, F., Riener, R., Quintern, J., (2001). Model-based control of FES-induced single joint movements. *IEEE Trans. Neural Syst. Rehabil. Eng.* 9, 245-257.
- Gottlieb, G. L., Agarwal, G. C., (1978). Dependence of human ankle compliance on joint angle. *J. Biomech.* 11, 177-181.
- Happee, R., (1994). Inverse dynamic optimization including muscular dynamics, a new simulation method applied to goal directed movements. *J. Biomech.* 27, 953-60.
- Happee, R., van der Helm, F. C., (1995). The control of shoulder muscles during goal directed movements, an inverse dynamic analysis. *J. Biomech.* 28, 1179-91.
- Hardt, D. E., (1978). Determining muscle forces in the leg during normal human walking---an application and evaluation of optimization methods. *J. Biomech. Eng.* 100, 72-78.
- Patriarco, A. G., Mann, R. W., Simon, S. R., Mansour, J. M., (1981). An evaluation of the approaches of optimization models in the prediction of muscle forces during human gait. *J. Biomech.* 14, 513-25.



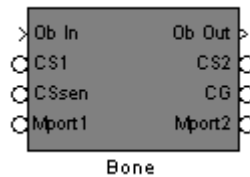
- Soetanto, D., Kuo, C. Y., Babic, D., (2001). Stabilization of human standing posture using functional neuromuscular stimulation. *J. Biomech.* 34, 1589-1597.
- Umberger, B. R., Gerritsen, K. G. M., Martin, P. E., (2001). A model of human muscle energy expenditure., University of California, San Diego, CA.
- Vaughan, C. L., Andrews, J. G., Hay, J. G., (1982). Selection of body segment parameters by optimization methods. *J. Biomech. Eng.* 104, 38-44.
- Winter, D. A., Patla, A. E., Prince, F., Ishac, M., Gielo-Perczak, K., (1998). Stiffness control of balance in quiet standing. *J. Neurophysiol.* 80, 1211-1221.
- Yoon, Y. S., Mansour, J. M., (1982). The passive elastic moment at the hip. *J. Biomech.* 15, 905-910.

# Appendix A. Biomechanical Modeling Elements

## A.1 Segments

The rigid body block (Figure A-1) can be used to represent a body such as a bone. The block contains a mass and inertia parameter. Each segment also has two muscle ports (MPort1 and MPort2) for attaching muscles. More muscles can be attached thorough the use of a mechanical branching bar. The segment can be connected to a joint block through the CS1 and CS2 ports. CS1 is a coordinate system with its location defined relative to the adjoining segment. CG is the center of gravity of the segment with its location defined relative to CS1. CS2 is another coordinate system with is location defined with respect to CS1. CSsen, which can be used for attaching a body sensor, is another coordinate system with is location defined with respect to CS1. To ensure muscles wrap over the segments properly, obstacle points can be input to the block and then passed through to the attached muscle.

**Figure A-1. Rigid body.**



## A.2 Joints

The planar joint block (Figure A-2) allows for rotation about one axis and translations along the other two axes. The user can specify which axis rotates and which axes translate. The joint has two Sensor/Actuator ports which allow measuring or applying moments/forces or rotations/displacements to the joint. Sensor data including position, velocity, and reaction force/moment are output through the Sensor Data port.



**Figure A-2. Planar joint.**

## A.3 Passive Elements

### A.3.1 Spring and Damper Parallel (1 DOF)

The Parallel Spring and Damper block (Figure A-3) models a single elastic element in parallel with a single viscous element. Therefore it only outputs a force/moment signal for 1 degree of freedom (DOF). The equation for each element is defined by the user and can be nonlinear. This block attaches to the Sensor/Actuator port of a joint block which provides the joint position and velocity information needed for the calculation.

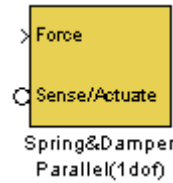


**Figure A-3. Parallel spring and damper (1 DOF).**

### A.3.2 Spring and Damper Parallel (3 DOF)

This block (Figure A-4) contains 3 sets of parallel elastic and viscous elements. This allows one to add passive properties to the Planar Joint block without combining 3 single DOF blocks. It attaches to the Sensor/Actuator port.

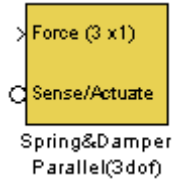


**Figure A-4. Parallel spring and damper (3 DOF).**

### A.3.3 Spring and Damper Series (1 DOF)

The spring and damper in series block (Figure A-5) has a single elastic element in series with a viscous element. Consequently it only provides force/moment data for 1 DOF. The equation for each element is linear and is defined by the user. It attaches to the Sensor/Actuator port on a joint block.

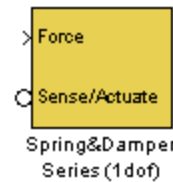


**Figure A-5. Series spring and damper (1 DOF).**

## A.4 Active Elements

The muscle block (Figure A-6) calculates the force generated by the muscle for a given length and activation. It then applies that force to the two segments connected by the muscle. The Base and Follower ports connect to the Muscle ports of two segments. The musculotendon force and length are outputted for debugging purposes. This muscle block also has the ability to wrap itself over one cylindrical obstacle. The location, orientation, and reference frame of the obstacle are input through the Ob data port.

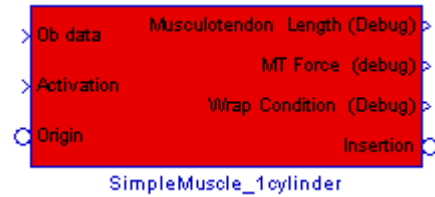


**Figure A-6. Muscle.**



**communications**

**Applied Technologies**

---

# **Overuse Injury Assessment Model, Part III: Preliminary pQCT Analysis of Tibia Changes due to Physical Exercises**

**Part III of Annual Report: J3181-06-298**  
under Contract No. DAMD17-02-C-0073

Prepared by:

Charles Negus, Ph.D.  
Weixin Shen, Ph.D.

**L-3 Communications/Jaycor**  
San Diego, California 92121-1002

**Prepared for:**

Commander  
**U.S. Army Medical Research and Materiel Command**  
504 Scott Street  
Fort Detrick, Maryland 21702-5012

# Summary

Images from a study conducted by the University of Connecticut for USARIEM were forwarded for analysis. The 16-bit grayscale images are of the tibia of 17 subjects before, during, and after a 13 week training regimen involving both aerobic and resistance exercises. Images were taken, for each subject at 4%, 38%, and 66% of tibial length (called “slice planes”), as measured from the distal end. This gave a total of nine images per subject. The images were analyzed to see what changes in bone morphology might be evident as training progressed.

Using threshold values of pixel intensity, the images were segmented to identify inner (endosteal) and outer (periosteal) boundaries of the tibial cortex. These boundaries were then used to register the images such that “post training” and “midtraining” images were aligned with the “pretraining” images for each slice plane. Defining the polar origin of the tibia cross section in each slice plane as the center of the inner cortical boundary, statistics were calculated for 10 degree sectors around each slice.

The analysis first looked for changes in bone quality in each sector from pre through post training. Bone was classified, according to pixel intensity value, as being either trabecular, transitional, or cortical. In each sector, differences in mean pixel intensity, standard deviation, area (as measured by number of pixels), cortical thickness, and canal radius were tracked. Additionally, overall medial-lateral (M-L) and anterior-posterior (A-P) lengths, cross sectional moment of inertia (CSMI), and cortical bone strength index (BSI) were calculated.

The second phase of the analysis was to look for correlations between bone geometry (i.e., cortical thickness, cortical area, cross-sectional moment of inertia) and bone mineral density. In so doing, we hoped to gain insight into the relationship between geometry and material properties and, consequently, stress fracture propensity itself.

The results showed there were no significant density changes as a result of the training regimen in any of the three classifications of bone. Certain trends in bone quality as a function of geometry did emerge however. Cortical bone was lower in density on the anterior sectors where the average thickness was significantly greater. Another result noted was that scalar measures of overall bone strength (such as the “Bone Strength Index”) were consistent for each subject from pre to post training. This indicates that while the scalar measures apparently did not capture any morphological adaptation, pQCT may be a reliably repeatable measurement of overall bone strength, and hence, stress fracture susceptibility.

The results also suggest that while changes in density over a time period commensurate with basic training are subtle, and may not be reliably ascertained by pQCT, it can still be used to accurately assess bone geometry and regional mineralization to a degree that may be very useful, when combined with anthropomorphic data such as body weight, for determining stress fracture propensity. To the knowledge of the investigators, no research has attempted to use pQCT as the basis for patient-specific tibial stress analyses. Given a population with some incidence of stress fracture, estimating tibial stresses for each individual could lead to individual predictions of stress fracture susceptibility.

# Contents

	<u>Page</u>
<b>1. INTRODUCTION .....</b>	<b>1</b>
1.1    PQCT BACKGROUND.....	1
1.2    PRECISION AND ACCURACY .....	1
1.3    SUBJECT TIBIA IMAGES .....	2
<b>2. METHODS .....</b>	<b>3</b>
2.1    IMAGE PROCESSING.....	3
2.1.1    Image Conversion .....	3
2.1.2    Image Registration.....	4
2.2    MEASUREMENTS .....	6
2.2.1    Cortical Thickness.....	7
2.2.2    Density Calculations .....	7
2.2.3    Moment of Inertia.....	8
2.2.4    Other Geometric Properties.....	8
2.2.5    Output.....	8
2.3    STATISTICAL ANALYSES.....	8
2.3.1    Changes due to Training.....	8
2.3.2    Bone Quality vs. Geometry .....	9
<b>3. RESULTS .....</b>	<b>10</b>
3.1    CHANGES DUE TO TRAINING .....	10
3.1.1    Trabecular Density.....	10
3.1.2    Transitional Density.....	14
3.1.3    Cortical Density.....	16
3.1.4    Average Radius .....	19
3.1.5    Geometry and Strength Indices.....	20
3.2    BONE QUALITY VS. GEOMETRY .....	28
<b>4. DISCUSSION.....</b>	<b>31</b>
<b>5. REFERENCE .....</b>	<b>33</b>

# Illustrations

	<u>Page</u>
1. HISTOGRAM FOR SUBJECT 48. ....	4
2. IMPORTED TIBIA IMAGES WITH A TIGHT BOUNDING BOX. ....	5
3. INNER AND OUTER BOUNDARIES FOLLOWING ALIGNMENT. LEFT: MID (BLUE) ALIGNED TO PRE(RED). RIGHT: POST (BLUE) ALIGNED TO PRE(RED). ....	6
4. EXAMPLES OF INNER AND OUTER CORTICAL BOUNDARY DEFINITIONS. ....	7
5. TOP LEFT: AVERAGE TRABECULAR DENSITY (PRE, MID, AND POST TRAINING) BY SECTOR OF THE 4% SLICE. (SUBJECTS 3 AND 11 POST-TRAINING IMAGES HAVE SOME IMAGE NOISE, BUT ARE INCLUDED.) ....	10
6. TOP LEFT: AVERAGE TRABECULAR DENSITY (PRE, MID, AND POST TRAINING) BY SECTOR OF THE 38% SLICE. ....	12
7. TOP LEFT: AVERAGE TRABECULAR DENSITY (PRE, MID, AND POST TRAINING) BY SECTOR OF THE 66% SLICE. ....	13
8. TOP LEFT: AVERAGE TRANSITIONAL DENSITY (PRE, MID, AND POST TRAINING) BY SECTOR OF THE 38% SLICE. ....	14
9. TOP LEFT: AVERAGE TRANSITIONAL DENSITY (PRE, MID, AND POST TRAINING) BY SECTOR OF THE 66% SLICE. ....	15
10. TOP LEFT: AVERAGE TRANSITIONAL DENSITY (PRE, MID, AND POST TRAINING) BY SECTOR OF THE 38% SLICE. ...	17
11. TOP LEFT: AVERAGE TRANSITIONAL DENSITY (PRE, MID, AND POST TRAINING) BY SECTOR OF THE 66% SLICE. ...	18
12. TOP: NORMALIZED CANAL RADIUS AT 38% OF TIBIAL LENGTH: PRE, MID, AND POST TRAINING. BELOW: DATA TABLE OF AVERAGE VALUES FOR ALL 17 SUBJECTS, 60° SECTORS. ....	19
13. TOP: NORMALIZED CANAL RADIUS AT 66% OF TIBIAL LENGTH: PRE, MID, AND POST TRAINING. BOTTOM: TABLE OF AVERAGE VALUES FOR ALL 17 SUBJECTS, 60° SECTORS. ....	20
14. AVERAGE AREA (TRABECULAR, TRANSITIONAL, AND CORTICAL) FOR THE 4% LEVEL: PRE, MID AND POST TRAINING. ....	21
15. AVERAGE AREA (TRABECULAR, TRANSITIONAL, AND CORTICAL) FOR THE 38% LEVEL: PRE, MID AND POST TRAINING. ....	21
16. AVERAGE AREA (TRABECULAR, TRANSITIONAL, AND CORTICAL) FOR THE 66% LEVEL: PRE, MID AND POST TRAINING. ....	22
17. AVERAGE CSMI (M-L, A-P, POLAR) FOR THE 38% LEVEL: PRE, MID AND POST TRAINING. UNITS ARE $PIXELS^4$ ....	22
18. AVERAGE CSMI (M-L, A-P, POLAR) FOR THE 66% LEVEL: PRE, MID AND POST TRAINING. UNITS ARE $PIXELS^4$ ....	23
19. AVERAGE BSI (M-L, A-P, POLAR) FOR THE 38% LEVEL: PRE, MID AND POST TRAINING. ....	24
20. INDIVIDUAL BSI (M-L) FOR THE 38% LEVEL: PRE, MID AND POST TRAINING. UNITS ARE $(PIXEL-INTENSITY)(PIXELS^4)$ . ....	24
21. INDIVIDUAL BSI (A-P) FOR THE 38% LEVEL: PRE, MID AND POST TRAINING. UNITS ARE $(PIXEL-INTENSITY)(PIXELS^4)$ . ....	25
22. INDIVIDUAL BSI (POLAR) FOR THE 38% LEVEL: PRE, MID AND POST TRAINING. UNITS ARE $(PIXEL-INTENSITY)(PIXELS^4)$ . ....	25
23. AVERAGE BSI (M-L, A-P, POLAR) FOR THE 66% LEVEL: PRE, MID AND POST TRAINING. UNITS ARE $(PIXEL-INTENSITY)(PIXELS^4)$ . ....	26
24. INDIVIDUAL BSI (M-L) FOR THE 66% LEVEL: PRE, MID AND POST TRAINING. UNITS ARE $(PIXEL-INTENSITY)(PIXELS^4)$ . ....	26



25. INDIVIDUAL BSI (A-P) FOR THE 66% LEVEL: PRE, MID AND POST TRAINING. UNITS ARE ( <i>PIXEL-INTENSITY</i> )( <i>PIXELS</i> <sup>4</sup> ).	27
26. INDIVIDUAL BSI (POLAR) FOR THE 66% LEVEL: PRE, MID AND POST TRAINING. UNITS ARE ( <i>PIXEL-INTENSITY</i> )( <i>PIXELS</i> <sup>4</sup> ).	27
27. AVERAGE CORTICAL THICKNESS (IN A 10° SECTOR) VERSUS AVERAGE CORTICAL DENSITY IN THAT SECTOR FOR THE 38% LEVEL: PRE, MID, AND POST TRAINING.	28
28. INDIVIDUAL CORTICAL THICKNESS (IN A 10° SECTOR) VERSUS AVERAGE CORTICAL DENSITY IN THAT SECTOR FOR THE 38% LEVEL: PRE, MID, AND POST TRAINING.	29
29. AVERAGE CORTICAL THICKNESS (IN A 10° SECTOR) VERSUS AVERAGE CORTICAL DENSITY IN THAT SECTOR FOR THE 66% LEVEL: PRE, MID, AND POST TRAINING.	30
30. INDIVIDUAL CORTICAL THICKNESS (IN A 10° SECTOR) VERSUS AVERAGE CORTICAL DENSITY IN THAT SECTOR FOR THE 66% LEVEL: PRE, MID, AND POST TRAINING.	30

# 1. Introduction

## 1.1 pQCT Background

Peripheral Quantitative Computed Tomography (pQCT) is a noninvasive diagnostic technique used to measure characteristics of bones on the skeletal periphery. pQCT results in higher accuracy and precision than standard densitometric measures such as DEXA, DPA, and SPA which only measure areal density (Fujita 2002). As such, it is widely used in studies involving volumetric bone mineral density measurements (see, e.g., (Riggs et al. 2004), (Ferretti et al. 2003), (Findlay et al. 2002), or (Veitch et al. 2005)).

pQCT machines employ X-ray tubes with small focal areas emit photons at various angles to compile a cross sectional image of the object of interest. The X-ray energy is attenuated in the process of passing through mass, and this reduced energy is then detected through an array of semiconductor-crystal collectors (Ferretti 1997; Ferretti et al. 2002; Stratec 2006). Attenuation coefficients are correlated with the pixel intensity of the final image.

Regardless of the manufacturer, the attenuation coefficients would have been calibrated using a phantom of solid hydroxy apatite of known density. This calibration procedure makes the machine “see” the mineralized portion of the bone tissue. As the manual for the Stratek XCT 3000 (one commonly cited pQCT machine in the literature) says, “By calibration with phantoms of a specified hydroxyl apatite concentration the attenuation coefficients can be transformed to density values (mg/cm<sup>3</sup>)”.

Knowing the BMD distribution of bone is useful because it is correlated with the overall stiffness (specifically, the Young’s Modulus) of the bone. A significant correlation of about 0.7 was found between both cancellous and cortical bone and Young’s modulus in the femur (Wachter, 2002), (Wachter et al., 2001).

## 1.2 Precision and Accuracy

In bone densitometry, “precision” refers to the reproducibility of a density measurement in a subject. “Accuracy” refers to the fidelity of the measured quantity to the actual value. The International Society for Clinical Densitometry recommends expressing precision error as the root mean square of the standard deviation of repeated measurements on a single subject. This can alternatively be expressed as the coefficient of variation ( $CV = STDEV/MEAN$ ). Using the CV, one can determine the “Least Significant Change” for a pQCT measurement. The Least Significant Change (LSC) is the least amount of measured change (such as trabecular area or BMD) that can be considered as statistically significant. Sievanen and coworkers (Sievanen et al. 1998) conducted precision

studies with the Stratec XCT-3000, a pQCT machine commonly used for human tibial measurements. From this study, we estimate that in order to be 95% confident that density changes are significant, they would have to be greater than:

2% in trabecular bone in the distal tibia

2% in cortical bone in the tibial shaft.

Other studies have calculated the precision of secondary density measurements arising from pQCT machines. Bone Mineral Density (BMD) can be correlated with Bone Mineral Content (BMC), which is the total density of a section of bone, as follows:

$$\text{BMC} = (\text{Cross sectional area}) * (\text{BMD}) * (\text{slice thickness}).$$

In the radius, using a Norland-Stratec XCT 960, cortical BMC had a 7-10% error (Louis et al. 1996). Total BMC error (cortical, subcortical, and trabecular) was reported as 17% (Louis et al. 1996) which may have been due to the larger trabecular content at the distal end, or perhaps, measurement error.

The Norland-Stratec XCT 3000 reports geometric area errors of about  $\pm 1\%$  ((Braun et al. 1998)), though the Sievanen study reported that the LSC for areal measurements was on the order of 5-10% for the same machine.

### **1.3 Subject Tibia Images**

Raw images were obtained from pQCT of tibia of 17 subjects. Images were taken at 4% of tibia length (measured from the distal end), 38%, and 66%. Each level will be referred to as a “slice plane”. Images were taken, at each location for each subject, before, in the middle of, and after a 13 week planned exercise regimen. The subjects in this study were from a group undergoing a training regimen which include both aerobic and resistance training

## 2. Methods

### 2.1 Image Processing

#### 2.1.1 Image Conversion

Raw image files were first converted to tiff format (630x630 pixels; 16 bits per pixel grayscale). This conversion produced no loss of bit-depth. The tibia cross-sections in each image were separated from the surrounding image by a two step process. First, all pixels were eliminated which were outside minimum and maximum pixel intensity bounds, determined by trial-and error. Then, the tibia cross section was found from the remaining pixels using the Matlab **bwareaopen** function in the Image Processing Toolbox. This function identifies objects (defined as connected pixels) with fewer than a given number of pixels.

The histograms for one subject are shown in Figure 1 and the threshold values are summarized in Table 1. These thresholds were used to extract the tibia from the surrounding image, and are not the same as the thresholds used to distinguish different types of bone (i.e., trabecular or cortical). Note in Figure 1 that the tibia at the 4% slice is essentially uniformly trabecular (pixel intensity of about 500) while the 38% and 66% slices reflect peaks in the trabecular and cortical regimes. The lower density peaks in the 38% and 66% images reflects the pixels in the canal center which includes nonosseous tissues and fluids.

Having extracted the tibia, the bounding box for each image is adjusted from 630x630 to the minimum box which will contain the image. These are shown in Figure 2.

Two subjects (14 and 60) were of the left tibia. These tibias were transposed so that meaningful comparisons could be made with the right tibia images.

Table 1. Threshold values used to separate the tibia from the surrounding image.

	<b>Lower Pixel Intensity Threshold</b>	<b>Upper Pixel Intensity Threshold</b>	<b>Maximum number of connected pixels in object</b>
4%	380	2000	2000
38%	500	2000	1250
66%	500	2000	1000

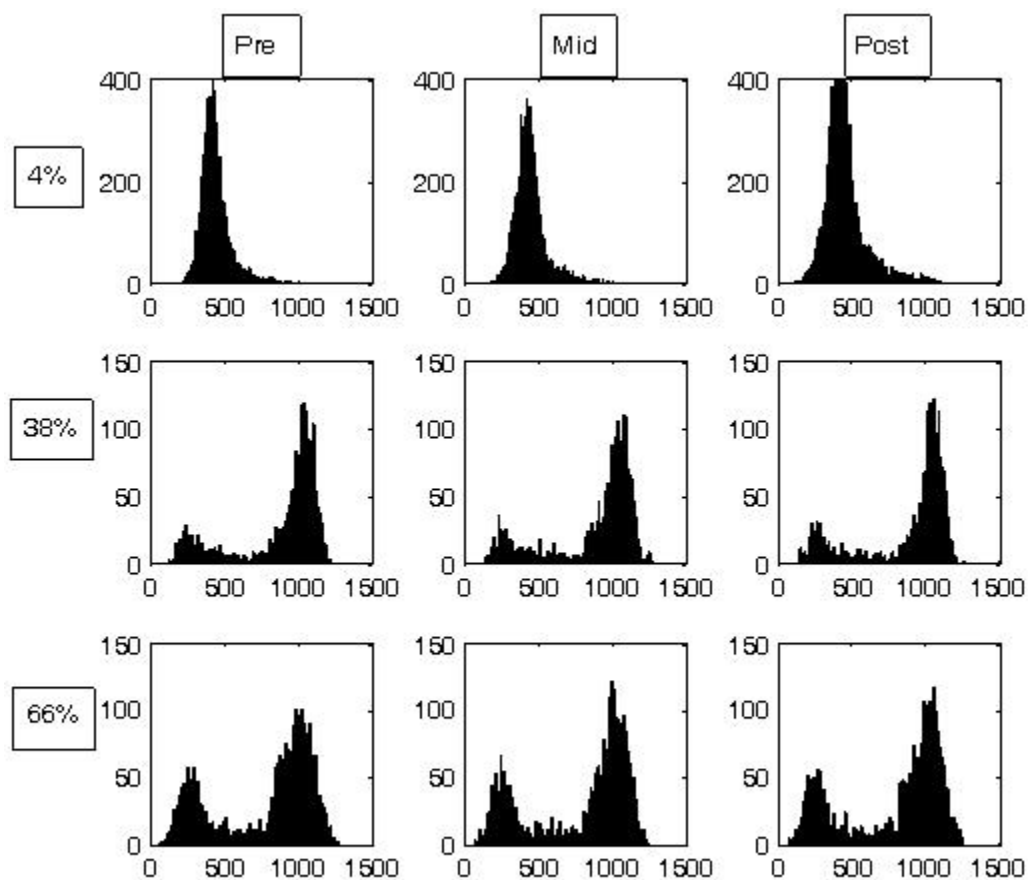


**Figure 1. Histogram for subject 48.**

*The pixel intensity distribution (a function of mineralized bone) is typical for each slice at each phase of training. Note that relatively few pixels exist between the trabecular and cortical thresholds.*

### **2.1.2 Image Registration**

In order to perform meaningful regional statistical comparisons between images, the images had to be aligned globally and with respect to each other.

For each subject, the “mid” and “post” images were aligned onto the “pre” image for a given slice plane (4%, 38%, or 66%). The registration procedure is summarized here:

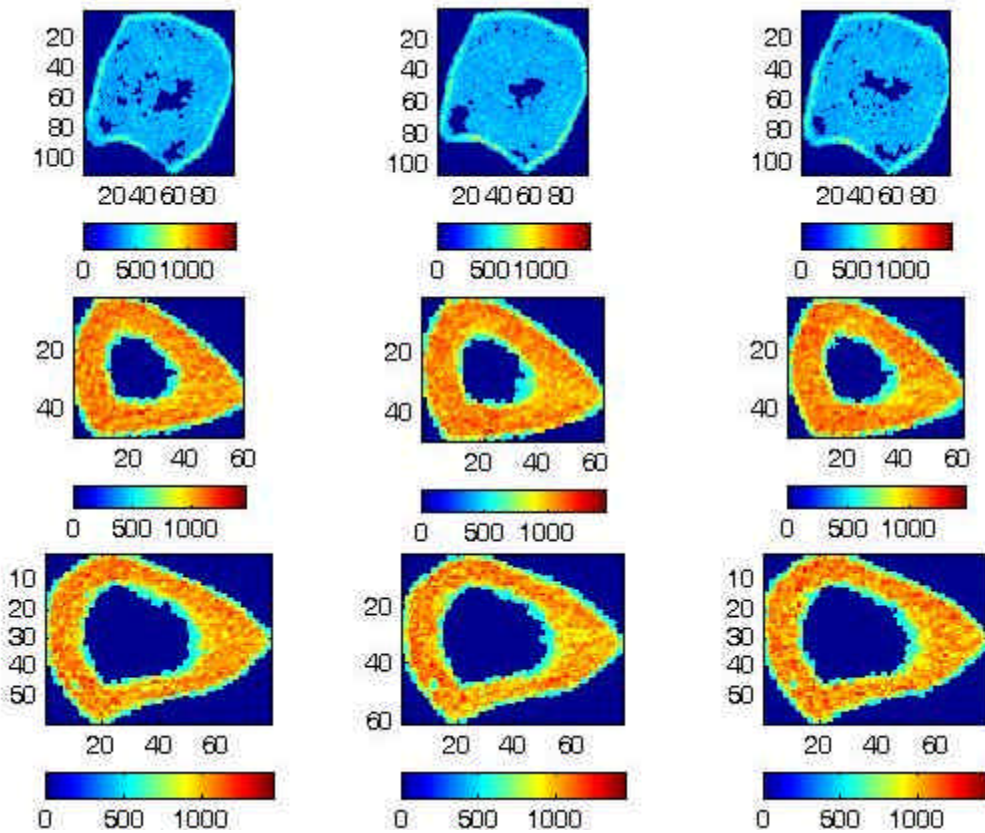


**Figure 2. Imported tibia images with a tight bounding box.**

1. The points on the outer boundary of the tibia are determined.
2. The image is re-centered horizontally on the average of the mean value of the 10 leftmost points and the mean value of the 10 rightmost points.
3. The image is similarly re-centered vertically.
4. Determine the points on the endosteal surface (38% and 66% slices only)
5. Edge of the endosteal surface is defined as a pixel with a minimum pixel intensity of 900.
6. Re-center the “mid” and “post” images on the mean value of the “pre” image endosteal boundary.
7. Rotate all nine images of a subject such that the “mid” and “post” are aligned

Once the images were registered, meaningful statistical comparisons could be made between “pre”, “mid” and “post” images and across subjects. An example of the result of the image registration process is shown in Figure 3.

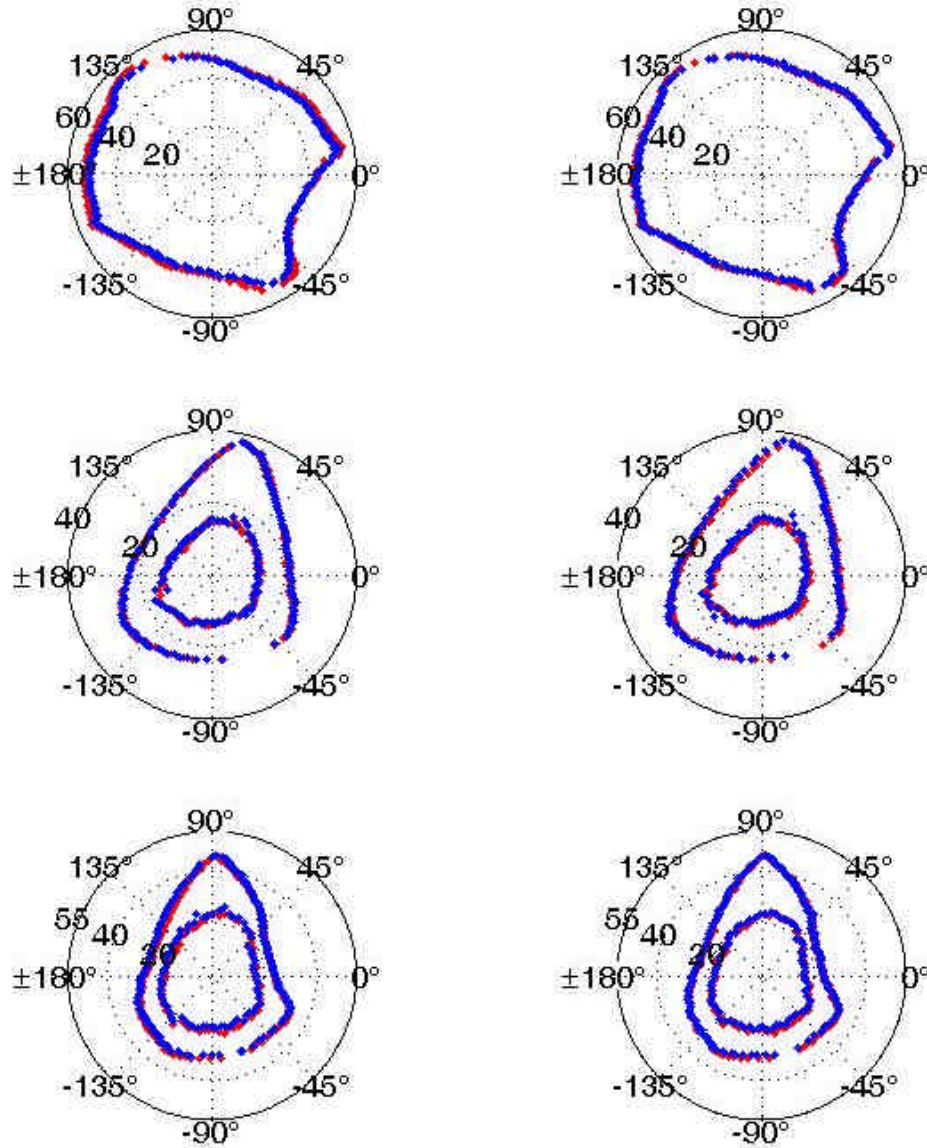


**Figure 3. Inner and outer boundaries following alignment. Left: Mid (blue) aligned to Pre (red). Right: Post (blue) aligned to Pre (red).**

## 2.2 Measurements

All measurements obtained from the images are dependent on the threshold values chosen to define different types of bone. These values were chosen such that trabecular bone would not, for example, include tissue or fluid, and cortical bone would not include pixels in a transitional region. These thresholds can typically set in the pQCT machine

itself at the time the image is acquired, but since they weren't, the analysis is based on trial-and-error.

### 2.2.1 Cortical Thickness

The cortical wall thickness was calculated for 10 degree sectors. In each sector, the minimum radial distance was calculated between the points defining the outer boundary and the points defining the inner boundary. Additionally, the normalized canal radius, defined as the ratio of endosteal radius to periosteal radius, was calculated for each sector. An example of the location of a tibial image in polar coordinates is given in Figure 4.

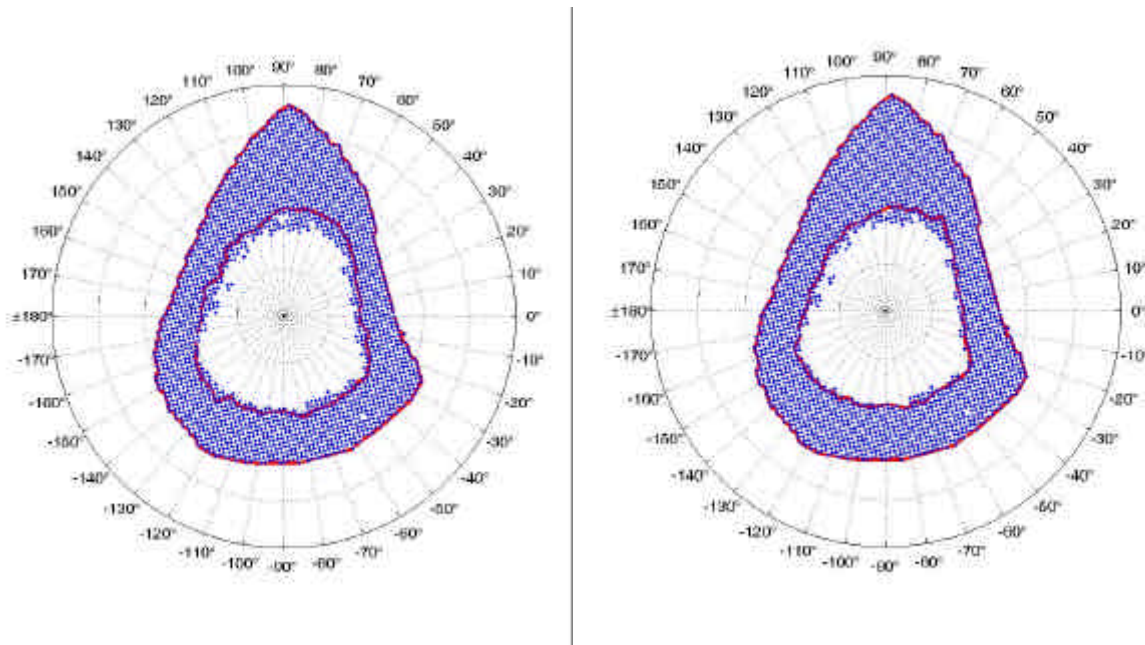


**Figure 4. Examples of inner and outer cortical boundary definitions.**

*The exact location of the inner boundary depends on the minimal pixel intensity defined as being cortical bone. Shown are two different intensity values. LEFT: using a pixel intensity of 900 and 750 (right) as lower cortical thresholds. Cortical thickness was measured for each 10 degree sector.*

### 2.2.2 Density Calculations

Average values for density were calculated for each sector as follows. Upper and lower pixel intensity values are chosen for the type of bone of interest. These values were set at:

- (a) Trabecular: 375 to 600
- (b) Transitional: 600 to 800
- (c) Cortical: 800 to 1500

Then for each 10 degree sector, the mean value and standard deviation of pixel intensity is calculated from among pixels within the specified thresholds.



### 2.2.3 Moment of Inertia

The geometric character a bone diaphysis can be described by both the amount of cortical bone present (the cross sectional area) and its spatial arrangement (architecture) (Ferretti 1997). A single scalar which captures both the amount and arrangement of compact bone in the diaphysis is the Cross Sectional Moment of Inertia (CSMI).

CSMI were calculated about two axes, the Medial-Lateral axis (M-L) and the Anterior-Posterior axis (A-P) using the center of the endosteal (inner) boundary as the origin. Units of pixels were used. The moment of inertia of each pixel was,

$$I_{pixel} = \frac{(b)(h)^3}{12} \quad 1$$

where  $b$  is the pixel base length and  $h$  is the pixel height, both of which are equal to 1. The parallel axis theorem was then used to sum the moments of inertia of each pixel,

$$I_{total} = \sum_{j=1}^{j=Num.Pix.} I_{pixel} + (A)(d^2) \quad 2$$

CSMI is needed to calculate the cortical Bone Strength Index , an index of the overall mechanical competence of the bone (Ferretti 1997). BSI was calculated for each CSMI as the product of the CSMI and the average cortical density:

$$BSI (M-L) = CSMI(M-L) * Ct.D.$$

$$BSI (A-P) = CSMI(A-P) * CT.D.$$

$$pBSI = BSI(M-L) + BSI(A-P).$$

### 2.2.4 Other Geometric Properties

The tibia area was calculated by summing the pixels in a given threshold range. The overall M-L was calculated using the difference between the average values of the 10 right-most and 10 left-most pixels. Similarly, the A-P length was calculated using the difference of the 10 upper-most and 10 lower-most values.

### 2.2.5 Output

All geometric data and the sector-by-sector density values were written to an Excel spreadsheet which processed and plotted the results. (Polar plots were generated by a separate Matlab program.)

## 2.3 Statistical Analyses

### 2.3.1 Changes due to Training

The intent of this portion of the analysis was to answer the following question: *“Did the 15 week training regimen result in measurable changes in density or shape?”*

To answer this question, statistical comparisons were made of the mean density in each sector of each image as well as the area occupied by trabecular, transitional, and cortical bone.

### **2.3.2 Bone Quality vs. Geometry**

The intent of the second phase of the analysis was to answer the question: “*What generalizations can be made regarding how density varies within a bone?*” And the related questions: “*Is density homogeneous throughout a cross section?*” and “*Does thinner bone tend to be more dense than thicker bone?*”.

### 3. Results

#### 3.1 Changes due to training

##### 3.1.1 Trabecular Density

The 4% slice images were composed primarily of pixels in the trabecular threshold bounds (375-600). For this reason, statistics involving cortical bone were not calculated for bones at the 4% level. Since trabecular bone requires, on average, 4 months to remodel versus 5 months for cortical bone, we hypothesized that any remodeling changes due to the training regimen would most likely be seen in trabecular bone, though not necessarily at the 4% slice.

##### Trabecular: 4% Slice

Trabecular density averaged among the 17 subjects for each 10 degree sector is shown in Figure 5. Shown are values obtained from the pre, mid, and post training images.

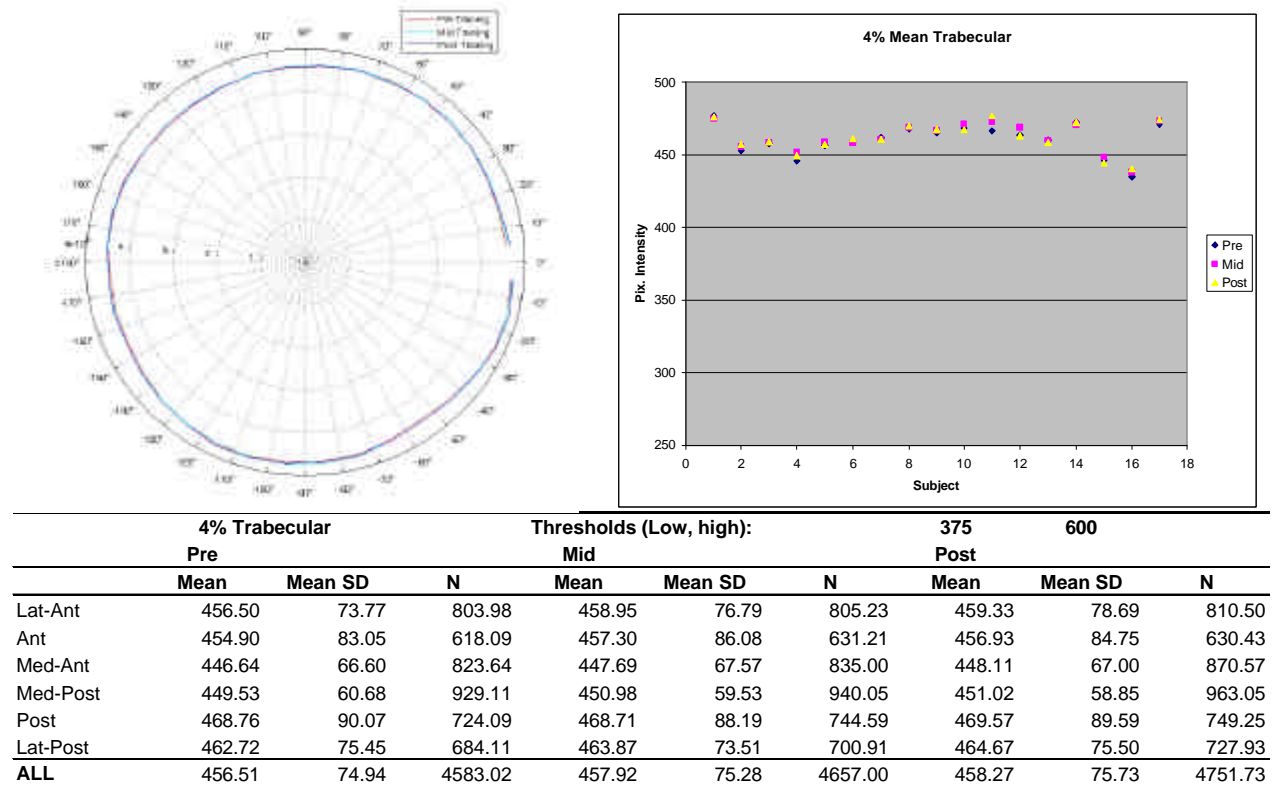


**Figure 5. Top left: Average trabecular density (Pre, Mid, and Post training) by sector of the 4% slice. (Subjects 3 and 11 post-training images have some image noise, but are included.)**

*Trabecular threshold limits: 375 to 600. Top right: individual mean trabecular values. Bottom: data table for 60° sectors, averaged among all subjects.*

The mean trabecular density measured for each subject was found to be very consistent at the three training intervals (pre, mid, and post). Peak densities were in the posterior and lateral sectors, but it should be noted that the Anterior-Posterior axis was estimated using the “cusp” of the 66% slice, and so these designations are approximate. Among all subjects, the sectors with the maximum density had a mean trabecular density 6% higher than the sectors with the lowest mean density. The maximum density difference between one sector and another seen in an individual was about 10% (between Medial-Posterior and Lateral-Posterior). The minimum density difference for an individual (that is, the most homogeneous bone at the 4% slice plane) was about 1.7%.

Trabecular apparent density measurements are most accurate at the 4% slice plane level due to the sheer number of pixels falling in trabecular threshold range (about 5000 versus 100 at 38% and 200 at 66%). While trabecular BMD measurements are less reliable than for cortical bone due to the higher collagen content of the former and the fact that trabecular bone is properly a structure, not a material, the fact that the measurements were consistent on an individual basis over the three measurement intervals suggest that *intratibial* density are probably highly patient specific.

Despite the apparent increase in trabecular area (“N” in the data table for Figure 5) a student’s t test was used to compare mean pretraining to mean post training areas among all 17 subject. The result showed there was no significant change from pre to post training at the 4% level.

#### Trabecular: 38% Slice

There are much fewer pixels in the trabecular range at the 38% level (note the average number N of pixels in the data table of Figure 6).

Trabecular bone comprised, on average, just 6.5% of the total bone area (“area” being defined simply as the number of “trabecular pixels” in the image).

Among the 17 subjects, there was no significant change in trabecular area from pre to post training at the 38% level. The average trabecular area change was 6% but had a standard deviation of  $\pm 17\%$ . With an outlier removed the average trabecular area change was 2% with a standard deviation of  $\pm 8\%$ .

#### Trabecular: 66% Slice

The bone at 66% of tibial length is also predominantly cortical. The trabecular average densities are given in Figure 7.

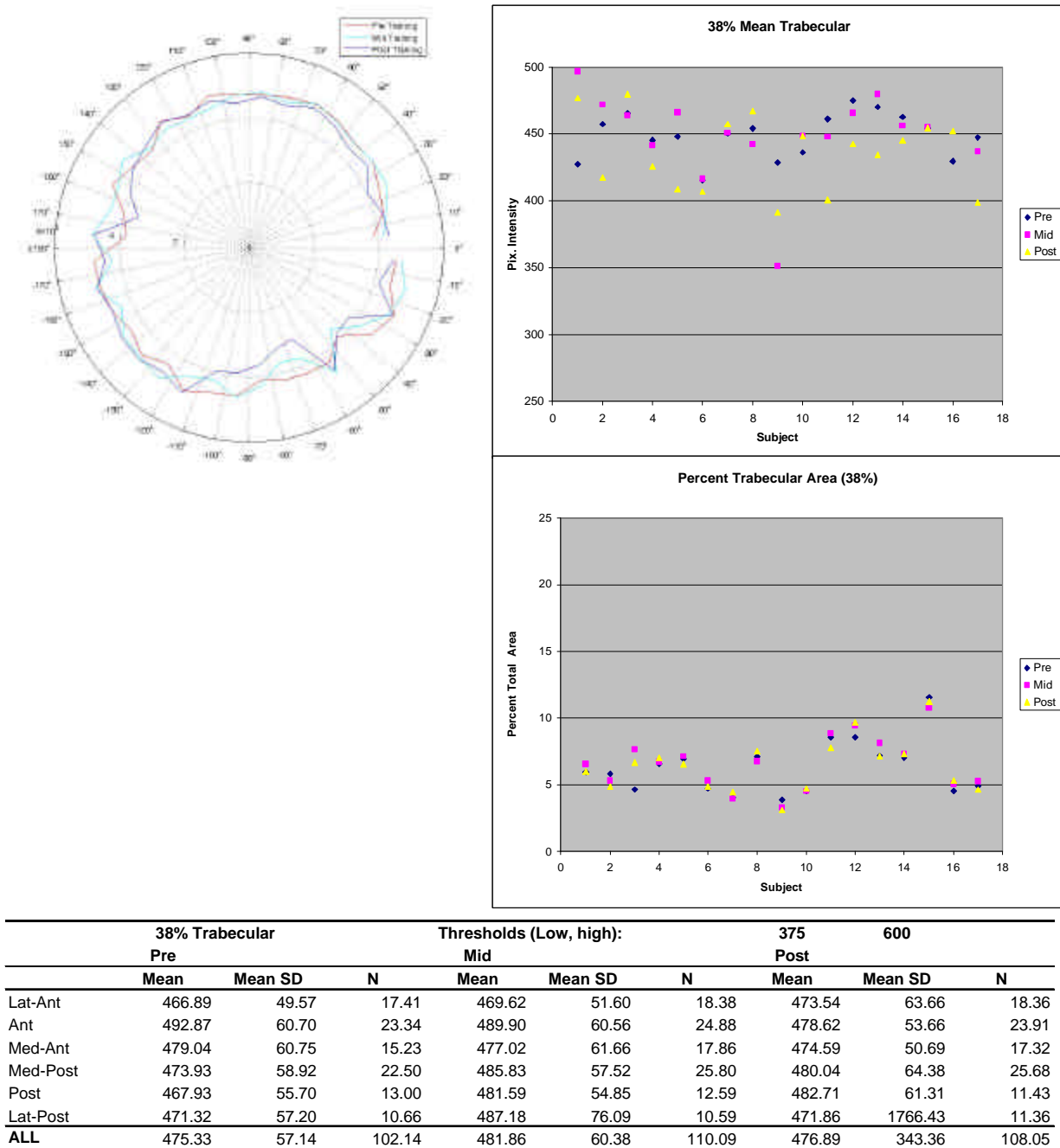
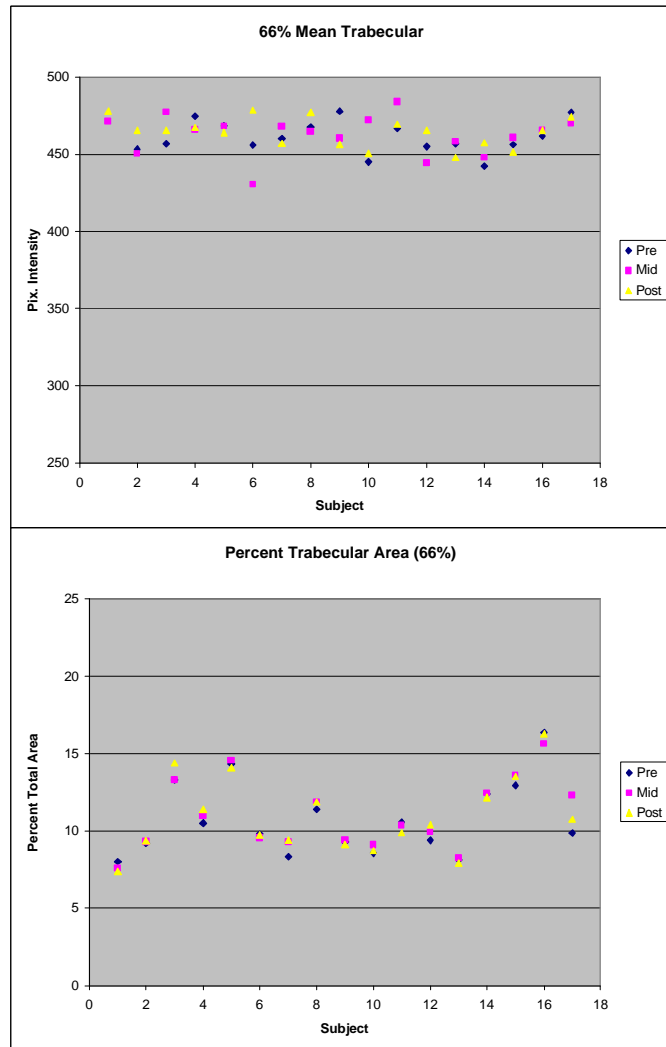
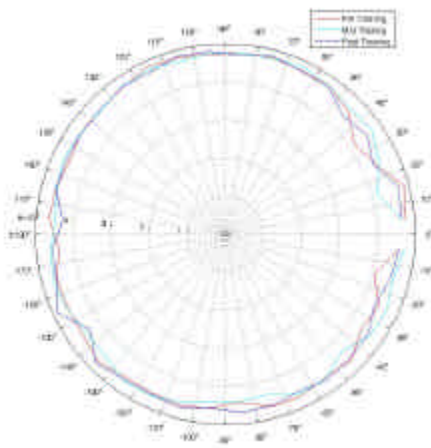


**Figure 6. Top left: Average trabecular density (Pre, Mid, and Post training) by sector of the 38% slice.**

*Trabecular threshold limits: 375 to 600. Note that the variability of density in any one sector is due to the few number of pixels in the trabecular range (N). Top right: individual trabecular averages. Middle row: individual trabecular area as a percent of total area. Bottom: data table for 60° sectors, averaged among all subjects.*



	66% Trabecular			Thresholds (Low, high):			375		600	
	Pre			Mid			Post			
	Mean	Mean SD	N	Mean	Mean SD	N	Mean	Mean SD	N	
Lat-Ant	465.03	55.51	39.46	464.51	59.38	37.96	464.45	58.50	39.79	
Ant	479.07	64.37	93.04	478.92	63.37	90.55	477.50	62.19	91.70	
Med-Ant	461.23	53.74	45.77	466.87	63.40	49.77	462.90	62.18	49.89	
Med-Post	470.09	59.34	28.34	457.77	65.84	25.30	464.06	56.28	27.27	
Post	460.66	58.70	26.88	462.15	59.69	25.82	469.50	61.09	24.96	
Lat-Post	464.44	67.22	20.89	463.16	60.28	24.34	461.90	54.31	21.34	
<b>ALL</b>	<b>466.75</b>	<b>59.81</b>	<b>254.38</b>	<b>465.57</b>	<b>61.99</b>	<b>253.75</b>	<b>466.72</b>	<b>59.09</b>	<b>254.95</b>	

Figure 7. Top left: Average trabecular density (Pre, Mid, and Post training) by sector of the 66% slice.

*Trabecular threshold limits: 375 to 600. Top right: individual average trabecular density values. Middle: trabecular area as a percentage of total area. Bottom: data table for 60° sectors, averaged among all subjects.*

Pixels in the trabecular threshold comprise, on average, 11% of the total. The maximum percentage of trabecular bone (pre, mid, or post training) is about 15% and the minimum trabecular percentage is about 8%.

Among the 17 subjects, there was no significant change in trabecular area from pre to post training at the 66% level. The average change in trabecular area from pre to post training was  $6\% \pm 5\%$ , but the range was -10% to 13%. Further, change in trabecular area at the 66% slice did not correlate with pretraining trabecular area or pretraining mechanical integrity (as measured by pBSI).

### 3.1.2 Transitional Density

The main reason for analyzing “transitional pixels” is to ascertain whether new bone might form near the cortex (at the boundary of cortical and trabecular bone) which may appear in the pQCT as subcortical. Results of the transitional data analysis for the 38% slice are given in Figure 8.

#### Transitional: 38% Slice

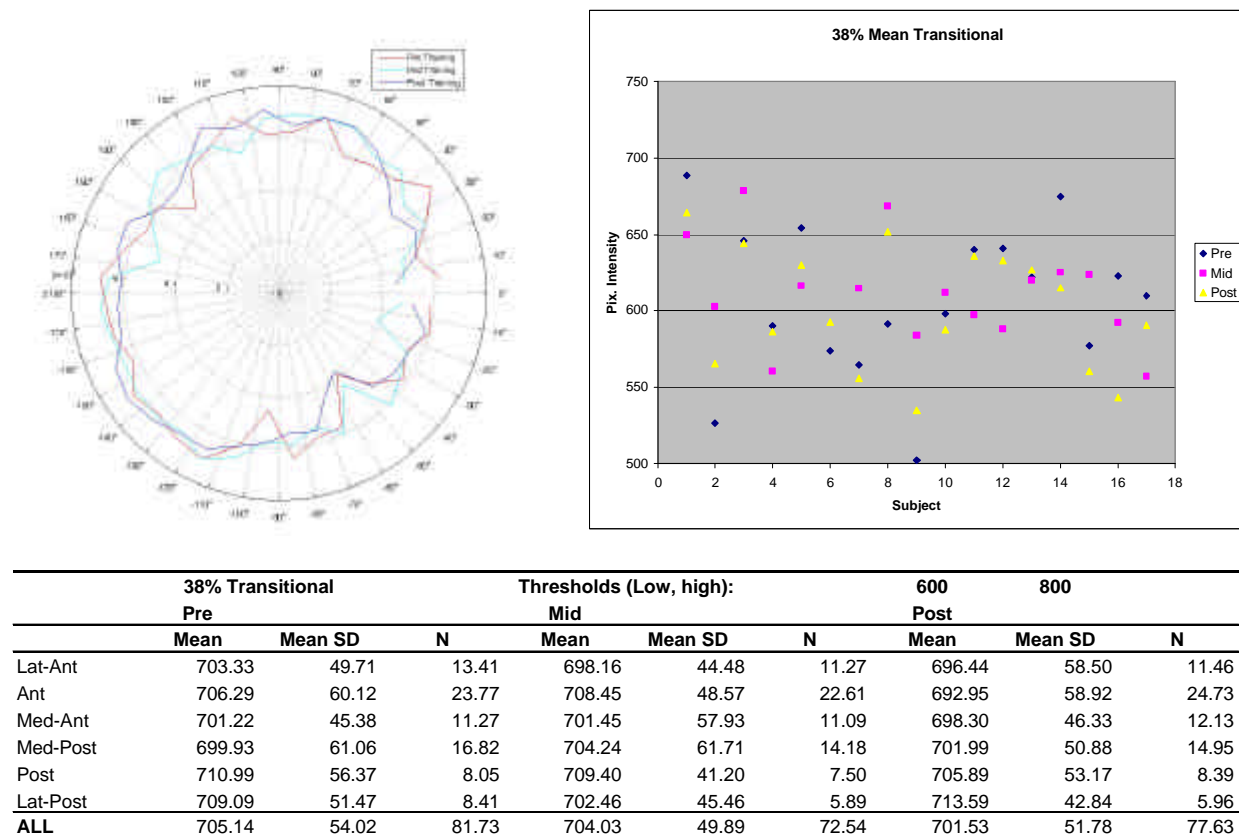


**Figure 8. Top left: Average transitional density (Pre, Mid, and Post training) by sector of the 38% slice.**

*Top Right: Individual mean transitional densities. Bottom: Data table for 60° sectors, averaged among all subjects. Transitional threshold limits: 600 to 800.*

The larger variation in average transitional density values at the 38% level is due to the small number of pixels falling in the transitional threshold range (about 110 pixels per picture).

No significant change was noted from pre to post training in transitional bone at the 38% level.

### Transitional: 66% Slice

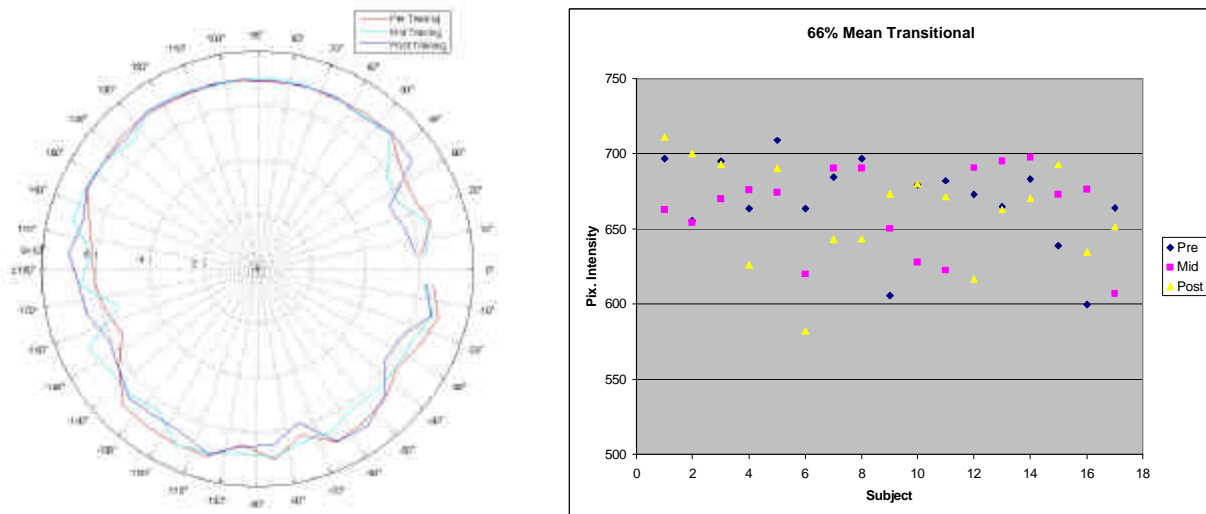


Figure 9 is a summary of statistics of transitional pixels in the 66% slice plane.

	66% Transitional			Thresholds (Low, high):			600 800		
	Pre			Mid			Post		
	Mean	Mean SD	N	Mean	Mean SD	N	Mean	Mean SD	N
Lat-Ant	696.44	58.50	17.20	699.11	59.09	15.77	696.02	53.62	16.07
Ant	692.95	58.92	45.91	699.61	58.11	46.70	696.54	60.17	47.09
Med-Ant	698.30	46.33	18.71	694.88	54.73	18.09	692.91	53.00	20.91
Med-Post	701.99	50.88	12.09	695.02	56.52	13.00	694.61	44.37	13.86
Post	705.89	53.17	22.14	707.08	53.43	23.41	711.50	55.47	22.61
Lat-Post	713.59	42.84	13.09	711.52	45.61	12.68	711.62	54.64	12.09
<b>ALL</b>	<b>701.53</b>	<b>51.78</b>	<b>129.14</b>	<b>701.20</b>	<b>54.58</b>	<b>129.64</b>	<b>700.53</b>	<b>53.54</b>	<b>132.63</b>

**Figure 9. Top left: Average transitional density (Pre, Mid, and Post training) by sector of the 66% slice.**

*Top right: Individual mean transitional densities. Bottom: Data table for 60° sectors, averaged among all subjects. Transitional threshold limits: 600 to 800.*

No significant change in transitional density or area was observed at the 66% level from pre to post training.



### **3.1.3 Cortical Density**

#### **Cortical: 38% Slice**

Average values of pixels in the cortical range for the 38% slice plane are given in Figure 10.

Among all subjects there was an average difference of about 4.7% between peak density in a Posterior sector and minimum density in the Anterior sector. The most homogenous cortical bone had peak density which about 2% greater than the minimum density. The largest density gradients seen were roughly 6.5%, typically in the Medial-Posterior direction. The Anterior sectors had the most homogeneous cortical bone, as indicated by a lower mean Standard Deviation (see standard deviation plot and data table in Figure 10).

Among all subjects, there was no significant change in mean cortical density or mean cortical area from pre to post training.

#### **Cortical: 66% Slice**

Average values of cortical bone for the 66% slice plane images are shown in Figure 11.

The average difference between peak sector cortical density and minimum sector cortical density was approximately 5%. The largest difference between Anterior and Posterior sectors was in Subject 52 with 8% at midtraining, the smallest was Subject 02 which had a 2.5% difference at midtraining. As was the case with the images from the 38% slice plane, the bone is most homogeneous in the anterior sectors.

Among all 17 subjects, there was no significant change in cortical density or area from pre to post training.

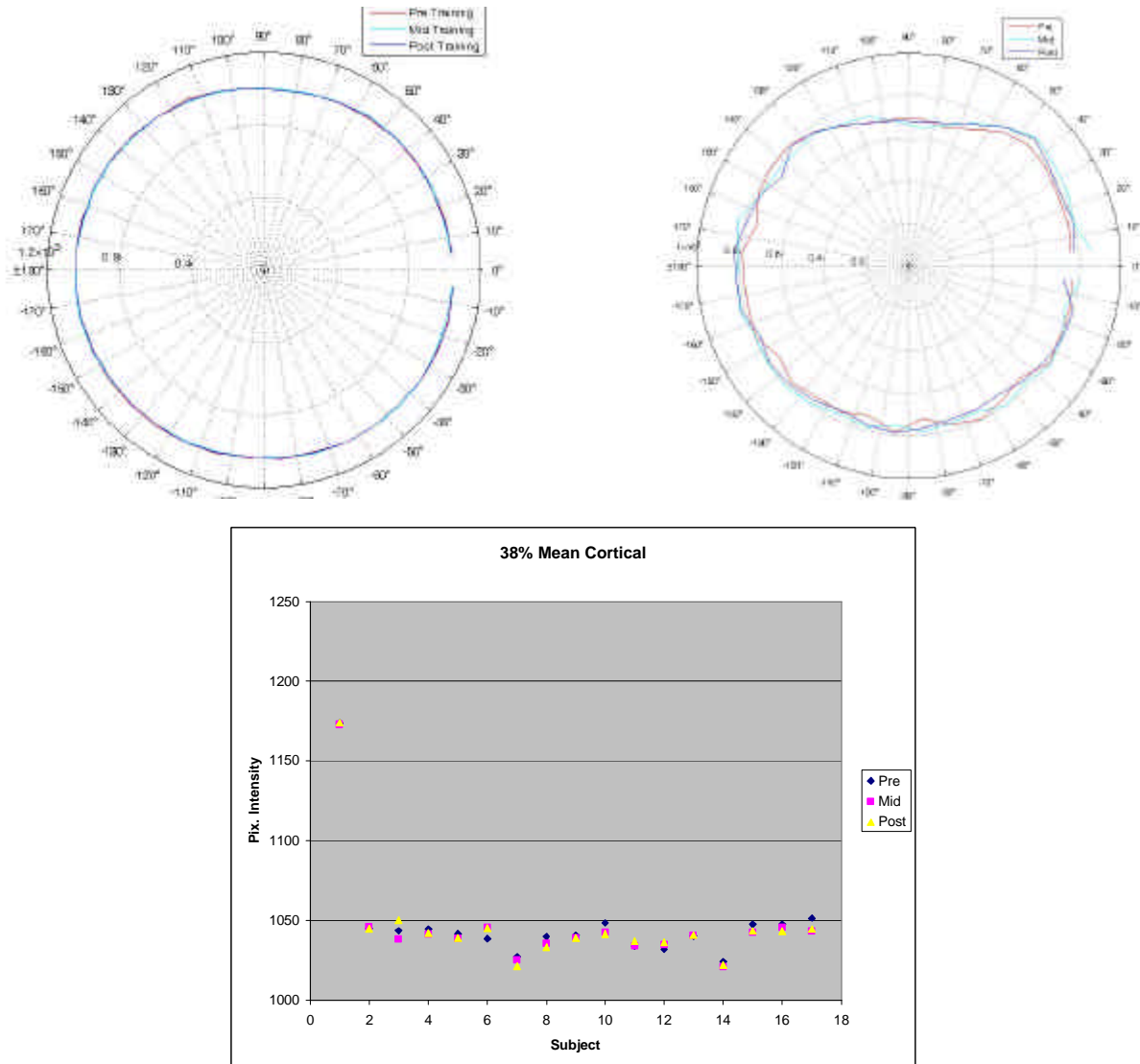
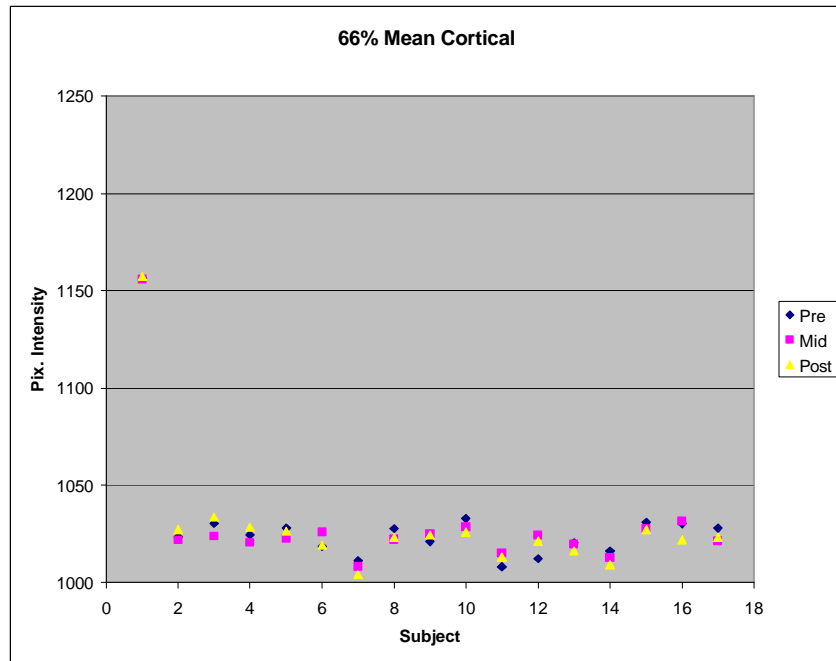
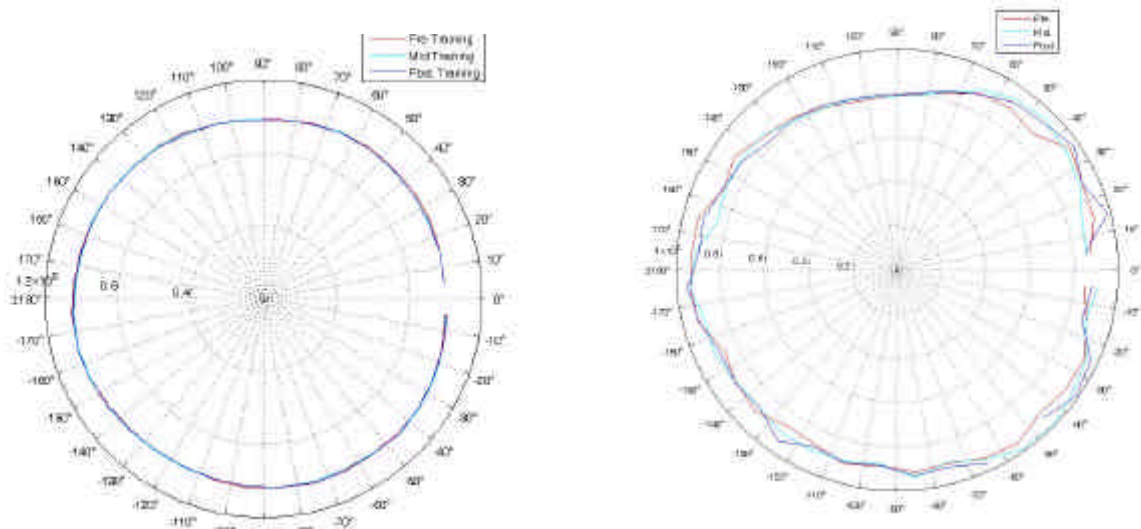


**Figure 10. Top left: Average transitional density (Pre, Mid, and Post training) by sector of the 38% slice.**

*Top right: average standard deviation (a measure of the homogeneity of the cortical bone). Middle: Individual mean transitional densities. Bottom: Data table for 60° sectors, averaged among all subjects. Cortical threshold limits: 800 to 1500.*



	66% Cortical			Thresholds (Low, high):			800 1450		
	Pre			Mid			Post		
	Mean	Mean SD	N	Mean	Mean SD	N	Mean	Mean SD	N
Lat-Ant	1006.96	88.52	168.45	1004.73	89.09	170.93	1001.87	91.92	165.29
Ant	998.59	83.59	457.55	1004.36	82.91	456.32	994.69	82.12	461.25
Med-Ant	1034.95	91.81	200.70	1034.68	87.11	200.84	1033.03	88.32	205.98
Med-Post	1043.71	91.28	256.89	1044.23	88.27	256.39	1041.28	91.37	263.05
Post	1039.36	91.05	355.61	1034.60	92.25	356.75	1035.45	93.59	357.02
Lat-Post	1034.74	91.01	249.25	1039.58	92.58	248.79	1034.52	95.04	246.46
ALL	1026.38	89.54	1688.45	1027.03	88.70	1690.02	1023.47	90.39	1699.05

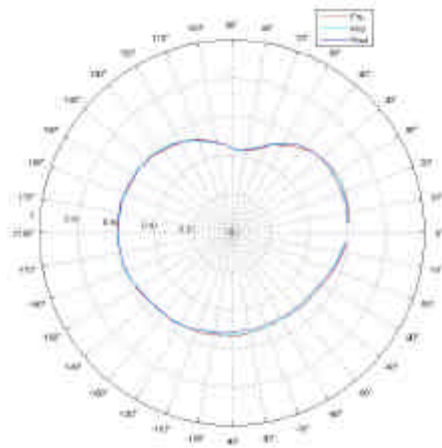
**Figure 11. Top left: Average transitional density (Pre, Mid, and Post training) by sector of the 66% slice.**

*Top right: Average standard deviation. Middle: Individual values for each subject. Bottom: Data table for 60 ° sectors, averaged among all subjects. Cortical threshold limits: 800 to 1500.*

### 3.1.4 Average Radius

Physical activity has been correlated with increased cortical thickness and periosteal circumference (Lorentzon et al. 2005), (Nordstrom et al. 1998). To ascertain whether the training regimen induced any changes in cortical bone size, the average canal radius is presented here for the 38% and 66% slice along with tables of normalized radius and cortical thickness. It was found that there was no significant increase in cortical thickness from pre to post training at either the 38% or 66% level.

#### Canal Radius: 38% Slice



38% Radius						
	Pre	Thickness	Mid	Thickness	Post	Thickness
	Norm.	Raw	Norm.	Raw	Norm.	Raw
Lat-Ant	0.6038	9.40	0.5997	9.41	0.5911	9.60
Ant	0.4782	15.65	0.4729	15.76	0.4703	15.80
Med-Ant	0.5867	8.85	0.5859	8.91	0.5789	9.02
Med-Post	0.5636	11.79	0.5589	11.95	0.5609	11.96
Post	0.5363	11.45	0.5363	11.38	0.5234	12.15
Lat-Post	0.5660	10.88	0.5585	11.11	0.5636	11.00
ALL	0.5558	11.34	0.5520	11.42	0.5480	11.59

**Figure 12. Top: Normalized canal radius at 38% of tibial length: pre, mid, and post training. Below: Data table of average values for all 17 subjects, 60° sectors.**

### Canal Radius: 66% Slice

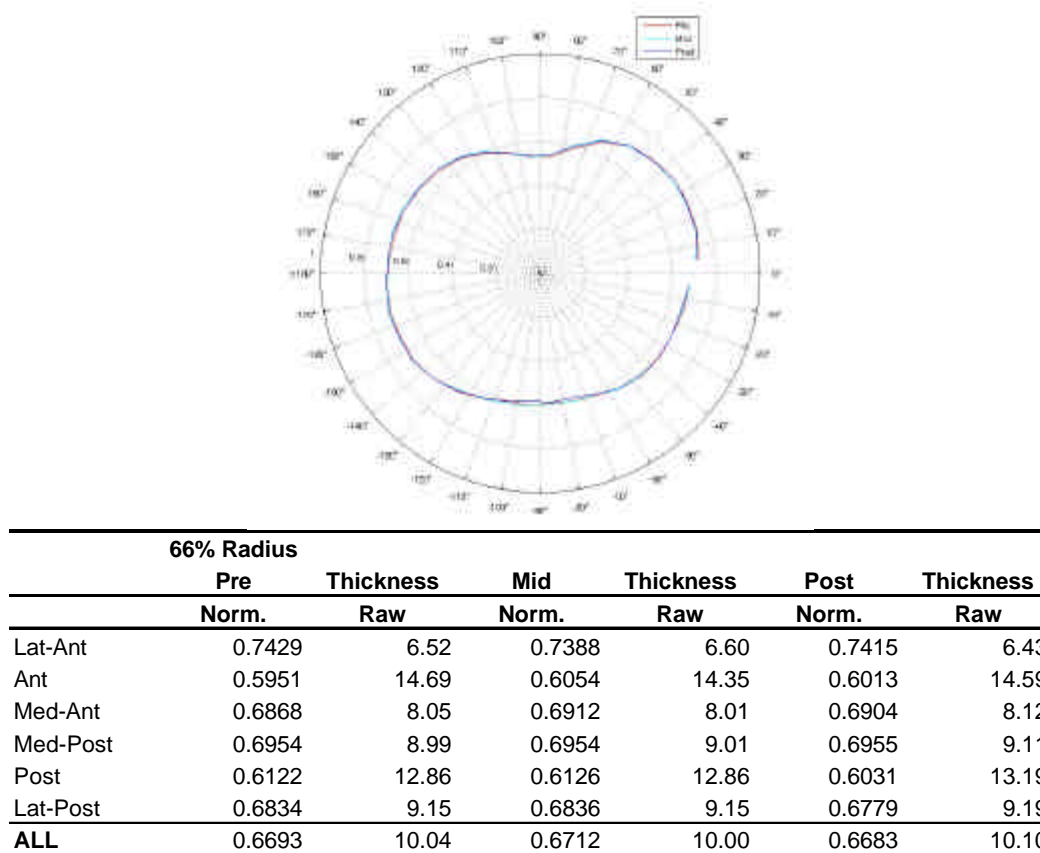


**Figure 13. Top: Normalized canal radius at 66% of tibial length: pre, mid, and post training. Bottom: table of average values for all 17 subjects, 60° sectors.**

### **3.1.5 Geometry and Strength Indices**

Scalar indicators of bone strength were calculated for each image to see if there was a strengthening trend from pre to post training, and also to evaluate the consistency of the measurement itself. Area, CSMI, and BSI are all quantities that can be calculated “on the fly” by the pQCT machine itself, and as such may be a useful way to make an initial assessment of bone health prior to the start of any long term physical regimen such as Basic Combat Training.

#### Area

Area measurements were subdivided for each image according to type of bone (trabecular, transitional, cortical) and are shown in Figure 14 to Figure 16. While no significant change in area was noted, areal measurements were found to be very consistent for each subject from Pre to Post training.

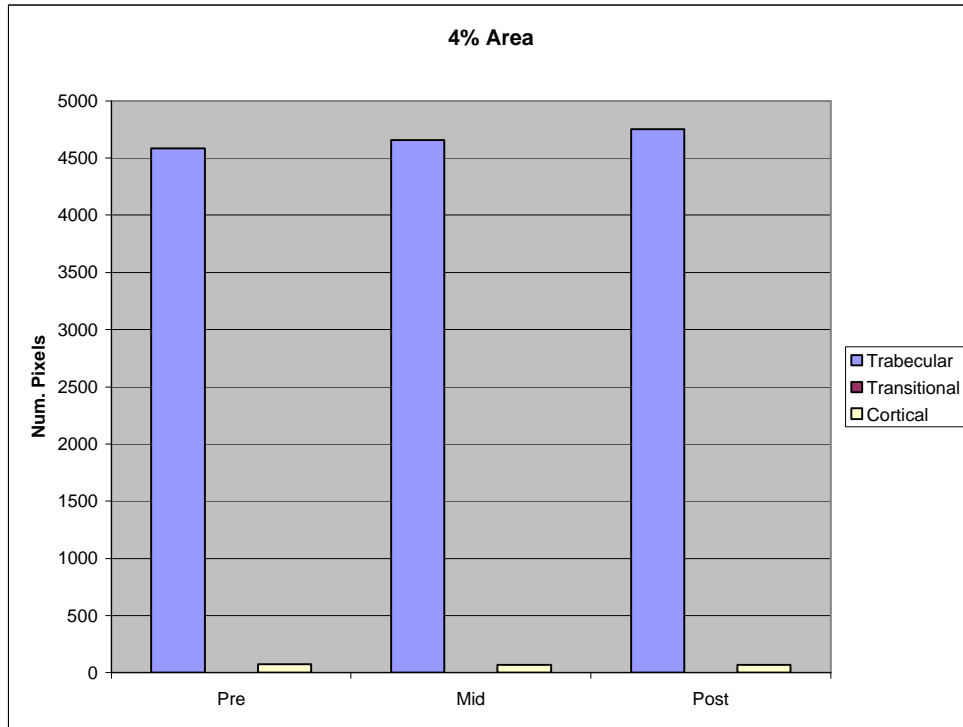


**Figure 14. Average area (trabecular, transitional, and cortical) for the 4% level: pre, mid and post training.**

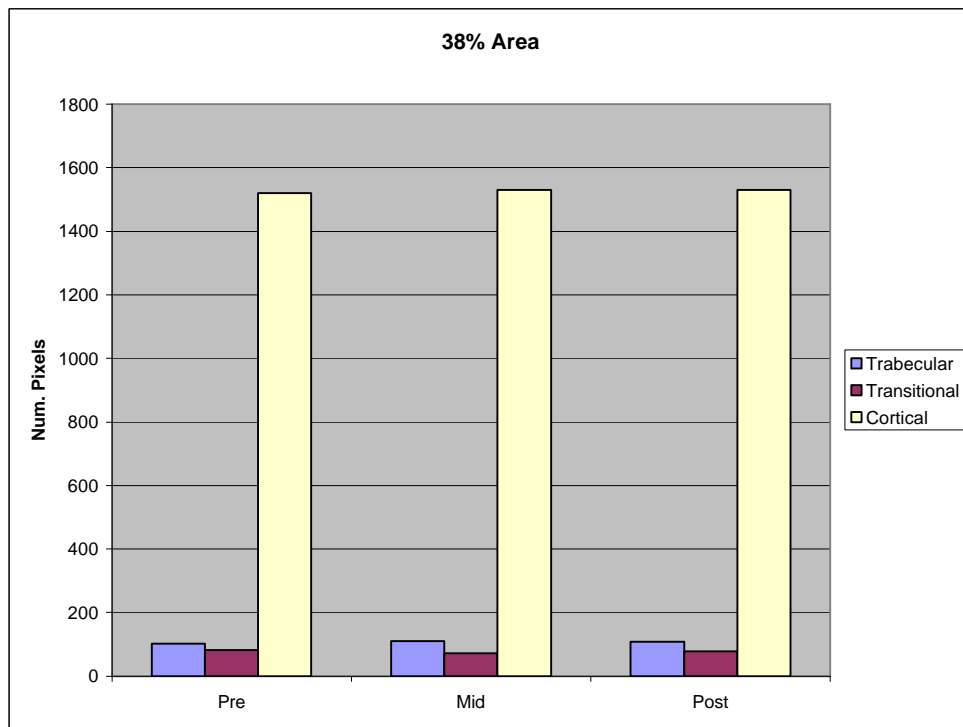


**Figure 15. Average area (trabecular, transitional, and cortical) for the 38% level: pre, mid and post training.**

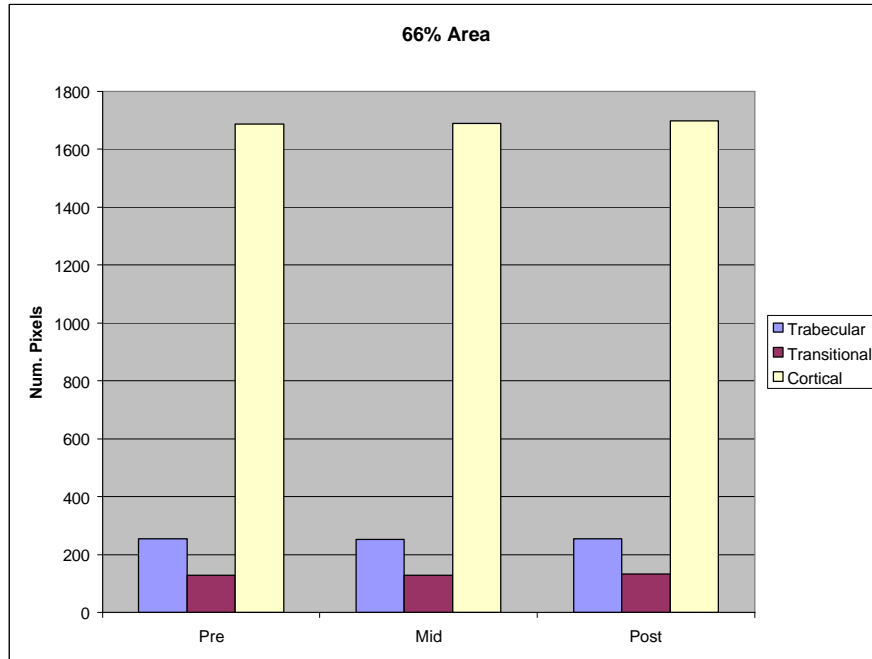


**Figure 16. Average area (trabecular, transitional, and cortical) for the 66% level: pre, mid and post training.**

### Moment of Inertia

Moments of inertia about various axes are shown for the 38% and 66% slice planes and averaged among all subjects in Figure 17 and Figure 18.

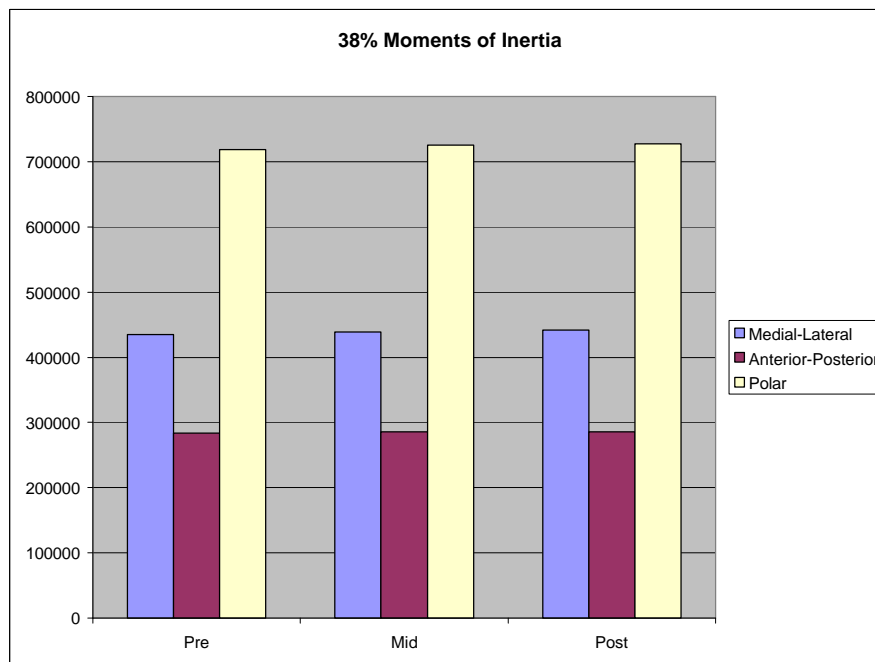


**Figure 17. Average CSMI (M-L, A-P, Polar) for the 38% level: pre, mid and post training. Units are  $\text{pixels}^4$ .**

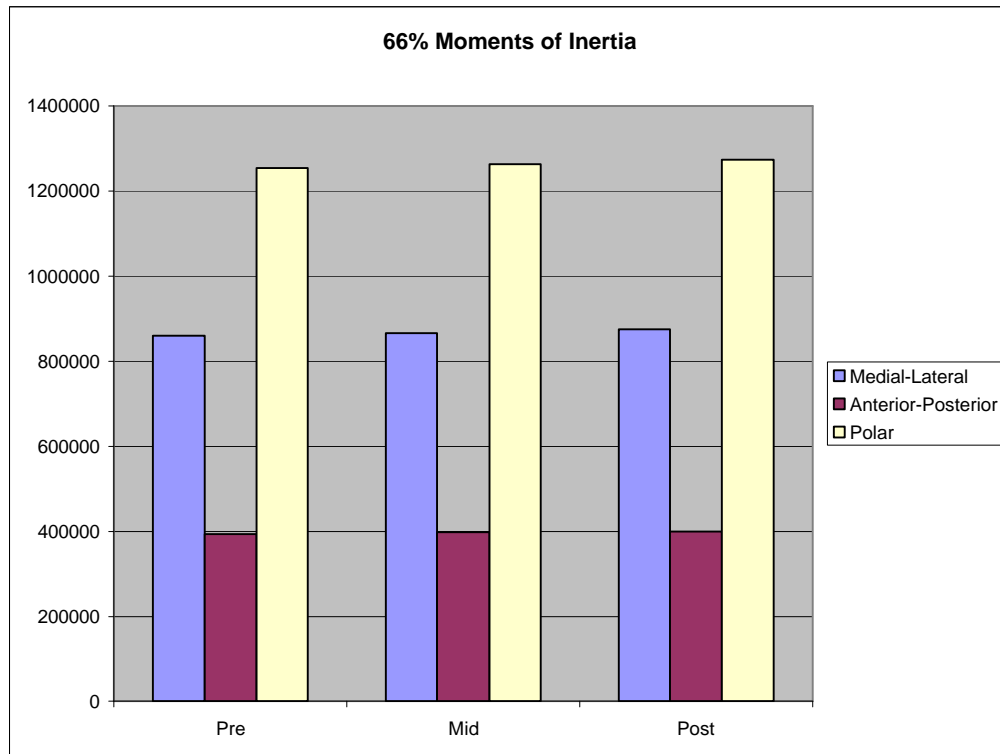


**Figure 18. Average CSMI (M-L, A-P, Polar) for the 66% level: pre, mid and post training. Units are *pixels*<sup>4</sup>.**

### Strength Indices

BSI was found to be a very repeatable and unique measurement for each subject. Figure 19 shows average values among all subjects. Values are consistent for BSI regardless of which axis they are measured about. Figure 20 through Figure 22 show various BSI values for each individual. The variation between “pre” values in subject 3 is due to image noise. Figure 21 and Figure 26 show BSI for the 66% level.



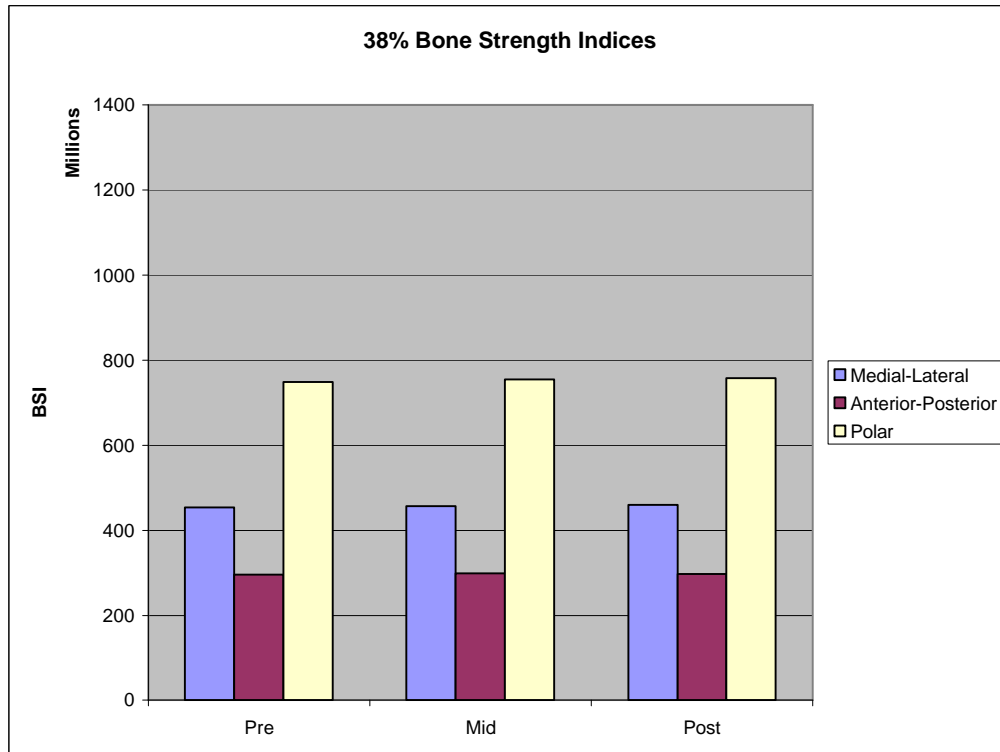


**Figure 19. Average BSI (M-L, A-P, Polar) for the 38% level: pre, mid and post training. Units are (pixel-intensity)(*pixels*<sup>4</sup>).**

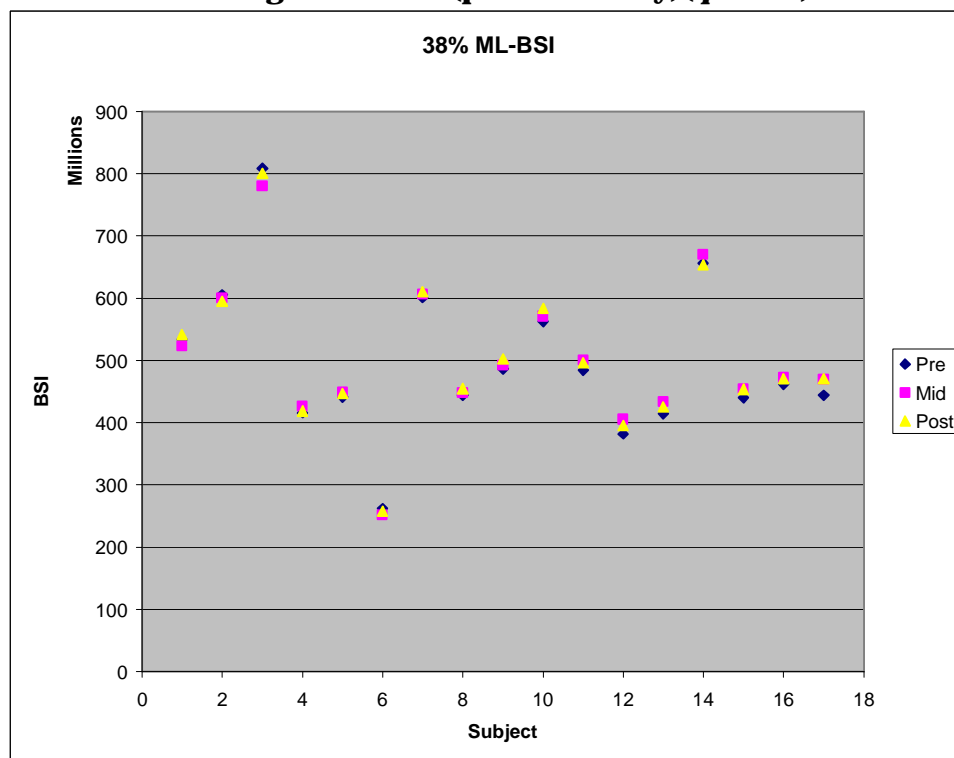


**Figure 20. Individual BSI (M-L) for the 38% level: pre, mid and post training. Units are (pixel-intensity)(*pixels*<sup>4</sup>).**

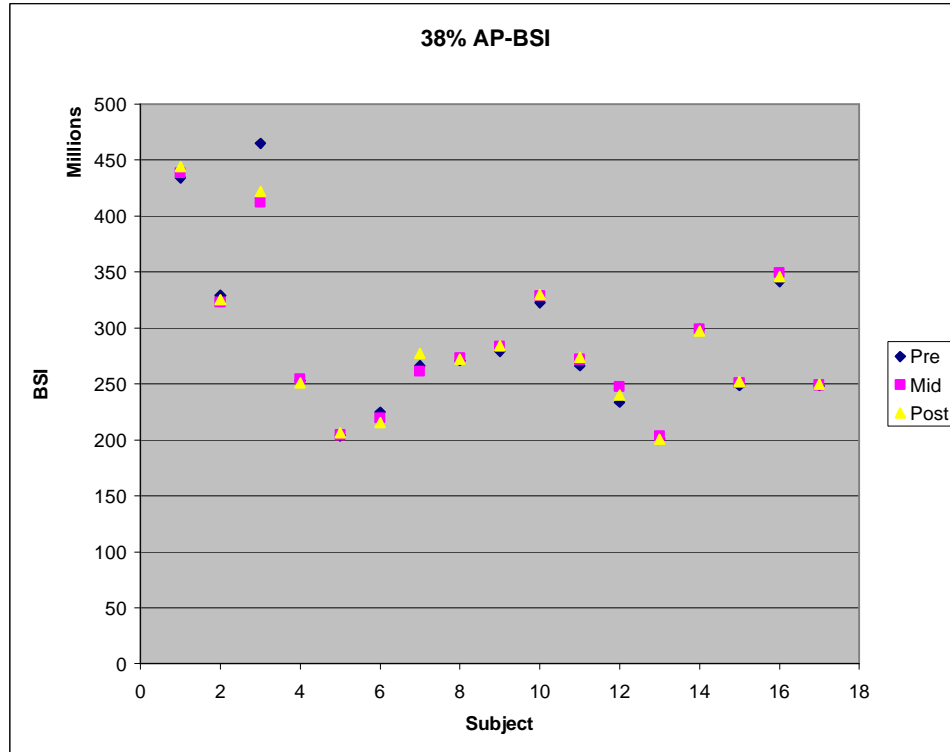


**Figure 21. Individual BSI (A-P) for the 38% level: pre, mid and post training. Units are *(pixel-intensity)(pixels<sup>4</sup>)*.**

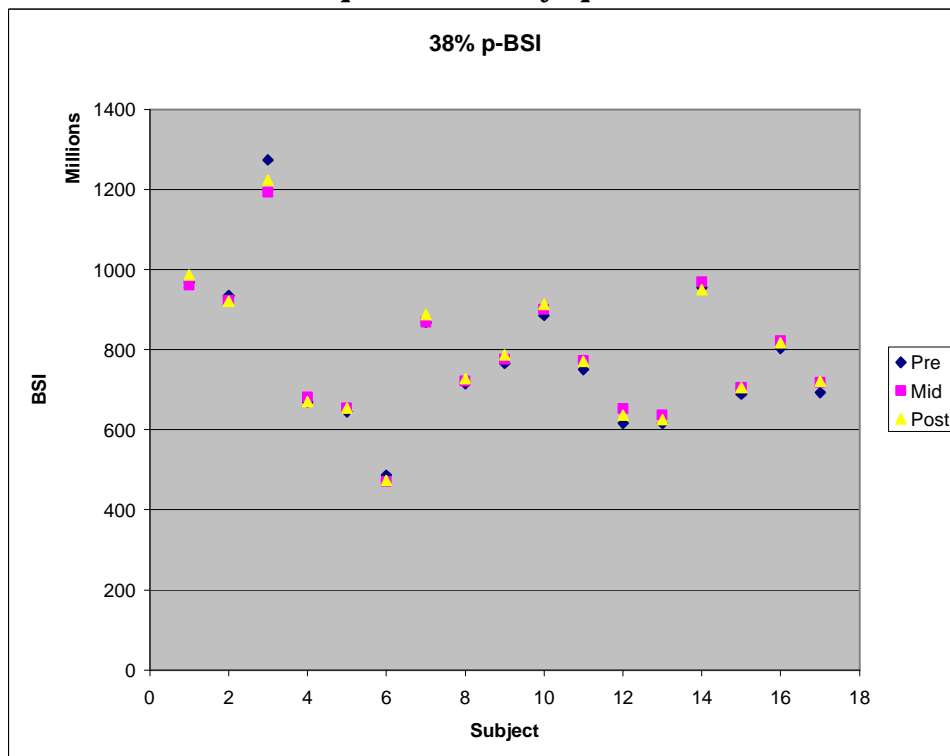


**Figure 22. Individual BSI (polar) for the 38% level: pre, mid and post training. Units are *(pixel-intensity)(pixels<sup>4</sup>)*.**

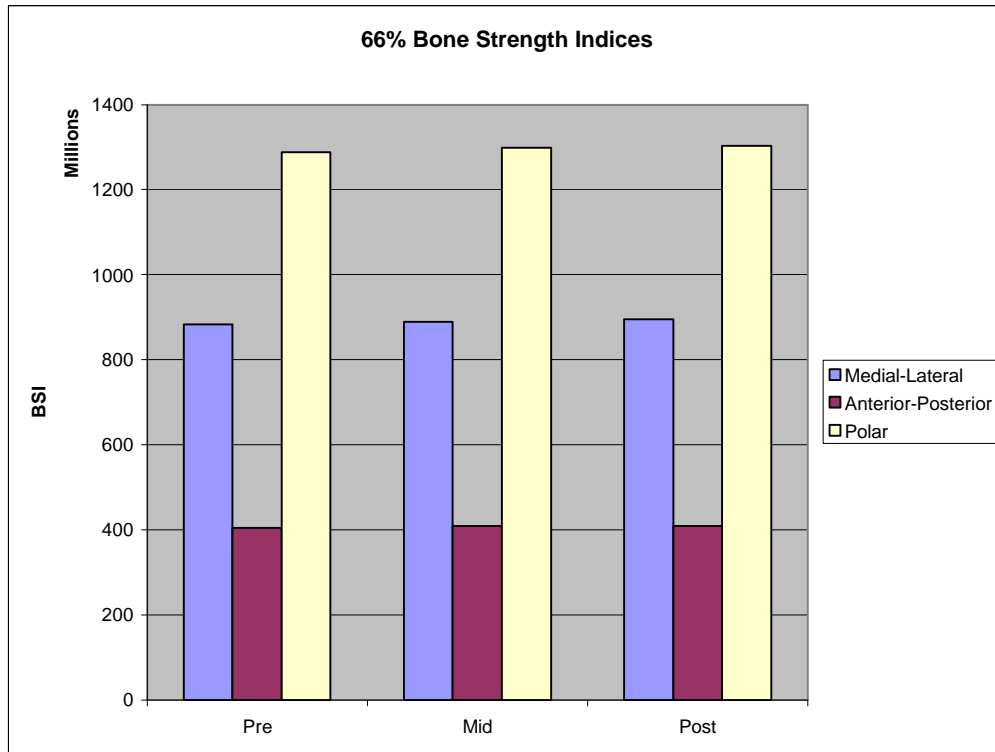


**Figure 23. Average BSI (M-L, A-P, polar) for the 66% level: pre, mid and post training. Units are *(pixel-intensity)(pixels<sup>4</sup>)*.**

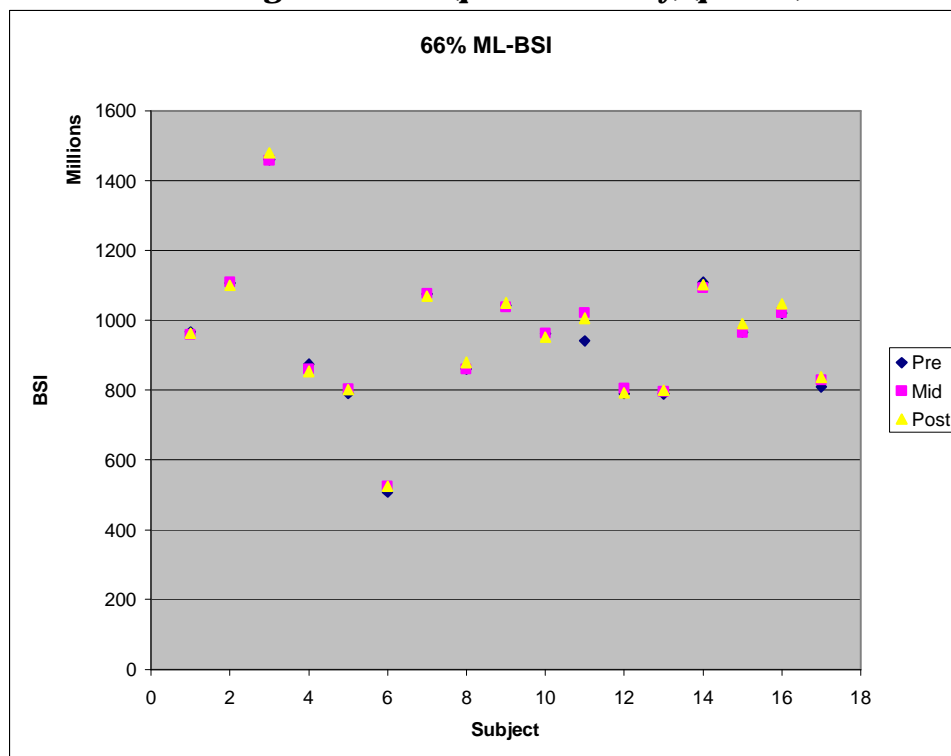


**Figure 24. Individual BSI (M-L) for the 66% level: pre, mid and post training. Units are *(pixel-intensity)(pixels<sup>4</sup>)*.**

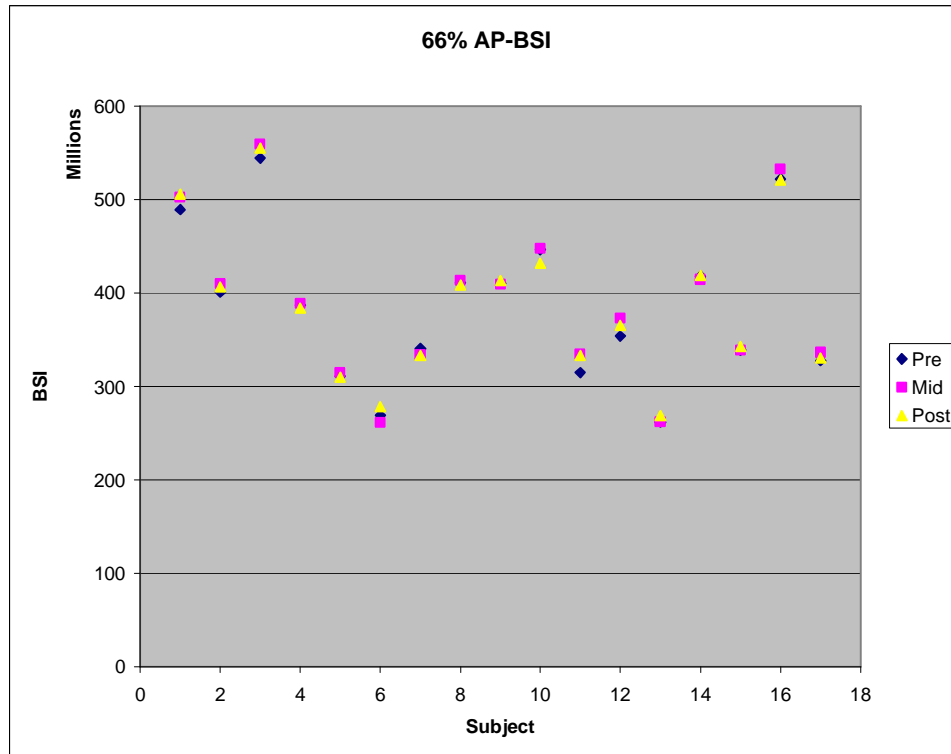


**Figure 25. Individual BSI (A-P) for the 66% level: pre, mid and post training. Units are *(pixel-intensity)(pixels<sup>4</sup>)*.**

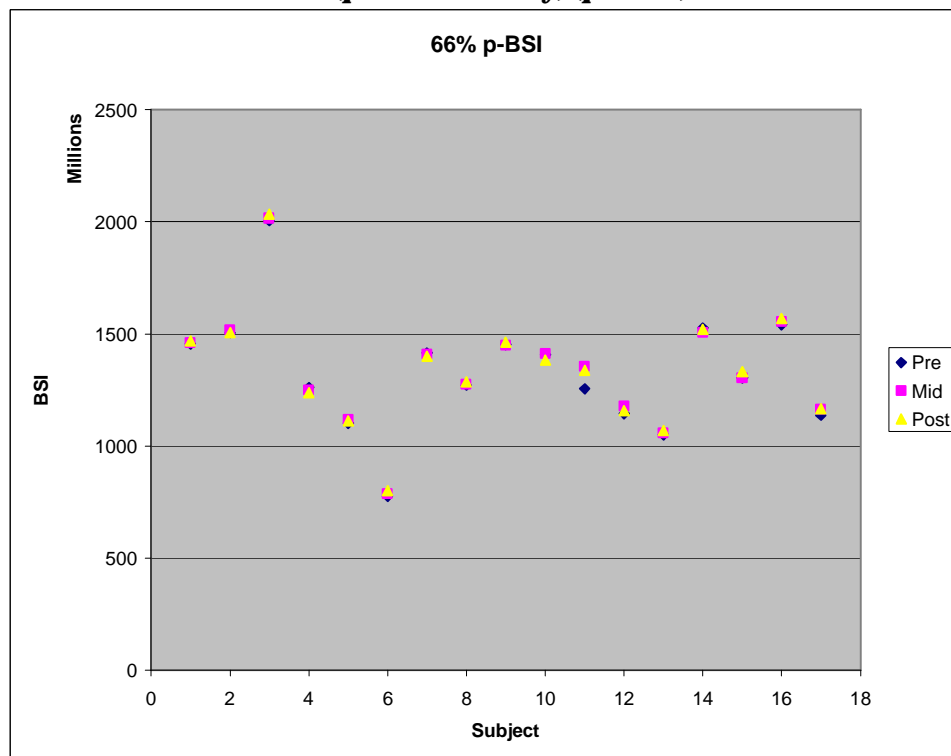


**Figure 26. Individual BSI (polar) for the 66% level: pre, mid and post training. Units are *(pixel-intensity)(pixels<sup>4</sup>)*.**

### 3.2 Bone Quality vs. Geometry

When the cortical bone at the 38% level are averaged among each of the 10° sectors and at each training interval (pre, mid and post), average values of cortical thickness can then be plotted against average values of density. The 36 data points from the average of the 38% slice plane images (and at each training interval) are shown in Figure 27. Values for each of the 17 subjects (36 sectors x 3 training intervals x 17 subjects = 1836 data points) are plotted in Figure 28. The average of the images at the 38% level show a clear linear trend becoming evident after a thickness (as measured by number of pixels) becomes greater than about 12 (see Figure 27). There is a 2.5% decrease in density (from about 1025 to 1000) that accompanies a 67% increase in thickness (from 12 to 20). This trend of having higher bone mineral density in the posterior portion is in keeping with observations of other researchers (see, e.g., (Lai et al. 2005),(Nonaka et al. 2006)).

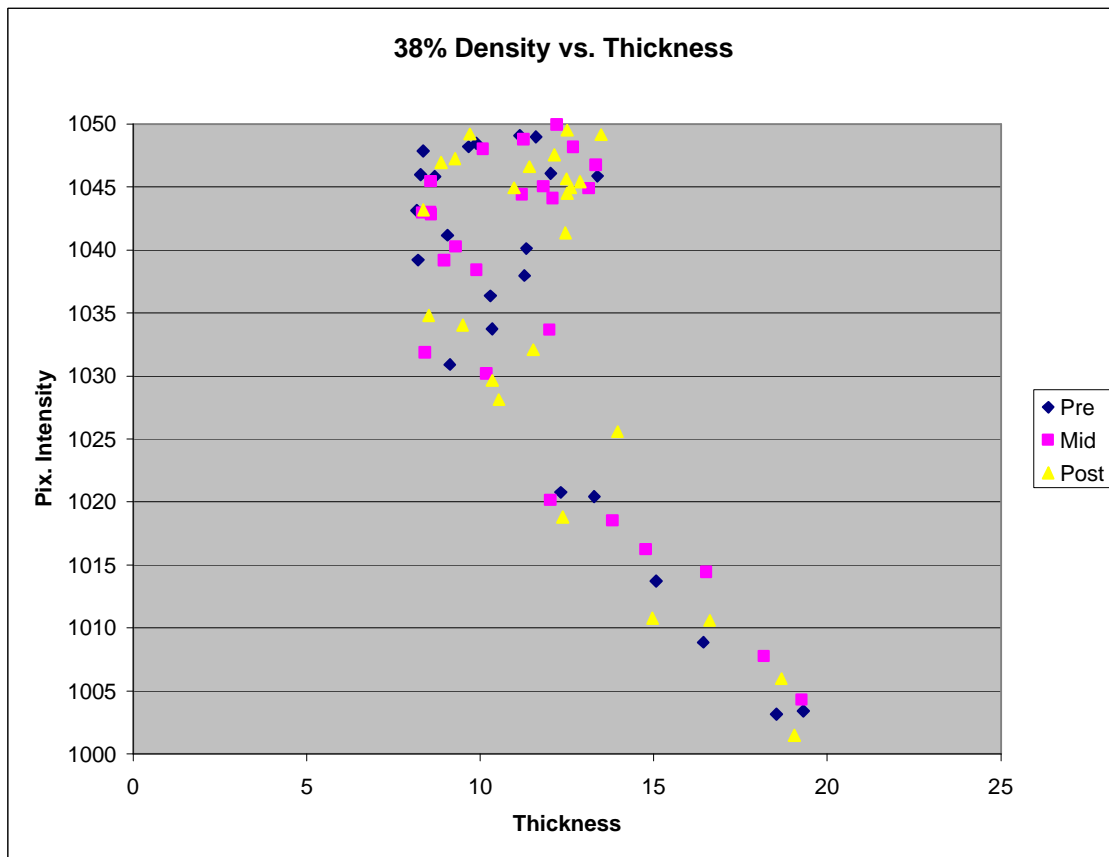


**Figure 27. Average cortical thickness (in a 10° sector) versus average cortical density in that sector for the 38% level: pre, mid, and post training.**

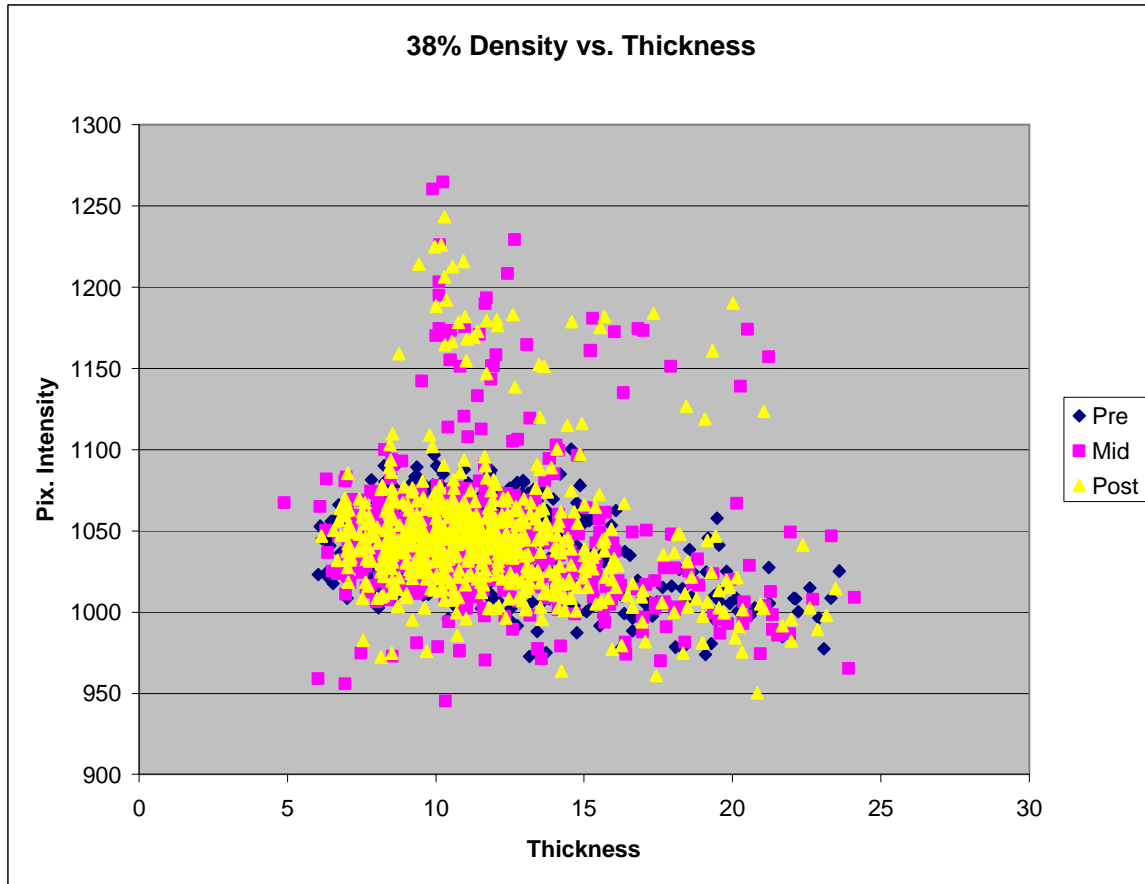


**Figure 28. Individual cortical thickness (in a 10° sector) versus average cortical density in that sector for the 38% level: pre, mid, and post training.**

Averaging the 66% slice plane images produced the cortical thickness-density points shown in Figure 29. Data for each of the 17 subjects are given in Figure 30. A similar linear relationship between thickness and density was seen at the 66% level as was seen at the 38% level. Here, a 2% decrease in density (from roughly 1005 to 985) accompanied a 67% increase in cortical thickness (from about 12 to 20).

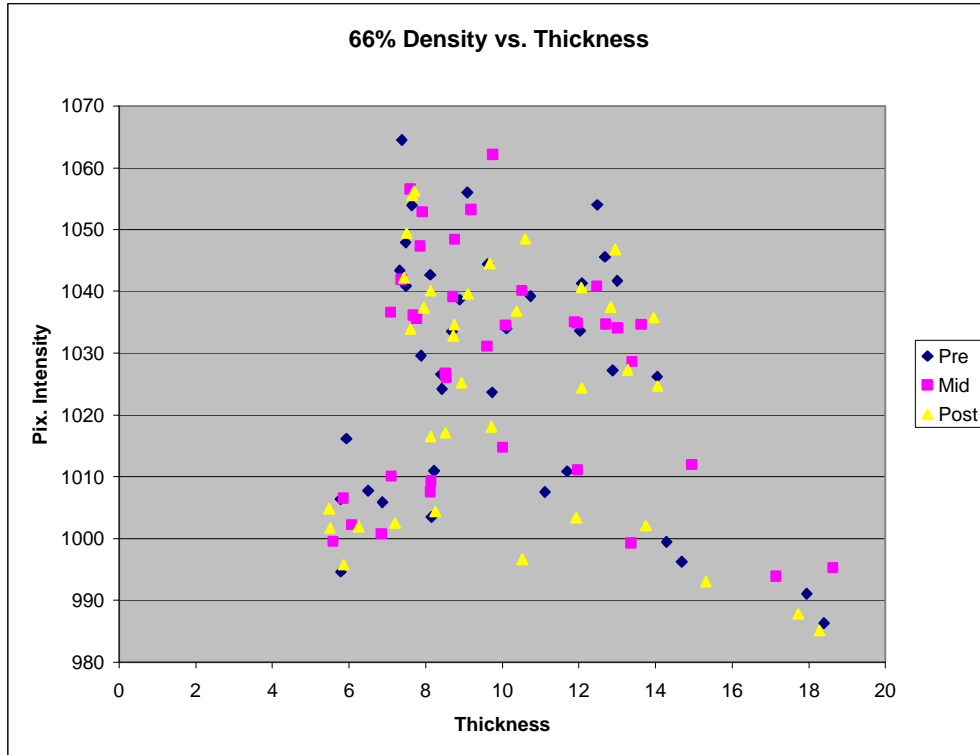


**Figure 29. Average cortical thickness (in a 10° sector) versus average cortical density in that sector for the 66% level: pre, mid, and post training.**

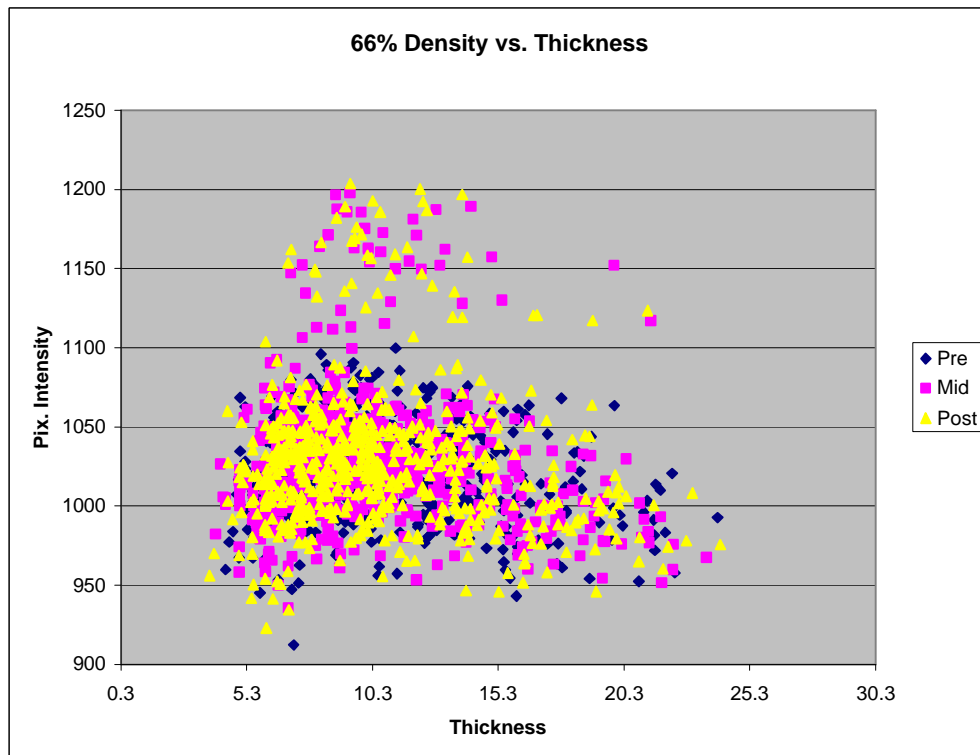


**Figure 30. Individual cortical thickness (in a 10° sector) versus average cortical density in that sector for the 66% level: pre, mid, and post training.**

## 4. Discussion

Even if the exercise regimen through which the subjects were tracked was more stimulatory than their previous daily activities, 13 weeks is probably the earliest than one would expect to see changes in bone density (most likely in distal trabecular bone) due to an increase in training. The remodeling process in bone consists of resorption of “old” bone followed by addition of new osteoid followed by mineralization of the new osteoid. The resorption process takes about 24 days in cortical bone. Osteoid formation can then take from about 3 (trabecular bone) to 4 (cortical bone) months. Mineralization is substantially complete 10 days later. While the whole remodeling process is on the order of 4 to 5 months, the process is obviously gradual. At any given remodeling location, bone resorption overlaps with bone formation which overlaps with mineralization. In light of these time periods, were short term adaptations to manifest themselves, it would be in either a *decrease* in cortical bone density (due to increased BMU remodeling activity) or an *increase* in bone area (probably trabecular, which forms faster). While a few subjects had localized trabecular apparent density changes that approached the Least Significant Change for an XCT-3000, overall neither trend was apparent.

While no significant change in bone morphology was noticed as a result of the training regimen, some striking observations were made regarding the subject bone images themselves. First, there was a wide variety of bone shapes represented in the study. Medial-Lateral lengths ranged from 47 to 62 pixels and Anterior-Posterior length ranged from 63 to 85 pixels. These unique cross sections manifest themselves in the range of individual CSMI and BSI measurements. Variations in bone morphology (shape) may have a double effect of an individual's peak tibial stress: in addition to the influence of shape on tibial stress, bone shape also influences the mechanical properties. Relationships between the morphology and the mechanical material properties of bone (brittleness and susceptibility to fatigue in particular) have been reported elsewhere in the literature (Tommasini et al. 2005). Further, tibial stresses and strains are related to individual ground reaction forces with the peak occurring on the anterior and posterior surfaces (Peterman et al. 2001). These ground reaction forces are themselves highly subject specific, being a function of body weight and gait. Anthropomorphic measurements, bone geometry, and bone material properties will all lead to a very individualized peak tibial stress. Given an estimate of an individual's basic anthropomorphic information, and a tibial density distribution and accurate representation of their geometry from pQCT, an assessment of the overall mechanical integrity of the bone should be possible.

Though the precise mechanism of tibial stress fracture remains unknown, one generalization that can be made is that stress fractures occur after microcracks induced by



repeated bone loading coalesce before having a chance to be cleared by the remodeling process. By correlating tibial stress (estimated on a subject-specific basis) with stress fracture morbidity data from its larger population (i.e., a BCT class), we should be able to begin to make generalizations about individual stress fracture propensity in the future. The investigators know of no studies which have attempted patient specific stress analyses on a population with the goal of being able to estimate stress fracture incidence *a priori*.

## 5. Reference

- Braun, M. J., Meta, M. D., Schneider, P., & Reiners, C. (1998). "Clinical evaluation of a high-resolution new peripheral quantitative computerized tomography (pQCT) scanner for the bone densitometry at the lower limbs." Phys Med Biol **43**(8): 2279-2294.
- Ferretti, J., Mazure, R., Tanoue, P., Marino, A., Cointry, G., Vazquez, H., Niveloni, S., Pedreira, S., Maurino, E., Zanchetta, J., & Bai, J. C. (2003). "Analysis of the structure and strength of bones in celiac disease patients." Am J Gastroenterol **98**(2): 382-390.
- Ferretti, J. L. 1997. "Noninvasive Assessment of Bone Architecture and Biomechanical Properties in Animals and Humans Employing pQCT Technology." J Jpn Soc Bone Morphom **7**, 115-125.
- Ferretti, J. L., Cointry, G. R., & Capozza, R. F. (2002). Noninvasive Analysis of Bone Mass, Structure, and Strength. In Orthopaedic Issues in Osteoporosis, ed. Yuehuei, H. CRC Press:pp. 145-167.
- Findlay, S. C., Eastell, R., & Ingle, B. M. (2002). "Measurement of bone adjacent to tibial shaft fracture." Osteoporos Int **13**(12): 980-989.
- Fujita, T. (2002). "Volumetric and projective bone mineral density." J Musculoskelet Neuronal Interact **2**(4): 302-305.
- Lai, Y. M., Qin, L., Hung, V. W., & Chan, K. M. (2005). "Regional differences in cortical bone mineral density in the weight-bearing long bone shaft--a pQCT study." Bone **36**(3): 465-471.
- Lorentzon, M., Mellstrom, D., & Ohlsson, C. (2005). "Association of Amount of Physical Activity With Cortical Bone Size and Trabecular Volumetric BMD in Young Adult Men:The GOOD Study." J Bone Miner Res **20**(11): 1936-1943.
- Louis, O., Soykens, S., Willnecker, J., Van den, W. P., & Osteaux, M. (1996). "Cortical and total bone mineral content of the radius: accuracy of peripheral computed tomography." Bone **18**(5): 467-472.
- Nonaka, K., Fukuda, S., Aoki, K., Yoshida, T., & Ohya, K. (2006). "Regional distinctions in cortical bone mineral density measured by pQCT can predict alterations in material property at the tibial diaphysis of the Cynomolgus monkey." Bone **38**(2): 265-272.
- Nordstrom, P., Pettersson, U., & Lorentzon, R. (1998). "Type of physical activity, muscle strength, and pubertal stage as determinants of bone mineral density and bone area in adolescent boys." J Bone Miner Res **13**(7): 1141-1148.

- Peterman, M. M., Hamel, A. J., Cavanagh, P. R., Piazza, S. J., & Sharkey, N. A. (2001). "In vitro modeling of human tibial strains during exercise in micro-gravity." J Biomech **34**(5): 693-698.
- Riggs, B. L., Melton, I. L., III, Robb, R. A., Camp, J. J., Atkinson, E. J., Peterson, J. M., Rouleau, P. A., McCollough, C. H., Bouxsein, M. L., & Khosla, S. (2004). "Population-based study of age and sex differences in bone volumetric density, size, geometry, and structure at different skeletal sites." J Bone Miner Res **19**(12): 1945-1954.
- Sievanen, H., Koskue, V., Rauhio, A., Kannus, P., Heinonen, A., & Vuori, I. (1998). "Peripheral quantitative computed tomography in human long bones: evaluation of in vitro and in vivo precision." J Bone Miner Res **13**(5): 871-882.
- Stratec 2006. "XCT 3000 Manual Software version 5.50."
- Tommasini, S. M., Nasser, P., Schaffler, M. B., & Jepsen, K. J. (2005). "Relationship between bone morphology and bone quality in male tibias: implications for stress fracture risk." J Bone Miner Res **20**(8): 1372-1380.
- Veitch, S. W., Findlay, S. C., Hamer, A. J., Blumsohn, A., Eastell, R., & Ingle, B. M. (2005). "Changes in bone mass and bone turnover following tibial shaft fracture." Osteoporos Int.